Modeling of the break process to improve tomato paste production quality

A thesis presented in partial fulfilment for the degree of Masters in Engineering (Bioprocess) at Massey University, Palmerston North

Arunee Srichantra

2002

Abstract

The pectic enzyme, Pectinmethylesterase (PE) and Polygalacturonase I and II (PGI and PGII), in the tomato fruit released after crushing during tomato processing reduce the viscosity of tomato paste by breaking down the insoluble pectin in the cell wall. To achieve higher viscosity tomato paste, the cold break (<60°C) or hot break (>60-95°C) processes can be used to inactivate the pectic enzyme and to achieve higher viscosity tomato paste.

The study of tomato solids and PG enzyme activity showed that the levels of insoluble solids, total solids, pectin, and °Brix in Ferry Morse tomatoes were independent of fruit ripeness. The amount of PG enzymes was high in orange and dark red tomatoes and the activity of PG enzymes increased as a function of ripeness, from green to dark red. In the dark red tomato, the inactivation of PG enzyme activity was required to retain the level of pectin. Cold break temperatures below 60°C can not inactivate the PG enzyme activity. The PG enzymes started to be denatured when the hot break temperature was above 65°C and be completely destroyed when the break temperature was above 80°C.

A mathematical model of the break process was formulated and Matlab programme was used to predict the effect of break temperatures on the pectin and PG enzyme concentration of the tomato pulp in the break tank for any inputs of feed rate (the flow rate to the break tank), feed ripeness, and residence time. The model was used to demonstrate the understanding and the optimisation of break process performance. Longer residence time of dark red tomato pulp in the break tank can decrease pectin fraction residual and increase enzyme inactivation in the tank temperature range 40 to 60°C. The pectin fraction remaining increased when the tank temperature was above 60°C because of the inactivation of PG enzymes. At 80°C there was no effect of residence time, the pectin fraction residual increased and reached 90% and enzyme fraction residual decreased to 10%.

The effect of mixed tomato ripeness between the ripe fruit (orange and dark red) with the unripe fruit (green, breaker, and turning), the level of PG enzymes in the break tank decreased and affected on the higher pectin fraction remaining. Lower break temperature can be therefore used in this process to inactivate the low amount of PG enzyme and to achieve the same extent of pectin hydrolysis.

The interruption of the feed coming into the break tank during tomato processing can increase the pectin fraction remaining and the enzyme fraction remaining in a new steady state when the feed was turned on.

Acknowledgements

I would like to thank Dr. John Bronlund who taught, encouraged, supported, and pushed me along with this work. Also thanks to Dr. Pak Lam Yu who spent time to expand my knowledge of enzyme and laboratory instructions.

Thanks to Colin Watson and Daya Vithanage at Heinz-Watties, Hastings, who let me take part in this research and sent me the tomato fruit every week during my experimental research.

I would like to salute in Thai manner (Khob-khun-ka) to Gavin Watson (an engineer at Chevron Niugini Ltd.), Worasit Tochampa, Stephen Werner and Gary Field-Mitchell. Thanks to your kindness to edit my Thai-English to Kiwi-English and supports useful advices. Thank you very much.

Special thanks to Anne-Marie Jackson, Mike, and Suzanne who support my laboratory work.

Weerawate Utto, one of my best friends who always encouraged and supported me along with this thesis.

Wisanu Srichantra, thank for your kindness to support me as a lab boy, cook and nice husband. Thank you to God to give us a little angel, Amy, who always cheers me up with her four teeth smile.

Table of contents

CHAPTER 3

CHARACTERISATION OF TOMATO SOLIDS

CHAPTER 4

CHARACTERISATION OF PG ENZYMES IN TOMATOES

CHAPTER 5

BREAK PROCESS MODEL

CHAPTER 6

MODEL APPLICATION

CHAPTER 7

CONCLUSION

List of Figures

List of Tables

Chapter 1
Project Overview

1.1 Problem definition

The tomato is an important ingredient in the present food industry. It can be consumed as a fresh fruit or processed to form tomato pulp, tomato juice, tomato puree or tomato paste. Tomato paste or concentrated tomato is widely used by food manufacturers as a starting material for a wide range of tomato products. The paste imparts viscosity, colour and flavour to formulated products. Concentrated product enables storage for long periods of time for use outside the tomato growing season.

Heinz-Watties Australasia Ltd., Hastings produces a wide range of tomato products such as soups, sauces, baked beans, spaghetti and pasta sauces for several different brands including Watties, Oak, Heinz, Weight Watchers. Tomato paste is used as the base ingredient for many of these products. Tomato paste processing comprises many stages including washing, crushing, evaporating, sterilising and packaging.

Campbell (2002) found that the viscosity of tomato puree after crushing was not uniform and that affected the subsequent viscosity of tomato paste. This was due to the activity of pectinmethylesterase (PE) and polygalacturonase I and II (PG I and II) enzymes (pectic enzymes). These enzymes breakdown the insoluble pectin in the cell wall and as a result, the viscosity was reduced. The hot break process is designed to keep the temperature greater than 80°C to help inactivate both enzymes and achieve the higher viscosity.

Campbell (2002) also showed that the ratio of soluble solid to total solids of paste produced at Heinz-Watties was variable. These findings were assumed to be due to the changing residence time in the break tank resulting in variable pectic enzyme inactivation and therefore varying the degree of the conversion of insoluble pectin into soluble sugars and organic acids. It was therefore assumed that tomato pulp with a short residence time in the break tank may result in high IS/total solid ratios, whereas tomato puree with a long residence time may achieve lower IS/total solid levels.

The aim of this work was to develop a model for the break process to allow process optimisation and thereby providing a more consistent tomato paste for Heinz-Watties. This involves characterisation of the kinetics of pectin hydrolysis and PG enzyme destruction in the process and the modelling of temperature and reaction in the break tank.

1.2 Project Aims

The intermediate aims to achieve these goals are;

- To measure the kinetics of PG enzyme activity.
- To measure of the kinetics of PG enzyme inactivation due to heat processing of tomato fruit at the temperature range 25 to 80°C.
- To mathematically model the break process to allow the prediction of break tank temperature, extent of pectin hydrolysis and enzyme inactivation as a function of time and temperature in the break process.
- To use the model to suggest strategies for the better control of tomato paste quality.

Chapter 2
Literature Review

2.1 Introduction

Tomatoes rank second to potatoes in dollar value among the vegetables produced in the world. In terms of per capita consumption, tomatoes are the leading processed vegetable. Two-thirds of the total world production of tomatoes are processed using heat treatment. The application of thermal preservation treatments significantly effects the viscosity and consistency of final products (Barrett *et al.*,1998). The consumption of tomatoes in tomato processing is limited mostly to *Lycopersicum esculentum* (Gould,1992).

2.2Tomato

There are many compounds in fresh tomato which changes as the fruit ripens. The extent of these changes is dependent on the environment, temperature, harvesting etc. The tomato physiology is described in Figure 2.1. The changes of tomatoes during ripening and the function of each enzyme in the fruit are discussed as below.

2.2.1Tomato physiology

Tomato is generally regarded as a berry since the seeds are formed within a fleshy mesocarp. The main divisions of tomato fruit are skin, pericarp, and locular contents. Tomato skin is composed of four or five layers of cells under a thin cuticle. The epidermal layer has a heavily cutinized outer surface, and both the epidermis and the underlying collenchyma are rather thick-walled. As the fruit matures, the pericarp cells become very large (100 to 500 μm) and thin-walled. During ripening, it has been found that the plasmalemma, tonoplast, and nuclei remain intact both physically and physiologically. All cytoplasmic structures detected in developing fruit persist during ripening with no loss of density of the cytoplasm. Vascular strands radiate from the stem end of the fruit, both round the pericarp and down the columella to the blossom end. From an early stage in development, the locules are filled by an outward growth of placental cells. As maturity approaches, the walls of these parenchymatous cells around the seeds become thin and wavy, and contain a large but diminishing number of starch grains (Davies and Hobson,1981).

The appearance of the jelly-like material in the locular cavities provides an excellent criterion whereby fruit may be designated "mature green" and the ripening is often first seen a pinkish tinge to this placental tissue. (Davies and Hobson,1981).

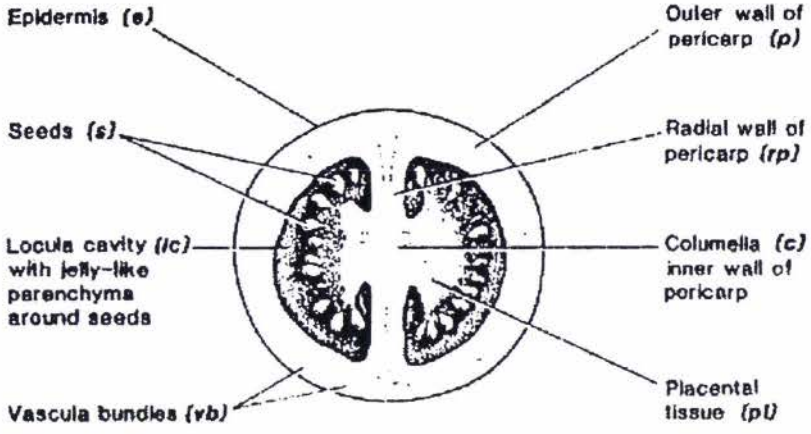

Figure 2.1 Tomato anatomy (Davies and Hobson, 1981)

2.2.2 Composition of tomatoes

Tomatoes are considered a high acid food (pH<4.6). The acid content varies due to maturation and storage conditions (Wiese and Dalmasso, 1994). The ranges of values for some constituents in tomato depend on the level of the dry matter, season, nutrition and environment. While the concentration of components in the tomato fruit depends upon light levels, the uptake of many elements is a result of a complex series of interactions with environment, pH of the growing medium, and with the other elements present (Davies and Hobson, 1981).

The composition of tomatoes affects the quality of tomato products. The compositions of the tomatoes and processed tomato products are sumarised in Table 2.1.

Table 2.1 Composition of fresh tomatoes (Gould, 1992)

Constituents	*%*
Total solids	7.0-8.5
Soluble solids	4.0-6.0
Sugar	2.0-3.0
Insoluble solids	1.0
Soluble protein and amino acid	0.8-1.2
Mineral constituents	0.3-0.6
Acid	0.3-0.5
Salt (sodium chloride)	0.05-0.1

2.2.2.1 Total solids

Total solids in the tomatoes consist of soluble solids and insoluble solids. The percentage of solids varies depending on the variety of tomatoes, character of soil, and especially the amount of rainfall during the growing and harvesting seasons.

Total solids of a tomato fruit is generally between 7.0-8.5 %. Generally, the tomatoes contains 1.0% of skins and seeds, and insoluble solids and 4.0-6.0% is soluble solids (Gould,1992).

2.2.2.2 Carbohydrates

Carbohydrates in tomatoes comprise of polysaccharides and free sugars. The polysaccharides in tomatoes consists of 0.7% of tomato juice which pectins and arabinogalactans constitute about 50%, xylans and arabinoxylans about 28% and cellulose about 25%. The reducing sugars in the tomatoes are glucose and fructose which is 50-65% of tomato solids (Gould,1992).

2.2.2.3 Proteins and amino acids

There are 19 amino acids in fresh tomato juice. Glutamic acid is at the highest concentration in fresh tomato juice and asparagine and glutamine are the second highest in concentration in tomato juice. The processing of tomato juice at the higher temperature results in a substantial increase in the free amino acids as a result of denaturation and partial hydrolysis of protein. The greatest increase occurs in glutamic and aspartic acids, which partially account for the increase in ammonia in the processed juice. The disappearance of glutamine and asparagine by deamination during the heat treatment causes the formation of pyrollidone carboxylic acid which is not presented in unheat treated tomato juice. The compositions of amino acids in tomatoes are summarised as Table 2.2.

Table 2.2 *Amino acid content of fresh and processed tomato juice (Gould,1992)*

Amino acid	*mg Amino Acids in 100g Tomato Juice*	
	Fresh	*Processed*
Glutamic acid	21.9	212.5
Asparagine and glutamine	7.8	-
Aspartic acid	5.5	51.6
Serine	2.3	12.7
Phenylalanine	1.4	10.8
Alanine	1.0	9.0
Threonine	1.0	9.0
Lysine	0.9	5.1
Histidine	0.9	7.5
Arginine	0.7	4.4
Isoleucine	0.6	3.8
Leucine	0.6	3.0
Tyrosine	0.5	3.4
Valine	0.4	1.7
Glycine	0.3	1.2
Methionine	0.2	0.9
Proline	0.1	0.4
Unknown	-	0.6
Total	45.1	337.6

2.2.2.4 Acids

The majority of organic acids in tomatoes are as citric acid, with minor levels of other acids. Processing of tomato juice results in an increase in total acid. Acetic acid is increased by 32.1%, apparently due to oxidation of aldehydes and alcohols and deamination of amino acids, such as alanine to pyruvic during processing. The organic acids in fresh and processed tomato juice are presented in Table 2.3.

Table 2.3 *Organic acids in fresh and processed tomato juice (Gould, 1992)*

Acid	*mEq/Litre tomato juice*	
	Fresh	*Processed*
Citric	60.92	66.92
Malic	3.72	5.39
Lactic	1.37	1.46
Alpha-ketoglutaric	1.10	0.53
Acetic	1.06	1.56
Pyrrolidone-carboxylic	0.81	8.10
Succinic	0.60	0.49

2.2.2.5 Minerals

The quantity of minerals in tomatoes varies between 0.3-0.6%. The minerals of tomato fruit are sumarised in Table 2.4.

Table 2.4 *Concentraion range of constituents in normal ripe tomato fruit per 100g fresh tissue (Davies and Hobson , 1981)*

Constituent	*Normal range*
Potassium (mg)	92-376
Chlorine (mg)	24-69
Phosphorus (mg)	7.7-53
Magnesium (mg)	5.2-20.4
Calcium (mg)	4.0-21
Nitrate (mg)	1.3-30
Sodium (mg)	1.2-32.7
Aluminum (mg)	0.5-2.95
Iron (mg)	0.35-0.95
Copper (mg)	0.05-0.2
Manganese (mg)	0.04-0.3
Boron (mg)	0.04-0.13
Lead (mg)	0.02-0.05
Zinc (mg)	0-0.25

2.2.2.6 Pigments in tomatoes

Lycopene is the main pigment in tomatoes and is responsible for the deep-red colour of ripe tomato fruits and tomato products. The loss of lycopene can be attributed to both oxidation and isomerization. The concentration of lycopene in the tomato fruit is 3.1-7.7 mg/100g of ripe fruit. In tomatoes, lycopene biosynthesis increases dramatically during the ripening process as chloroplasts undergo transformation to chromoplasts. Table 2.5 illustrates the carotenoid levels in tomato fruit (Shi and Maguer,2000).

Table 2.5 *The contribution of carotenoid species in tomato fruits (Shi and Maguer, 2000)*

Carotenoid species	*Composition (% of total carotenoid)*
Lycopene	80-90
Neurosporene	7-9
Phytoene	5.6-10
β-carotene	3-5
Phytofluene	2.5-3.0
ξ-carotene	1-2
γ-carotene	1-1.3
α-carotene	0.03
Lutein	0.011-1.1

2.2.2.7 Nutrients in tomatoes

Fresh tomato, tomato juice, and other processed tomato products contain several nutrients as shown in Table 2.6. Tomatoes are a good source of vitaminA which is present in the form of carotene and makes a very important contribution to the vitamin A requirement of the human diet (Davies and Hobson,1981).

Table 2.6 *Vitamin range in normal ripe tomato fruit per 100g fresh tissue (Davies and Hobson,1981)*

Constituent	*Normal range*
Vitamin A (IUs)	833-1667
Vitamin B_3 (μg)	280-340
Vitamin B_2 (μg)	20-78
Vitamin B_1 (μg)	16-80
Vitamin C (mg)	8.4-59
Vitamin B_6 (mg)	0.074-0.15

2.2.2.8 Volatile components in tomatoes

The volatile components present in tomato products has been studied by Sieso and Crouzet (1977) using combined gas chromatography-mass spectrometry. After a prolonged heat treatment of tomato paste, it was found that the most volatile components decrease or disappear. Table 2.7 is shown the volatile components of tomato before and after heat processing.

***Table 2.7** Relative amounts of the most characteristic compounds present in fresh and heated juice (100°C for 10 minutes) (Sieso and Crouzet, 1977)*

Compounds	*Fresh juice*	*Heated juice*
Trans-2-hexenol	30	21.8
Cis-3-hexenol	12.4	10.4
Hexanol	11.4	12.7
6-methyl-5-heptene-2-one-and n hexanol	9.7	11.2
Trans-2-hexenol	9	19.5
Pentanol	3.8	3.25
Carvone	2.05	0.79
2-isobutylthiazol	1.37	1.08
2,6-dimethyl-2,6-undecadien-10-one	1.04	2.45
Xylenes	0.93	1.08
α-terpincol and isopropyl-4-phenyl alcohol	0.5	1.3
Toluene	0.47	0.73
2-phenyl ethanol	0.44	1.02
Furfural	0.14	0.42
5-methyl furfural	0.13	0.47
Furfuryl alcohol	0.09	0.4
Benzaldehyde	0.07	0.30
5-methyl-2-acetylfuran	0.07	0.15
Phenyl acetaldehyde	0.05	0.66
2-acetyl furan	0.05	0.14
Linalol	0.03	0.19
Trimethyl benzene	0	0.51

2.2.3 PG and PE enzyme biochemistry in tomato

Tomatoes contain many enzymes but the pectolytic enzymes are particularly important during tomato processing. Tomatoes are the richest plant source of polygalacturonase. McColloch and Kertesz (1949) found that pectinmethylesterase (PE) and a pectic acid depolymerase (PG) in fresh tomatoes resulted in the loss of pectinic substances in processed tomato products. This confirmed that there are two enzymes present in tomatoes responsible for pectin hydrolysis.

2.2.3.1 Polygalacturonase (PG)

PG catalyses the hydrolytic cleavage of α-1-4-glycosidic bonds of pectin galacturonic acid chains. There are two main PG isoenzymes in tomatoes, PGI and PGII. Both are endopolygalacturonases, but they differ in molecular size and thermostability. PGII is composed of a single polypeptidic chain. PGI is composed of two subunits; the polypeptidic chain of PGII which is the catalytic subunit, and the so-called β subunit (McColloch and Kertesz,1949). Though PGI is known as a part of PGII but the relationship between them is unknown (Giovannoni,1992).

2.2.3.2 Pectinmethylesterase (PE)

Pectin methylesterase catalyses the hydrolysis of the methyl ester bonds of pectin which causes the degradation of pectic cell wall. Although there are also different PE isoenzymes in tomato fruit, their heat resistance seems to be quite similar (Lopez *et al.*,1998). Because of its discrete thermoresistance, it may cause cloud instability when partially inactivated in products such as pastes and/or sauces (Sio *et al.*,1995).

2.2.4 Mechanism of changes during ripening and storage

Ripening of tomato fruit involves dramatic changes in colour, texture, aroma, flavour, and composition. At the beginning of ripening, there is a rise in ethylene production and respiration rate. The initial colour changes occur in the locular region, chlorophyll is replaced by carotenoids, mainly lycopene (Hayes *et al.*,1998 and Giovannoni *et al.*,1992).

During growth, the plant forms insoluble protopectin that firmly binds with the cell wall. Pectin is also associated with cellulose to form plant cell walls (Hayes *et al.*,1998).

Pectin is the major component of the middle lamella. It occurs in most plant materials but it is particularly high in young fruit tissues. The composition of pectin varies greatly from source to source and even from the same plant at different stages of growth. Pectins are mixtures of polysaccharides that originate from plants that contain pectinic acids as major components. Pectins are water soluble and able to form gels under suitable conditions. Pectin solutions exhibit the Non-newtonian and pseudoplastic behavior characteristic of most polysaccharides (Fisherman and Jen,1986).

BeMiller (1986) established definitions of pectin substances in current commercial use. Firstly, pectic acids are galacturonoglycans (poly (α-D-galactopyranosyluronic acids)) without methyl ester groups or with a negligible content of methyl ester groups. Salts of pectic acids are called pectates. Secondly, pectinic acids are galacturonoglycans with various contents of methyl ester groups. Salts of pectinic acids called pectinates.

Pectin is basically a linear α-1,4-galacturonan, a native polysaccharide that is insoluble. The solubilization of pectin can be accomplished by degradation. The degradation of pectin can occur from lyases or transeliminases which cleave the α-1,4-galacturonisidic bond by a *trans* elimination of the proton bond and

poly-α-1,4-galacturonide glycanohydrolase (polygalacturonase) which de-esterified galacturonans. However, the degradation of galacturonan chain of pectin can be interrupted by α-1,2-linked rhamnose residues, arabinose and galactose (Pressey ,1986).

The cell wall-middle lamella softens from the inside out. Protopectin is converted to soluble pectin by the enzyme protopectinase, and the pectin so formed binds the cells together but less firmly. The pectin in turn is further broken down by the pectinolytic enzymes, polygalacturonase (PG) and pectin methylesterase (PE) (Hayes *et al.*,1998 and Hobson,1965). Knegt *et al.* (1988) confirmed that the PG activity during ripening increases by measuring the extent of the depolymerization of the pectin of the middle lamellae between the cells of pericarp. Hobson (1965) found that the activity of polygalacturonase increased very rapidly as tomato fruit turn red. Polygalacturonase was suggested as fulfilling an important role on the changes in firmness of tomato fruit throughout maturation and ripening.

Hayes *et al.* (1998) divided PG enzymes to be two types, endo-PG and exo-PG. Endo-polygalacturonase (endo-PG) hydrolyses the (1-4) link between two adjacent galacturonic acid residues within a polygalacturonic acid chain. The activity of endo-PG increases dramatically during ripening. The action of PG is limited by a number of factors including the amount of calcium bound to pectin, the distribution of PG in the cell walls and the extent of methyl esterification in the polygalacturonic acid molecules.

On the other hand, the activity of exo-polygalacturonase comprises only a small fraction of the total polygalacturonase activity in ripening and it is not likely to play a significant role in softening. As endo-PG is more active in degrading nonesterified rather than methyl-esterified pectin, pectinesterase (PE) is another important enzyme in the softening process. This enzyme carries out demethoxylation at the C6 position of galacturonate methylesters of the pectin molocule. The presence of PE enhances the ability of PG to solubilize polyuronide which the degree of esterification is a critical factor in the solubilization of the cell wall (Barrett *et al.*,1998). The overall mechanism of enzymatic changes to pectic substances during ripening is shown in Figure 2.2.

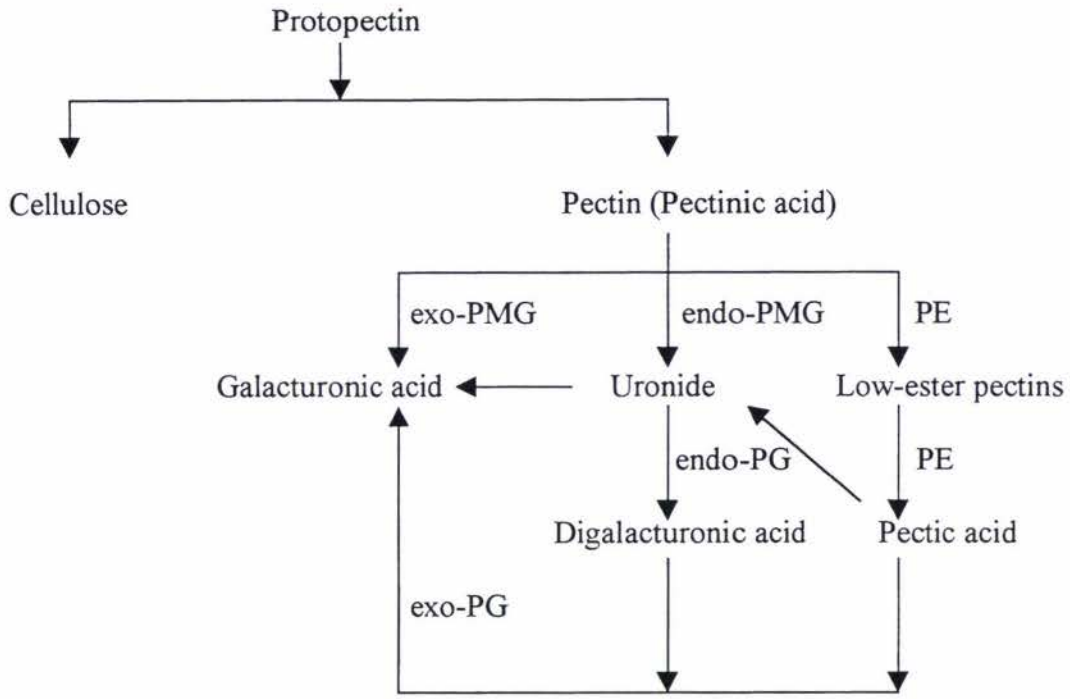

PE: Pectinesterase
PG: Polygalacturonase
PMG: Polymethylgalacturonase

***Figure 2.2** The actions of enzymes in tomatoes (Gould, 1992)*

The fruit then becomes soft and mushy. The solubilization of the cell wall continues more extensive as more ripening proceeds, leading to fragile walls in very ripe fruit (Hayes *et al.*, 1998).

PG and PME can bring about a large reduction in the viscosity of the product unless inactivated by 'Hot braking'. The hot braking is carried out by heating the tomato pulp as quickly as possible to 82°C or above to denature PG and PME and preserve as much of the potential viscosity as possible (Hayes *et al.*, 1998).

2.3 Tomato paste production

Tomatoes may be processed to give many tomato products. This section describes the tomato paste production process; which is the focus of this project.

2.3.1 Definition of processed tomatoes

Tomatoes can be processed to give tomato juice, and concentrated tomato juice, tomato puree, and tomato paste. Hayes *et al.*(1998) defined the useful definitions of these processed tomato products as shown in Table 2.8.

Table 2.8 Definitions of the processed tomato products (Hayes et al., 1998)

Tomato products	*Definitions*
Tomato pulp	The crushed tomatoes either before or after the removal of skins and seeds.
Tomato juice	The juice (the crushed tomatoes which skin and seeds are removed) is intended for consumption without dilution or concentration.
Tomato serum	The tomato juice which is filtered or centrifuged to completely remove suspended solid material.
Tomato pulp solids	The suspended solid material in tomato juice, puree or paste which can be separated by centrifugation.
Tomato syrup	Tomato syrup which has been concentrated.
Tomato puree	A low concentration tomato paste which contains 8% to less than 24% natural total soluble solids.
Tomato paste	The products are resulted from the concentration of tomato pulp after the removal of skins and seeds and contains 24% or more natural tomato soluble solids (NTSS).

2.3.2 Desired qualities in processed tomatoes

The principle quality parameters for tomato paste are colour, consistency and flavour and in addition there are compositional standards. The absence of a world-wide standardization of methods and instruments to define tomato paste quality and composition has been the main cause of disputes among companies dealing with the tomato products (Hayes *et al.*,1998).

The quality of processed tomato products is highly variable. The sensory characteristics are the major attributes influencing the buying behavior of the consumers. The attractive bright red colour, good aroma, high consistency, low pH and high acidity, and low serum separation are some of the factors that are expected Thakur *et al.*(1996a).

Thakur *et al.*(1996a) discussed the factors that affected the quality of processed tomato products as follows:

2.3.2.1 Colour

Colour has a strong influence on the buying behavior of the customers because they notice colour first. It is important to make a favorable initial impression with standard and familiar colour that consumer want to buy and expect to see. In this study, the model will allow optimisation of the process to achieve good colour tomato paste.

2.3.2.2 Flavour

Flavour is an important quality attribute of processed tomato products. It is affected by agricultural practices, time of harvest, postharvest treatment, and genetic control (cultivar). The characteristics sweet-sour taste and the flavour intensity of tomato and tomato products are affected by almost all of tomato constituents. They may influence

the flavour directly as a flavour substance or indirectly by providing either an appropriate medium for chemical or biochemical reactions leading to the formation of flavour. Therefore, flavour is an important factor influencing the quality of tomato products.

2.3.2.3 Consistency

Viscosity is also an important characteristic of high quality tomato products. It determines the acceptability of tomato products to the customer and is an integral part of the quality grade standard. In addition to its role in product quality, consistency also has economic implications for tomato processors. The higher consistency lowers the amount of tomato needed in a product to obtain a certain level of quality and thus reduce the cost of product. The highest consistency of tomato paste will be optimised using the mathematical model in this study.

2.3.2.4 Serum separation

Serum separation, or degree of settlement, is a significant problem in maintaining the quality of tomato products. Serum separation in tomato products can occur in two ways are:

(a) There is too much liquid for a given concentration of insoluble particles.

(b) A gradual collapse of precipitate occurs under gravity during storage of the product.

Therefore, the problem of serum separation in the market should be avoided.

2.3.2.5 Total acidity and pH

Generally, acid concentration and pH influence the acceptance of consumers in addition to flavour and viscosity. The higher acidity of tomato products necessitate longer processing times which affect the product quality. The average acidity of processing tomatoes is about 0.35% expressed as citric acid.

2.3.2.6 Nutritive value

Tomato is one of the most important crops because it is full of minerals and vitamins. Extended heat treatments can decrease the amount of vitamins in tomato products. Therefore, a balance has to be set between various factors to obtain a product with high nutritional and desirable product quality.

2.3.3 Tomato processing & diagram

The basic sequence of operations in the production of canned tomato paste from raw material are sumarised as Figure 2.3. This diagram based on an economic study of a typical, medium-sized Italian plant (Hayes *et al.*,1998)

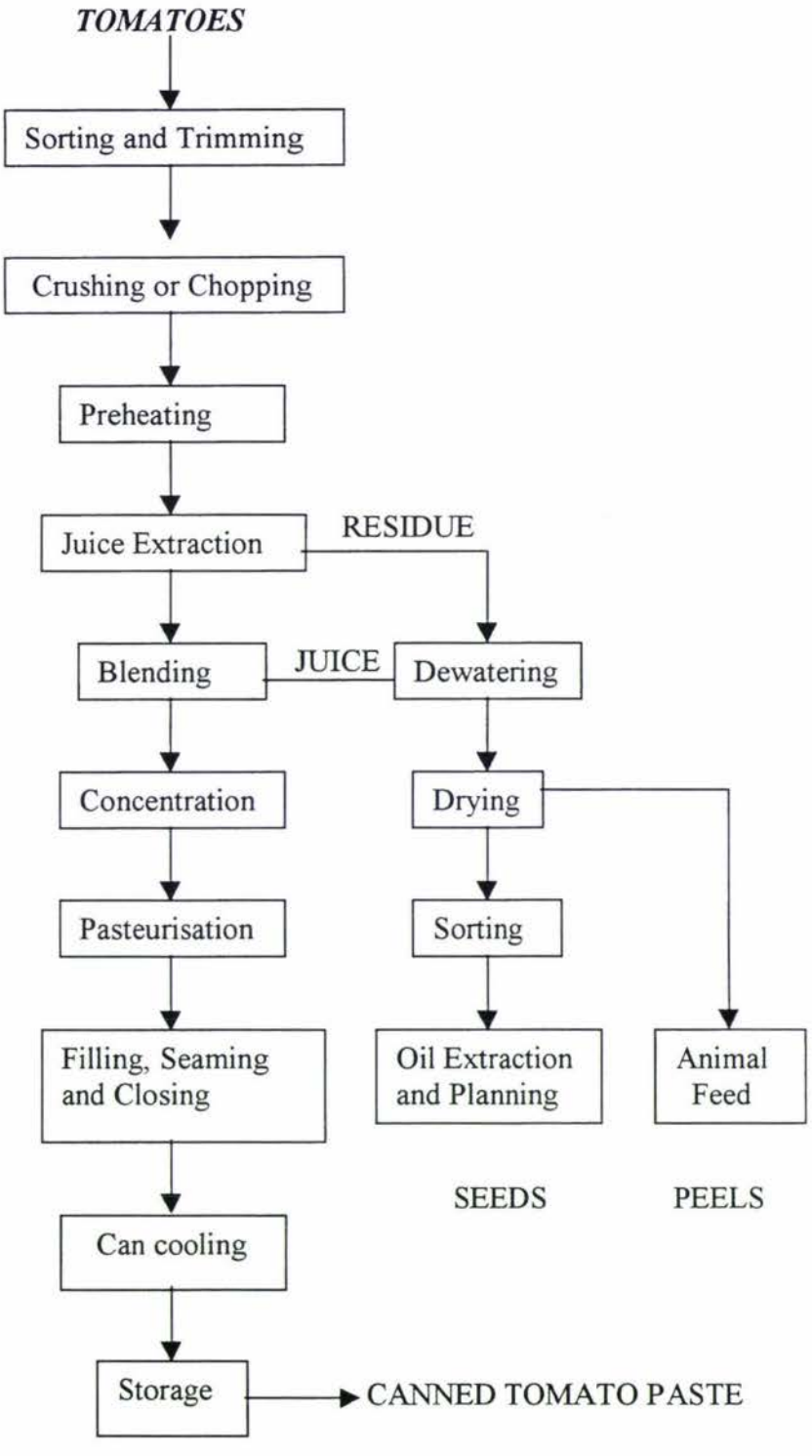

Figure 2.3 *Flow diagram for canned tomato paste production (Hayes et al., 1998)*

The description of tomato processing steps can be summarised as described by Hayes *et al.*(1998) as follows:

2.3.3.1 Washing, sorting, and trimming

Tomatoes are washed in water tanks agitated with compressed air, followed by rinsing with high-pressure water sprays to remove pesticide residues, microorganisms, dirt, mold fruit fly eggs, and larvae adhering the fruit. The wash water is chlorinated to 5 to 10 ppm to maintain sterility. The unfit whole fruit is picked out and discarded, while partly defective fruit is trimmed by hand. Sorters and trimmers remove off-colour fruit and parts. A low mould count is the final control point to ensure the safe number of mould in the final product.

2.3.3.2 Breaking process

The washed tomatoes are chopped into small pieces by a rotary comb chopper, and then are pumped into a heat exchanger and preheated to either 60°C for 'a cold break' or preheated to 90 to boiling and held for 1 to 2 minutes for 'a hot break'.

2.3.3.3 Juice extraction

The heated tomato pulp is passed through two (or three) juice extractors to remove the skin and seeds, and to squeeze the juice out of the remaining pulp. Juice extractors may be either of the screw type or paddle type, a screw-type extractor uses an expanding helical screw to subject the pulp to increasing pressure against a screen, whereas a paddle type extractor beats the pulp against a screen. In the teminology of tomato precessor the first juice extractor is known as a 'pulper' and the second juice extractor is known as a 'finisher'. A further screw press may be added to extract more juice from the residue leaving the juice extractors. Blending of the juice from this dewatering stage with that leaving the juice extraction stage increased the yield. In addition, seeds in the residue may be recovered for animal feed or fuel.

2.3.3.4 Concentration

Tomato juice is concentrated by evaporation under partial vacuum either in a batch or continuous process. In a batch process, the evaporation may be entirely carried out in steam-jacketed vacuum pans (known as 'boules') fitted with agitators, or the juice may be preconcentrated in a tubular evaporator to about 12% solids before transfer to the boules. Evaporation at low pressure reduces the boiling point of the juice so that the resulting paste retains most of its colour and flavour. Continuous processes, such as multiple effect evaporators with backwards feed (flow), produce a more consistent paste than batch processes. The concentration of tomato juice for paste results in a large increase in viscosity during evaporation.

2.3.3.5 Pasteurisation

Continuous pasteurisation of tomato paste in a tubular heat exchanger at 90 to 92°C, before it is canned, prevents spoilage by lactobacilli. The recirculation tube around the heat exchanger returns the hot paste to the receiving tank if flow through the filling nozzles is restricted, to prevent 'burning on' fouling of the heat exchanger and loss of product quality.

2.3.3.6 Filling, closing, and cooling

The pasteurised paste is automatically hot-filled into lacquered tin cans that have been prepasteurised with steam and immediately seamed, inverted to sterilise the lids, and held for 3 min. prior to cooling. The retention of heat leads to deterioration off flavour and colour. Cans are cooled as quickly as possible by air or water. Water cooling involves agitating the cans for about 2 hr. under a spray of 15 ppm chlorinated water.

2.4 Characterisation of tomato paste

After tomato juice is concentrated to produce tomato paste. The characteristics of tomato paste is investigated in this section in terms of the composition, colour, viscosity, and total solids.

2.4.1 Compositional and functional properties of tomato paste

Tomato paste is a tomato product that is concentrated by evaporating the tomato juice. The composition of tomato paste after heat processing is considerably changed from the tomato juice. Weise and Dalmasso (1994) studied the chemical and physical changes before and after heat processing of tomato products. It was found that the organic acids in tomato juice are immediately higher after heat processing. Therefore, heat treatment always decreases the constituents of fruits. The composition of tomato paste and products is shown in Table 2.9.

Table 2.9 *Composition of fresh tomato and tomato products (100g) (Thakur et al., 1996a)*

Compositions	***Tomato fruit***	***Tomato juice***	***Tomato paste***	***Tomato ketchup***
Water (%)	93.5	93.6	75	68.6
Carbohydrate(g)	4.7	4.3	18.6	25.4
Protein (g)	1.1	0.9	3.4	2.0
Fat (g)	0.2	0.1	0.4	0.4
Ash (g)	0.5	1.1	2.6	3.6
Ascorbic acid (mg)	23	16	49	15
Vitamin A (IU)	900	800	3300	1900
Food energy (cal.)	22	19	82	106

2.4.2 Measurement of colour changes of tomato paste

There are many systems to determine the colour of agricultural products. Gould (1992) suggested many systems to measure the colour of tomato products as following.

2.4.2.1 Ridgway Charts

The Ridgway Charts were developed in 1886. It comprises 1113 colours and 36 hues that are reduced by regular proportions of white, grey, and black to give systematic groupings.

2.4.2.2 Maerz and Paul Colour Dictionary

The Maerz and Paul Colour Dictionary was published in 1930. It contains 7056 colours on 56 charts. The charts are divided into seven main groups. These colour charts were used for colour-matching purposes since the dictionary has one of the widest number of colours available. Because the charts could not be accurately reproduced in the future editions, the application of this dictionary declined.

2.4.2.3 Munsell Colour System and Charts

The Munsell Colour system is based on the use of three visual colour attributes such as hue, lightness and chroma. The Munsell charts contain 982 colours in 40 hues. The results of colour measurement are expressed in terms of colour order rather than colour mixture, and allowed an interpretation of results directly in terms of the visual qualities known in the Munsell System. Data obtained by the Munsell System can be translated or be given in figures of the ICI System, which is internationally reconized, or they can be translated into many other colour systems and notations.

2.4.2.4 CIE or ICI system

The Commission Internationale de l'Eclavinge system is based on the effect any colour may have on an agreed "standard observer". Three beams of fully saturated spectral colours isolated from the spectrum of white light (blue, green, and red) are considered to be the vertices of an equilateral triangle. It is assumed that at the corners of the triangle the amount of the particular colour is 100% and that as the light progresses further away from the corner it becomes uniformally weaker, so that as it reaches any point on the opposite side its intensity is zero. Therefore, the position of any point in the triangle can be defined mathematically by means of coordinates. This enables values to be quoted which may be converted into actual colour.

2.4.2.5 Macbeth-Munsell Disk Colorimeter

The Macbeth-Munsell Disk Colorimeter is a method of subjectively measuring colour that depends on a visual comparison in tomatoes and tomato products. The unit was developed especially for the colour grading of tomato products such as tomato juices, tomato pulp, tomato ketchup, tomato paste, chilli sauce, and tomato sauce. It consists of an arrangement of two spinning disks mounted directly beneath a colour-corrected light source with controlled viewing conditions. These disks are held together with a suitable binding post at the center and spun at a speed great enough to eliminate flicker, the colour seen by the eye is the sum of the different segments exposed.

The requirement of colour for grade A tomato pulp, according to the USDA, is that shall be "equal or better than that produced by spinning a combination of the following Munsell disks: R65% glossy finish,Y21% finish, glossy; black and grey 14% total or any combination of the two (Black N1 glossy finish and/or Grey N4 mat finish). For minimum Grade C, 53% Red, 28% Yellow, and 19% of the Black and Grey in any combination are used according to the USDA and the FDA.

2.4.2.6 Hunterlab and Colour and Colour Difference Meter

The Hunterlab and Colour Difference Meter is a tristimulus colorimeter that measures colour on three scales by the use of three filters that approximate the X, Y, and Z functions of the Commission Internationale de l'Eclairage (CIE) system. Three values are obtained for each colour measured : Rd (45 degrees-0 degree luminous reflectance) or L (visual lightness on a scale of 0-100; 0, perfect black; 100, perfect white) and parameters a and b which are defined below in Table 2.10.

Table 2.10 *The colour of a and b for Hunterlab and Colour Difference Meter (Gould,1992)*

Parameters	+	***zero***	-
a	red	grey	Green
b	yellow	grey	Blue

Hunter values can be converted to CIE values by the following equations:

$$L = 100(Y^{1/2})$$

$$a = \frac{175(1.02X - Y)}{Y^{1/2}}$$

$$b = \frac{70(Y - 0.847Z)}{Y^{1/2}}$$

The dimensions of colour measurement system in Hunter lab can be shown as Figure 2.4.

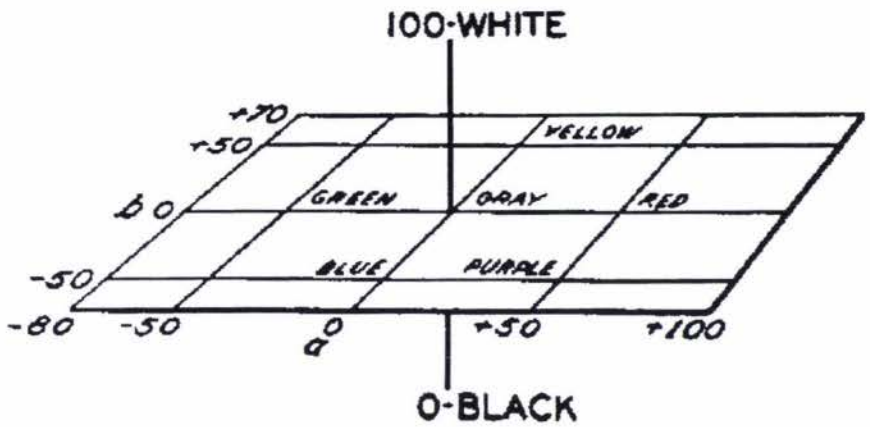

Figure 2.4 *Diagram showing dimensions of the Hunter L, a, and b colour solid (Gould, 1992)*

The Hunter instrument is standardized according to known values as assigned to each standard. The colour of the sample is determined by reading the three tristimulus values from the dials. The reading may be plotted in Munsell Chromaticity Charts as shown in Figure 2.5.

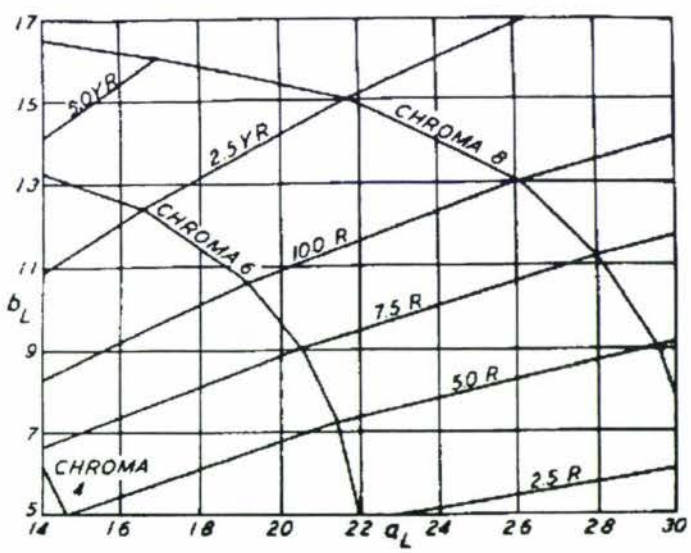

Figure 2.5 *Munsell hue and chroma coordinates in terms of Hunter a_L and b_L (Gould, 1992)*

From Figure 2.5, the hue or chroma values can be determined from Hunter a and b values for any given *L* value.

The samples used in the Hunterlab should be prepared as a homogeneous mass and free from air bubbles. The instrument should be located where the medium is, under subdued illumination, no drafts, and relatively dry air of constant temperature. The procedure of measurement varies with each particular model.

2.4.3 Measurement of consistency/viscosity of tomato paste

The viscosity of tomato product is greatly dependent on the degree of polymerization of pectic substances. Enzymatic depolymerization of pectin in pulp or serum causes a great reduction in the viscosity of the product. Pectolytic enzymes liberated during crushing, act very quickly, thus they should be promptly and thoroughly inactivated (Lopez *et al.*,1998).

Tomato paste is a mixture of liquid, insoluble solids, and coagulated flocs of pectin which generates high solids in the range of 24-30% solids and high viscosity. Gould (1992) suggested the application of penetrometers and potentiometric viscometry to determine the viscosity of tomato paste.

2.4.3.1 Penetrometer

A penetrometer measures the degree of penetration by a selected instrument into the material being tested, as produced by a given force applied over a given area for a measured length of time at a specified temperature. Penetration cones and plunger rods of different weights are furnished with the instrument to cover a wide range of consistencies. A constant penetration time interval must be used in order to obtain accurate and reproducible results. The degree of penetration of is increased in penetration of 6 scale divisions for every 10°C over the temperature range of 0 to 80°C. All samples is required to measure at the same temperature. A temperature of 25°C is a convenient temperature to standardize.

The advantage of the penetrometer to measure the consistency is that it is a convenient and rapid method. A few equipments are required to set up the measurement. However, the penetrometer could be used in the temperature range between 0-80°C only and the samples of the same lot are required to be the same temperature.

2.4.3.2 Potentiometric viscometer

The Potentiometric viscometer is designed to measure consistencies in food products such as tomato purees, ketchups, and pastes. It consists of two rotors, one spiral-shaped and the other shaped in a manner similar to a tuning fork which the spiral-shaped rotor is best suited to measure tomato paste consistency. The rotor consists of a stainless steel tapered wire helix. An action path formed by a given turn of the spiral of continuously is closed by the other turns of the wire. The test medium is submitted to a force tending to pump it up and turns the spiral. The force is from the medium resisting the pumping action which forms the consistency measurements of tomato paste. The calibration curve could be prepared using a standard solution of known viscosity. The Potentiometric viscometer could measure the samples with the total range of viscosity between 300 to 10000 centipoises.

Thakur *et al.*(1996b) determined the viscosity of tomato paste using "Bostwick consistency", although other instruments (e.g. the Brookfield viscometer) are also available. The Bostwick consistometer measures the consistency of a viscous material by determining how far the material flows under its own weight along a sloped surface in a given period of time. It measures the shear stress under the fixed

condition of shear rate whereas efflux viscometers measure shear rates under fixed conditions of shear stress

2.4.4 Measurement of tomato solids of tomato paste

Total solids and water make up the whole composition of tomato. After the water is removed in processing, the products are more concentrated. For this work, methodologies to quantify the levels of tomato solids are necessary.

2.4.4.1 Determination of total solids

The total solids are the better method of indicating tomato quality over time. The official method to determine total solids was mentioned in Gould (1992). It was suggested that the total solids in tomato pulp can be determined in various ways such as drying in vacuum at 70°C, drying at atmospheric pressure at the temperature of boiling water, calculating from the specific gravity of the pulp, or using the index of refraction of the filtrate. The direct refractometer reading is commonly used to determine the amount of concentration. Using the refractometer the scale should be checked periodically by taking the reading of distilled water.

2.4.4.2 Determination of soluble solids

The soluble solids content can be measured as °Brix. The reading from refractometer is not a true sugar reading because it is the value of soluble solids in the tomato. The refractometer measures the refractive index. It measures the angle of refraction of light passing through a substance compared to the refractive angle of light passing through air.

After the reading of soluble solids in tomato is achieved, the number can be correlated to °Brix (The conversion table from refractive index to °Brix is given on p.321 in Gould (1992).

2.5 Effect of break process

After the tomatoes are crushed, the PE and PG enzymes in the cell wall are released. Therefore, the heat processing should immediately be applied to the tomato pulp in order to retain the high viscosity of the tomato puree by a cold break or hot break process (Hayes *et al.*,1998).

The tomatoes are preheated to 60°C for a cold break or 90-95°C for a hot break process and held for 1-2 min (Gould,1992). It was widely agreed that the hot break method produces the better more highly viscous tomato products than the cold break method (Hayes *et al.*,1998).

The advantage of hot break method is that a more viscous product is obtained that does not separate upon standing. A heavier body of tomato is obtained in hot break because heat destroys the pectic enzymes and permits more efficient extraction of pectin. The heat stability of pectic enzymes is of importance during processing. PE enzyme is less stable, when heat is applied, than PG enzymes.

The advantages of cold breaking over hot breaking can be summarized as (Hayes *et al.*,1998).

1. The juice is less likely to foul heat exchangers and evaporators.
2. The juice is easier to pump.
3. Higher final concentrations of tomato paste are possible.
4. The final paste has a more natural colour and a fresher tomato flavour.

In addition, Gould (1992) gave the advantages and disadvantages of cold break. The product has a more natural tomato colour and it has a fresher tomato flavour. In terms of nutrition, the product from the cold break contains more Vitamin C content because less heat treatment is applied to.

Hayes *et al.*(1998) suggested that a hot break process is selected if the final paste is required to have a high viscosity for use in products such as pizza sauce and ketchup, and a cold break process is suited to paste that is intended to be diluted for tomato juice and vegetable cocktails. In addition that Vitamin C losses due to oxidation during crushing and breaking can be partly overcome by deaerating the tomatoes immediately after crushing.

2.5.1 Enzyme activation in broken pulp

When the tomatoes are crushed, the pectolytic enzymes are liberated. They act very quickly to depolymerize pectin which causes a great reduction in the viscosity of product. Therefore, the hot break process has to be applied quickly to retain the pectin substances.

Broeck *et al.*(2000) investigated the effect of pressure and temperature on the activity of tomato pectinesterase (PE) on a kinetic basis. It was illustrated that using high pressure potentially increases the activity and stability of PE. At atmospheric pressure, the highest PE enzyme activity was found at neutral pH and a temperature of 55°C. Increasing the pressure shifted the optimal temperature for enzymatic reaction higher to 60-65°C.

In this study, the mathematical model of the pectin hydrolysis will be required as a function of temperature.

2.5.2 Kinetic of enzyme inactivation

There are two enzymes that must be inactivated during tomato processing, PE and PG because they cause the reduction of viscosity after the tomatoes are broken.

Laratta *et al.*(1995) studied the inactivation of PE in tomato puree induced by heat. The denaturation of PE in these tomato purees were assumed to follow a two-state reversible process which described by sigmoidal thermal denaturation curves using Decimal reduction time (D_T) and Z values. It was found that PE inactivation depends on pH, the higher pH the higher rate of PE inactivation was achieved.

In addition, galacturonic acid is normally present in trace amounts in fresh tomato. It is formed as a result of processing and its absence is a sign of total enzymatic

inactivation undergone by crushed tomatoes before subsequent processing (Porretta, 1991).

Adams (1991) developed mathematical models for enzyme inactivation in real foods. There are three distinct aspects of enzyme inactivation covered. The fundamental aspects of structure, thermodynamics and kinetics on heating, a mathematical model of the heat inactivation of enzymes and the heat stability of enzymes in various foods were considered. He concluded that the kinetics of enzyme inactivation as a function of temperature can be described by Arrhenius law or activated-complex models. Modelling can give reasonable estimations to determine the inactivation rate constants and temperature distribution in the food.

Gould (1992) considered the fastest method of pectic enzyme inactivation is by steam injection. Another method of pectic enzyme inactivation can be achieved by heat treatment in a rotary coil tank (vertical or horizontal), follow by a heat exchanger and holding tube to achieve 104°C. A rotary coil tank procedure has the added advantage that the violent boiling occurring at the designed heat transfer capacity is an excellent means of deaeration. Air removal is important nutritionally because tomato juice containing dissolved air and processed at a high temperature will not retain all the original vitamin C.

In this study, a kinetic model of enzyme inactivation as a function of temperature will be developed and included in the overall break process model.

2.5.3 Ultrasound application

Lopez *et al.*(1998) found that combined use of heat pressure and ultrasound (manothermosonication) could accelerate pectic enzyme inactivation in tomatoes. This technology could result in improved colour and nutrient levels for high viscosity products. An overview of ultrasound technology is given below.

The application of ultrasound for food processing operations relies on the three important properties. They consist of the velocity at which an ultrasonic wave propagates through a material, the extent to which the wave is attenuated, and the acoustic impedance which determines the amount of ultrasound reflected from a boundary between two materials (Gaonkar,1995).

The principles of ultrasound are discussed in the next section as the following.

2.5.3.1 Ultrasound velocity

The ultrasonic velocity is the velocity that an ultrasonic wave travels through a material and is related to its physical properties. There are two methods to calculate the ultrasonic velocity. The first method depends on the physical state of the material and the type of wave;

$$c^2 = \frac{E}{\rho}$$

where c = the ultrasonic velocity
ρ = density of material
E = the appropriate elastic modulus

Table 2.11 *Elastic moduluses for different materials* (Gaonkar, 1995).

Materials	***Elastic modulus***
Liquid and gases	The reciprocal of the adiabatic compressibility.
Solid rods	***Young's modulus*** (where K = the bulk modulus and G is the shear modulus)
Bulk solids	$K + \frac{4G}{3}$ (where K= Bulk modulus, G = Shear modulus)

The second method to determine the ultrasonic velocity is the measurement the wavelength of ultrasound at a known frequency.

$$c = \lambda * f$$

where λ = the wavelength of ultrasound (m.)
f = the frequency of ultrasound
= $1/t$
t = time taken for a pulse of ultrasound

2.5.3.2 Attenuation

As an ultrasonic wave propagates through a material, its amplitude decreases and the wave is attenuated. The major causes of attenuation by a material are adsorption and scattering. The adsorption occurs due to mechanisms which convert some of the energy stored as ultrasound into other forms such as heat, viscous forces, thermal conduction and molecular relaxation. Scattering is important in heterogeneous materials and occurs when an ultrasonic wave encounters a discontinuity and is scattered in directions which are different from that of the incident wave. The attenuation can be defined by measuring the dependence of the amplitude of an ultrasonic wave on distance using the following equation;

$$A = A_o e^{-\alpha x}$$

where				
	A	=	amplitude of wave	(m.)
	A_o	=	initial amplitude of wave	(m.)
	α	=	attenuation coefficient	(dB m^{-1})
	x	=	the traveled distance	(m.)

2.5.3.3 Acoustic Impedance

The acoustic impedance determines the proportion of an ultrasonic wave reflected from a boundary between two materials. When a planar ultrasonic wave is propagated incidental to a planar interface separating two materials of different acoustic impedance, it is partly reflected and partly transmitted. The greater the difference in acoustic impedance between the two materials the greater the fraction of ultrasound reflected. This has important consequences for the design and interpretation of ultrasonic measurement techniques.

2.5.3.4 Applications of ultrasound in food processing

Because an ultrasonic pulse travels back and forth across the measurement cell, a series of echoes is observed on the oscilloscope. The presence or absence of an object between a pair of ultrasonic transducers can be detected by measuring the amplitude of the received signal. If an object is present, the amplitude of the received signal will be reduced. As such, low intensity ultrasound is used for measuring food composition and structure.

To avoid the viscosity problems associated with the catalytic activity of pectic enzymes. Tomatoes are rapidly heated at the hot break temperature (90-95°C) after chopping or crushing to inactivate PE and PG enzymes. However, heat treatments have also a negative impact on colour, flavour, and nutritional value which could be avoided by using other enzyme inactivation procedures with little or no heating (Lopez *et al.*,1998). High intensity ultrasound is one such technique that is commonly used at the laboratory scale.

Lopez *et al.*(1998) investigated the inactivation of tomato pectic enzymes using monothermosonication (MTS), a combined treatment of heat and ultrasound under moderate pressure. PE, PGI and PGII were extracted from ripe tomato fruit and separated by gel filtration chromatography. The PG activity was determined at 40°C for 10-60 min. by measuring the increase in reducing groups of the polygalacturonic acid substrate. The PME activity was assayed by acid-base titration at room temperature, pH 7.0. Ultrasonic irradiation was performed at a pressure of 200 kPa, an ultrasound amplitude of 117 μm and a frequency of 20 kHz. Enzyme inactivation rates were expressed as D values, the time required for the original enzyme activity to decrease by 90%. The inactivation efficiency of MTS was much higher than the simple heating for all enzymes. In addition, the MTS inactivation of the three pectic enzymes followed first-order kinetics which allows the expression of reaction rates in terms of D values. D values for the pectic enzymes heat inactivation at 62.5°C were reduced 52.9-fold by MTS and for PGI at 86°C and PGII at 52.5°C, 85.8-fold and 26.3-fold, respectively.

This indicates that this technology shows potential for tomato processing and it can be applied on a large scale in an economical way. To date industrial scale application of ultrasound is rare.

2.5.4 Kinetics of colour changes

Colour in the tomato is due to carotenoids. Carotenoids are a class of polyene compounds with yellow to red colour. Almost all carotenoids are derived from tetraterpenes. Many types of carotenoids have been isolated and quantified in the tomato fruit and in processed tomato products: lycopene, lycope-5,6 diol, α-carotene, β-carotene, γ-carotene, δ-carotene, lutein, xanthophylls (carotenol), neurosporene, phytoene, and phytofuene. Lycopene is a major carotenoid of tomato and comprises about 83% of the total pigment present (Thakur *et al.*,1996b).

Lycopene degradation in tomato products is the principal cause of colour change during processing. The *trans* form isomerises to the *cis* structure during heating, resulting in changes in colour (Barreiro *et al.*,1997).

Colour loss of tomato juice is accelerated by high temperature and longer storage. It is due to degradation of colour pigments. The main cause of carotenoid degradation in foods is oxidation which is complex and depends upon many factors, such as processing conditions, moisture, temperature, and the presence of pro- or antioxidants and lipids (Thakur *et al.*,1996a).

2.5.4.1 Factors contributing to tomato colour

As discussed above, colour in tomato is a result of the presence of carotenoids. The stability of carotenoids is higher than other animal and plant pigments such as chlorophyll, anthocyan, hemoglobin, and myoglobin. However, the destruction of carotenoids can occur under conditions of low water content in tomato products, heating, the presence of metallic ion (Cu^{2+}, Fe^{3+}, etc.), or the presence of oxygen which can affect the discolouration of tomato products with reducing lycopene. Therefore, the destruction of carotenoid should be prevented (Gould,1992).

Gould (1992) discussed the correlation of carotenoid in the fruit with factors such as size, degree of ripeness, mineral nutrient supply of the product, soil conditions, and variety as follows:

1. Large fruit were only slightly richer in percentage carotene than small fruit.
2. Wide variations in the supply of the nutrient during tomato growing in some cultivars produced only slight variation in the carotene content of the fruit, eventhough the variations in the nutrient supply greatly affected plant growth and fruit fullness.
3. Difference in carotene content were correlated with varietal differences.
4. Ripe fruits produced in the greenhouse, whether in summer or winter, were lower in carotene content than fruit produced outside during the summer.
5. Fruits picked green and ripened in storage were very much lower in carotene than vine-ripened fruit.

2.5.4.2 Effect from lycopene

Lycopene is the most abundant carotenoid in ripe tomatoes, comprising approximately 80 to 90% of the whole pigments present. The amount of lycopene in tomato fruit depends on variety, maturity, and the environmental conditions. Normally, tomatoes contain about 3 to 5 mg lycopene per 100 g of raw material (Shi and Maguer,2000).

Lycopene and other highly unsaturated hydrocarbon based carotenoids (α-carotene, β-carotene, γ-carotene, and ξ-carotene) contain no oxygen and is orange and red in colour (Shi and Maguer,2000).

2.5.4.2.1 Physical properties

In ripe tomato fruits, lycopene takes the form of elongated, needle-like crystals that are responsible for the typical bright-red colour of ripe tomato fruits. Shi and Maguer (2000) sumarised the physical properties of lycopene as Table 2.12.

Table 2.12 *Physical properties of lycopene (Shi and Maguer,2000)*

Properties	***Characteristics***
Molecular formula	$C_{40}H_{56}$
Molecular weight	536.85 Da
Melting point	172-175°C
Crystal form	Long red needles from a mixture of carbon disulfide and ethanol
Powder form	Dark reddish-brown
Solubility	Soluble in choroform, hexane, benzene,carbon disulfide, acetone, petroleum ether Insoluble in water, ethanol, methanol
Sensitivity	Light, oxygen, high temperature, acids

2.5.4.2.2 Chemical structure

The chemical structure of lycopene, a polyene hydrocarbon, an acyclic open-chain unsaturated carotenoid having 13 double bonds, of which 11 are conjugated double bonds arranged in a linear array. Colour and antioxidant activities of lycopene are a consequence of its unique structure, an extended system of conjugated double bonds. The molecular structure of lycopene is illustrated as Figure 2.6.

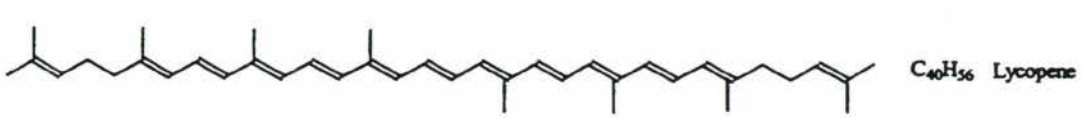

Figure 2.6 *Molecular structure of lycopene in tomato (Shi and Maguer, 2000)*

Lycopene exists in nature in all-*trans* form and seven of these bonds can isomerize from the *trans*-form to the mono or poly-*cis* form under the influence of heat, light, or by chemical reaction.

2.5.4.2.3 Biochemical properties and lycopene oxidation

Lycopene with its acyclic structure, large array of conjugated double bonds, and extreme hydrophobicity exhibits many unique and distinct biological properties. It is an antioxidant. Lycopene quenches highly reactive singlet oxygen ($O_2^{\cdot-}$) and traps peroxyl radicals (ROO.). Lycopene-oxygen radical interactions can be considered as second-order rate reaction. The reduction of lycopene is related to the formation of the superoxide radical anion, $O_2^{\cdot-}$ (Shi and Maguer,2000).

$$\text{L-C} + \text{ROO}^{\cdot} \longrightarrow \text{L-C}^{\cdot} + \text{ROOH}$$

$$\text{L-C} + \text{ROO}^{\cdot} \longrightarrow \text{L-ROO-C}^{\cdot}$$

The all-*trans* isomer of lycopene is the most predominant isomer in fresh tomatoes and is the most thermodynamically stable form. Lycopene can undergo trans-to-cis isomerization during tomato processing and storage.

The oxygen functions are introduced by reactions of two main types:

(1) Substitution of a methyl or methylene group.
(2) Addition to a carbon-carbon double bond.

Sharma and Maguer (1996) studied the kinetics of lycopene degradation in tomato pulp during heating at 100°C and storage at –20, 5 and 25°C with and without exposure to air and light. The results showed that lycopene content in tomato pulp decreased during heating and the kinetics of lycopene degradation followed a pseudo first order reaction at 100°C under different processing conditions. The apparent reaction rate constant for lycopene degradation increased with increase in concentration of lycopene, acids, sugars and overall pulp TS.

2.5.4.2.4 Lycopene isomerization

Natural lycopene from plants exist predominantly in the all *trans* configuration which it is the most thermodynamically stable form. When lycopene is degraded, the transformation of *cis-trans* isomers is readily occurred. *Cis* isomers of lycopene have distinct physical characteristics and chemical behaviors from their all-*trans* counterpart. The observed results of *trans* to *cis* isomerization reaction include decreased colour intensity, lower melting points, smaller extinction coefficients, a shift in the lambda maximum, and the appearance of a new maximum in the ultraviolet spectrum. The decrease in colour intensity is of paramount importance during quantitative analysis of lycopene isomers to avoid underestimation (Shi and Maguer, 2000).

Boskovic (1979) studied *trans-cis* isomerization of all-*trans* lycopene during tomato processing and proposed the reaction pathway scheme, based on known isomer characteristics and constituent reactions, includes lycopene autoxidation/isomerization

relationships. Thermal trans-cis isomerization of carotenoids can take place during cooking, heating, or drying of foods, relative to time-temperature exposure as shown in Figure 2.7.

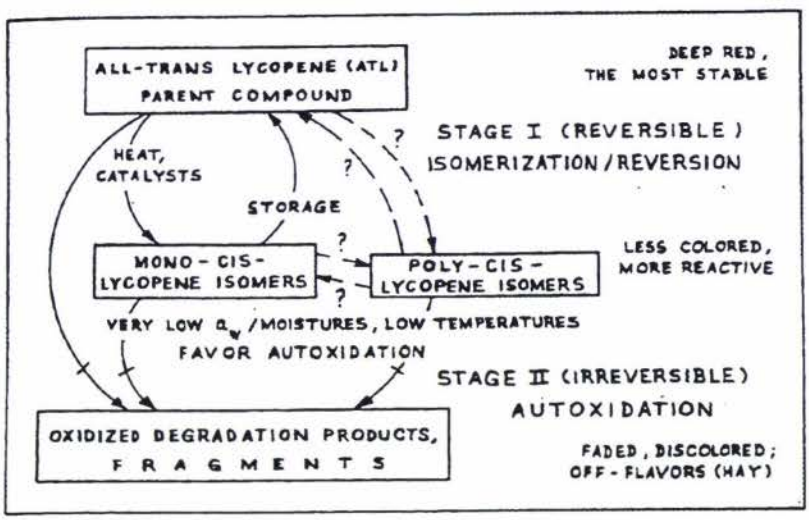

***Figure 2.7** Transformation of cis-trans lycopene degradation pathway during production and storage (Boskovic, 1979)*

Barreiro *et al.*(1997) studied the kinetics of colour degradation in concentrated tomato paste during heating at temperatures between 70 and 100°C. Samples were drawn after the concentration process before thermal processing for hot-filling. The processing plant used a cold-break rupture process. The samples were kept in glass jars under refrigeration (about 4 to 7°C), protected from light with aluminium foil, and properly closed until used for the experiment. The determination of the colour parameters was done using a tristimulus colorimeter (Gardner XL-23) with the scales '*L*', '*a*', '*b*'. The equipment was calibrated against a red tile standard No. CG-6802 GCS-1 with the following colour parameters: '*L*'=28.3; '*a*'=+49.6; '*b*'=+16.4. The parameters '*L*', '*a*' and '*b*' of the sample were read and the values of ΔE, *SI*, '*a*/*b*', and Hue angle were calculated.

$$\Delta E = \sqrt{(L_o - L)^2 + (a_o - a)^2 + (b_o - b)^2}$$

$$SI = \sqrt{a^2 + b^2}$$

$$\text{Hue angle} = tan^{-1}\ b/a$$

where L_o, a_o and b_o denote the colour parameters for the control samples (unheated)
L, a and b denote the colour parameters of the heated samples.

The values of reaction order and activation energy for all colour parameters change reactions were obtained and are shown in Table 2.13.

Table 2.13 *Reaction order and activation energy for the kinetics changes during heating of double concentrated tomato paste* (Barreiro *et al.*,1997)

Colour parameters	***Reaction order***	***Activation Energy (kJ/ mol)***
L (first phase)	1	48.30
L (second phase)	1	24.07
a	1	41.12
b	1	86.10
a/b	1	28.81
ΔE	0	42.84
SI	1	42.42
Hue angle	1	31.79

Porretta and Sandei (1991) studied the effects of ascorbic, malic, galacturonic, citric and glutanic acids to the formation of HMF and degradation of reducing sugars (fructose and glucose) in nonenzymatic browning reaction of tomato juice. The presence of galacturonic acid was found to slow browning reactions. Cold-break products would have a lower HMF formation and consequently less browning. It was concluded that fructose is the most reactive reducing sugar in nonenzymatic browning.

Bontovits (1981) studied the colour changes of tomato processing. Tomato samples were processed on a pilot plant and taken on 3 occasions during 24 hours. They were taken 6 different points of processing line every 30 minutes interval. The 7th sample included a paste stored for 2 months. The *L*, *a*, *b* values of Hunter D25-D3 colorimeter were coincided with the red-yellow ratio indicating the colour or redness of tomatoes expressed as the a/b ratio.

It was found that the rate of average colour deterioration was 0.5 *a/b* ratio therefore an a/b value of raw material at 2.5 should be used if the a/b ratio of tomato paste at 2.0 is needed.

2.5.5 Consistency of tomato paste

Consistency, or gross viscosity, is paramount as a quality attribute in determining the acceptability of tomato products to the consumer and is an integral part of the quality grade standard. The consistency is dependent on a number of factors including cultivar, geographical location, fruit maturity, processing conditions, solid level, viscosity of the serum, and amount and physical characteristics of cell walls as described below (Thakur *et al.*,1996a).

Thakur *et al.*(1996a) described the factors affected the viscosity of tomato products as follows:

2.5.5.1 Cultivar

The cultivar used is the most important factor influencing the consistency of tomato products. Each cultivar has a different chemical composition, and this affects the

consistency. Tomato juices and pastes made from different cultivars under similar processing conditions have different consistencies.

2.5.5.2 Break temperature

Temperature during processing greatly influences the consistency of tomato products as discussed previously. Products processed at higher break temperature exhibit higher viscosity due to greater degree of inactivation of pectolytic enzymes, pectingalacturonase (PG) and pectinmethylesterase (PE). Prolonged heating at high temperature causes denaturation of pectin, leading to reduced consistency. However, high temperature could also lead to high viscosity, due to disruption of cell structure and the consequent increased leaching of pectin from the cell walls. More pectin in the sample will bind more water, leading to high flow resistance.

Porretta *et al.*(1995) investigated the effects of ultra-high hydrostatic pressure treatments on the quality of tomato juice. By the response surface method, it was shown that viscosity was strongly dependent on the pressure, but independent of treatment time. This is presumably also due to enzyme inactivation but by a different mechanism that caused by heat.

2.5.5.3 Role of pectin

Pectins are structural, cell wall polysaccharides found in all higher plants. Fruit tissue is particularly enriched in the pectin substances, with amounts about 7% in tomato fruit. In tomato processing, the pectolytic enzymes are liberated from cell wall during crushing and act very quickly to depolymerise pectin in pulp or serum of tomato product. This causes a great reduction in the viscosity of the product. Therefore, the high heat is applied to inactivate pectolytic enzymes, resulting in high viscosity due to higher retention of pectin. However, the 100% retention of pectic substances is not obtained even under the best commercial conditions.

2.5.5.4 Cell walls

Consistency depends upon the quantity, quality, shape, degree of subdivision, and character of the cell wall present. Cell wall concentration in juice is influenced by maturity of tomatoes, native differences in cell wall thickness, type of pre-heat treatment of fresh fruit, and manner of extracting or comminuting tomatoes to form juice. In addition, homogenization of juice increases linearity of cell walls, thus increasing consistency.

2.5.5.5 Screen size and speed of blades in pulper or finisher

Screen size and blade speed are important factors in controlling the gross viscosity of tomato juice. At any given screen size, higher blade speeds resulted in better consistency of tomato juice and puree. Screen size affects the gross viscosity of tomato juice in two different ways. One is by enhancing viscosity due to exclusion of small particles and the other is by reducing the viscosity due to exclusion of large particles.

2.5.5.6 Electrolytes

Electrolytes influence the viscosity of tomato juice by keeping the cell wall in suspension. Viscosity of tomato juice is kept at a relatively low level by the presence of naturally occurring and added electrolytes. Removal of naturally occurring electrolytes including soluble pectins, organic acids, and mineral salts may cause the remaining fraction of juice to thicken to a semigel. In addition, the addition of NaCl decreases the viscosity of dilute pectic substances because NaCl decreases the charge on the pectin molecule, thus allowing formation of parallel dimers and trimers as well as increases in molecular folds in pectin molecules.

2.5.5.7 Pectin-protein interactions

Tomato juice is a complex mixture of carbohydrates, proteins, pigments, organic acids, and minerals. Interaction between these molecules, especially between pectin and proteins, influences the consistency of tomato juice by forming a reversible electrostatic complex.

The complex formation is pH dependent. The maximum juice viscosity is reached between pH 4.0 and 4.5 due to maximum pectin-protein interaction in this pH range. Prolonged heating during concentration of tomato juice may denature the protein and stabilize its complex with pectin.

2.5.5.8 Fruit solids

Tomato solids are an important quality factor in the tomato-processing industry. They influence the final yield, consistency, and overall quality of the finished product. The high solid in fruits is desirable because making concentrates to a specified solid level with high-solid tomatoes provides greater product yield and also requires less water evaporation reducing the cost.

From the effects on consistency of tomato paste, the break temperature and pectin play important roles in the break process. Figure 2.8 show the relationship between break temperature and pectin retention.

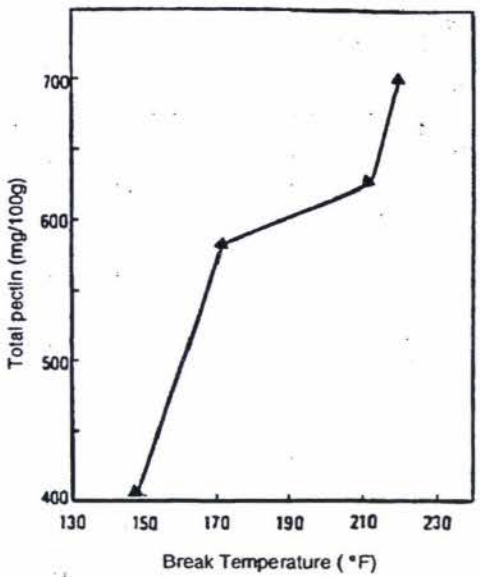

Figure 2.8 *Effect of break temperature on pectin retention of canned tomato paste (Thakur et al.,1996a)*

In tomato processing, when the higher temperature is applied to the hot break to inactivate pectolytic enzymes, resulting in higher viscosity due to higher retention of pectin.

The high consistency can be reached by applying (for enzymatic inactivation) severe heat treatment but this may impair other quality parameters of the finished product (eg.colour, nutrients) (Siviero *et al.*,1996)

2.5.6 Rheological properties of tomato paste

Tomato concentrates are non-Newtonian fluids. The relationship between shear stress (R) and shear rate (γ) for a Newtonian fluid is linear and the gradient of the line is equal to the dynamic viscosity (μ). The equation of motion can be written as;

$$R = \gamma \mu$$

Food liquids, including tomato concentrates, are often non-Newtonian.

The Power Law is one of the most widely application of all rheological models that was fitted to each fluid as;

$$R = K \gamma^n$$

where R = Shear stress
K = Consistency coefficient
γ = Shear rate
n = Flow behavior index

The flow behavior index is used to determine the apparent viscosity of fluids. When n is less than unity, the apparent viscosity decreases with increasing shear rate and such fluids display the property of shear thinning. If n is greater than unity, the fluids are presented the property of shear thickening or dilatant. The apparent viscosity can be obtained as below.

$$\mu_a = K\gamma^{n-1}$$

Figure 2.9 shows the characteristics of flow behaviour of different fluids

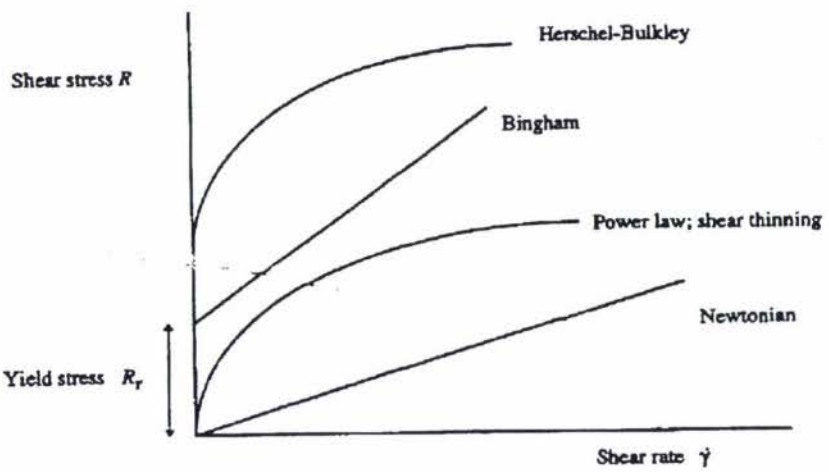

Figure 2.9 *Flow behavior of Newtonian, Power Law, Bingham and Herschel, Bulkley fluids (*Hayes *et al.*,1998)

Xu *et al.*(1986) studied the rheological properties of tomato juice and the paste affected to the breaking process at different temperature, 85, 96 and 107°C using Power Law. The study showed that the tomato juices and pastes are pseudoplastic fluids. The flow index varied between 0.302-0.423 for the paste. The consistency index (K) increased with the increased total solids of the concentrates. The highest viscosity of pastes was highest at the break temperature of 107°C which was apparently related to a highly disrupted cell structure and the high pectin levels achieved by enzyme inactivation.

2.5.6.1 Effect of Shear rate on viscosity

Tanglertpaibul and Rao (1987a) proposed the apparent viscosity at a shear rate of 100 s^{-1} (μ_{100}) as a suitable rheological characteristic for tomato concentrates. Tanglertpaibul and Rao (1987b) obtained the apparent viscosity of the concentrates (μ_{100}) and found that it was related to the viscosity of serum (μ_{serum}) and pulp content by the expression as;

$$\mu_{100} = \mu_{serum} + A * P^B$$

The viscosity of serum can be expressed to depend on the dissolved pectin content. The sugar content (°Brix) did not play an important part on viscosity of the serum.

$$\mu_{serum} = C + D\,p^{E}$$

where p = pectin content (% wt. of serum)
P = pulp content
A = 1.32 = the coefficient of the contribution to viscosity of a unit amount of pulp (Hayes *et al.*,1998).
B = 1.485 = the influence of pulp content on viscosity of concentrates from different tomato cultivars and/or processses (Hayes *et al.*,1998).
C = 0.00492
D = 0.0153
E = 1.483

2.5.6.2 Prediction of viscosity for changing temperature

Hayes *et al.*(1998) confirmed that the consistency index and the flow behavior index to vary with temperature and suggested the following relationships.

$$K = K_0\, a^{1000/T}$$

$$n = n_o + 1000*b/T$$

where K_o, a, n_o, and b = material specific constants
T = absolute temperature (K)

Tanglertpaibul and Rao (1987b) also proposed the Arrhenius relationship with the values of the activation energy ranging from 8.4 to 12.6 kJ/mol can describe the effect of temperature on μ_{100}.

$$\mu_{100} = \mu_\infty \exp(E_a/RT)$$

The apparent viscosity was found to depend on the total solids concentration of tomato concentrates raised to a power in the range of 2.0 to 2.5.

2.6 Conclusion

In tomato processing, the high viscosity of tomato paste is an expected result. This literature review shows that paste viscosity is affected by total solids content and the extent of pectin hydrolysis during tomato processing. PG enzymes are released when tomatoes are crushed, this results in pectin in cell wall and locular gel being hydrolysed to D-galacturonic acid which causes the decreasing of paste viscosity. Therefore, the critical processing step that affects pectin hydrolysis is the break process which pectin hydrolysis and enzyme inactivation are the main reactions.

It is clear from the literature that pectin levels vary with ripeness whereas the levels of PG enzymes may vary with fruit ripeness. Time and temperature history in the break process can be controlled to account for changes in these variables to produce paste of consistant viscosity. However, colour and nutrient losses also occur at high

temperature, therefore these factors should also be considered when the process is optimised.

A mathematical model will be a useful tool in process optimisation and require quantification of the kinetics of pectin hydrolysis and enzyme inactivation as a function of temperature and methods of characterising fruits composition (enzyme levels, pectin levels) variability due to fruit at different ripeness.

Chapter 3
Characterisation of tomato solids

3.1 Introduction

Tomato paste is prepared from a series of operations including maceration, blending, sieving, and heating. In order to control the paste production process, the quality of the paste must be measured. The tomato paste can be characterised in terms of compositional and functional properties. One of the most important measures is tomato solids. Tomato solids is often used to predict overall finished product quality. Variation of tomato solids can be caused by differences in the variety, maturity, area of production, climatic conditions, and practices undertaken during production of the tomato fruit used (Gould,1992).

In this chapter, tomato fruit are characterised in terms of total solids, soluble solids, °Brix, water insoluble solids, and pectin quantity. These methods were then used to quantify the effect of the variations in the feed conditions to commercial tomato paste production.

The specific goals of this chapter were to;

- Develop a method to characterise tomato fruit ripeness.
- Outline experimental methodologies to characterise tomato fruit;
  - Brix levels
  - Total solids levels
  - Insoluble solids level
  - Pectin levels
- Use these methods to characterise how these levels vary with respect to fruit ripeness.

3.2 Tomato ripeness

The ripeness of tomatoes involves dramatic changes in colour, texture, aroma, flavour, and composition. The texture of a particular tomato fruit depends on the cell turgor, cell shape and size, the chemical composition of cell wall and middle lamella, and all the whole polymer constituents of the cell wall. The plant cell wall is a very complex structure as discussed in the literature review (Chapter 2). The tomato is ripen from the central to the outside. The changes in the composition and solubility of polysaccharides in the cell wall also play a major role in ripening. The activity of PG enzymes in pericarp and locular gel in the tomatoes is increased dramatically during ripening. They degrade pectins in the cell wall and cause softening when the tomatoes are ripen. Pressey (1986) stated that ripe red tomatoes have 600 times more PG activity than green tomatoes. This suggests that the degree of ripeness in the fruit entering the production process will effect the ultimate quality of the tomato paste. It also follows that the level of intact pectin or insoluble solids could be significantly higher in green fruit the in ripe tomatoes.

To investigate the differences in tomato compositions as a function of ripeness. Some measurements of the fruit must be developed. Tomatoes can be classified on the basis of colour, into five ripeness as shown in Figure 3.1 and Table 3.1 (Barrett *et al.*,1998).

Table 3.1 *USDA tomatoes classes (Barrett et al.,1998)*

Class	*Description*
Green	Fruit surface completely green, varying from light to dark green.
Breaker	First appearance of external change in colour; pink, red, or tannish yellow colour on not more than 10% of fruit surface.
Turning	Over 10% but not more than 30% fruit surface is red, pink, or tannish yellow.
Orange	Over 60% surface shows orange, but not more than 90%.
Dark red	Over 90% dark red.

GREEN

BREAKER

TURNING

ORANGE

DARK RED

Figure 3.1 *Five different ripeness of the tomato fruits*

In this work tomatoes were categorised into these broad groupings.

3.3 Tomato fruit supply

To carry out experimental work throughout the year, it was necessary to grow tomato fruit out of season in a green house environment. Commercially available Ferry Morse processing variety tomatoes were grown in the Plant Growth Unit at Massey University, Palmerston North over the spring 2000 - summer 2001 months. No pesticide was applied to the fruit to ensure there was no effect on enzymatic levels in the fruit. In the normal tomato season (March-April 2001), fruit of the same variety were sourced from Heinz-Watties, Hastings tomato paste production feed stock.

3.4 Tomato pulp preparation

Before the tomatoes are characterised the levels of °Brix, insoluble solids, total solids, and pectin levels, the pulp preparation is required and shown as below;

3.4.1 Fresh tomato pulp preparation

A new batch of fresh tomato pulp was prepared in the laboratory before the analysis using Ferry Morse tomatoes.

- The harvesting was performed before starting the analysis and kept in a refrigerator at 4°C.
- About three tomato fruits at 5 different levels of ripeness (Green, Breaker, Turning, Orange, Dark red) were chopped in to quarters and any rotten parts were discarded.
- The fruit was blended in a Sunbeam food processor (Model LC-AX, 272) for 2 minutes at 22°C.
- The tomato puree was then put through a laboratory finisher (0.51mm mesh) to separate the seeds and skin. The thin tomato pulp passed through the screener was immediately placed into an ice bin, ready for subsequent analysis.

3.4.2 Microwave-heated tomato pulp

Three fruits of the Ferry Morse tomatoes at 5 levels of different ripeness were washed and dried.

- The PG enzymes were inactivated in the tomatoes by heating the fruits under high level power of a National microwave (The Genius model) for 2-3 min until the centre temperature of each fruit reached 85-90°C.
- The heated tomatoes were chopped, blended by a Sunbeam food processor (Model LC-AX, 272), and screened using a laboratory finisher (0.51 mm mesh).
- The thin tomato pulp was then used to determine total solids, insoluble solids, and soluble solids.

The screener could conceivably have an effect on the viscosity of prepared tomato pulp and therefore choice of screen size could be important when attempting to characterise tomato fruit composition. Robinson *et al.*(1956) studied factors influencing the degree of settling in tomato juice. It was found that the degree of settling in tomato juice was not related to the particle size of tomato pulp. Therefore, the mesh of screener used in this work is not likely to be an influence on the settling of prepared tomato pulp.

3.5 Total solids measurement

Total solids (TS) comprise all the solid components of the tomato and are determined by calculating the ratio of total solids to tomato product weight after removing the water by drying in a vacuum oven (Barrett *et al.*,1998). Total solids measurement is the prefered method to indicate tomato quality, although the technique is not fast enough for production line operations (Gould,1992). There are several literature reports which have examined total solids in the tomatoes as following.

Luh and Daoud (1971) investigated total solids of tomato pulp in order to study the effect of break temperature (60-115°C) and holding time on pectin and pectic enzymes in the tomato pulp. Diatomaceous earth (3.0000g) was dried in an aluminum dish at 110°C for 1 hour. The dishes were cooled in a desiccator for 30 min, and weighed with a Mettler analytical balance. 12.0000 g of tomato pulp was weighed accurately and put into the aluminum dish and mixed with the diatomaceous earth. The aluminum dish was then placed on a steam bath until the contents became almost dry and then further dried in a vacuum oven for 2 hours at 70°C and 29in Hg. The dish was then cooled in a desiccator for 30 min, weighed, and the percent of total solids was then calculated. It was found that the total solids of canned tomato pulp ranged from 4.3 to 4.5% at the hot break temperature, 60 to115°C respectively. The variation of total solids between the samples was explained by the amount of steam incorporated into the product from steam injection process.

Sherkat and Luh (1976) characterised the quality of tomato paste made at different break temperatures. The tomato paste was prepared on the commercial scale, canned and stored at 20°C. Tomato paste total solids was determined using the AOAC (1975) vacuum oven method with some modifications. Diatomaceous earth (0.5g) was dried in an aluminum weighing dish for 30 min at 110°C in a convection oven. The weighing dishes were cooled in a desiccator for 30 min and weighed on a Mettler Analytical Balance. About 12.000 g of the fresh tomato pulp or 5.000 g of the tomato paste was weighed accurately into an aluminum weighing dish. The samples were mixed with the diatomaceous earth and placed on a steam bath until the mixture became almost dry. Drying was completed in a vacuum oven after 2 hours at 70°C under pressure of 50 Torr. The dried samples were allowed to cool in a desiccator for 30 min and then weighed. The percent of total solids in the tomato products was calculated. It was found that the tomatoes in this study contained 5.5% total solids.

Chin *et al.* (1985) developed a method for the determination of total solids in processed tomato products using a microwave oven. The results compared well with the official AOAC method, vacuum oven procedure. The AOAC method requires 2 hours drying in a vacuum oven with repeated weighing of drying dishes and samples. Alternative means of determination total solids until now have been unreliable, particularly total solids with

a high content of carbohydrates. The advantages of microwave oven drying are short drying time and a minimum of sample handling.

Sharma *et al.* (1996) studied the effect of composition on the rheological properties of tomato thin pulp for six different cultivars. Total solids in thin pulp fraction was determined by a simple gravimetric method. About 3±0.05 g of samples were dried on aluminum dishes in a vacuum oven at 75°C for 24 hr in duplicate. The dishes were kept in a desiccator for 1 hr before recording their final weights. Total solids were estimated by calculating the difference in weight before and after oven drying. It was reported that total solids of six cultivars are different and ranged from 4.66 to 7.66%.

The AOAC Official method (2000) suggests the use of a microwave oven drying method be used for determining total solids in the tomatoes. A CEM microwave (Drying moisture solids analyser Model AVC-MP) is calibrated prior to use by analyzing laboratory samples of known solids content. Two dried pads are placed on the balance and the balance is tared. 2g of tomato sample is placed on rough side of a fiberglass pad. A spatula is then used to spread the test sample evenly over the entire pad. A second dried pad is placed on top of sample. This process must be completed rapidly to minimize evaporation. The pads are then inverted, placed on the balance ring, and the samples covered. A four minute drying cycle is then carried out and the weight change used to quantify the total solids content.

The method used in this study was applied from the literature cited above with a few modifications as below;

- The aluminum dishes and lids were dried for 1 hr at 75°C, in a vacuum oven (Townson & Mercer Ltd.,England) and cooled down in a desiccator for 1 hr.

- The dishes and lids were weighed with a Mettler analytical balance (AE 200).

- About 3.00 g of fresh or microwave-heated tomato pulp at 5 different ripeness was weighed accurately into the aluminum dishes. Samples were measured in triplicate for each ripeness.

- The aluminum dishes were placed in the vacuum oven for 48 hr at 75°C. The dishes were then cooled and kept in a desiccator for 1 hr before being weighed. The percentage of total solids in the tomato pulp was then calculated.

$$\% \text{ Total solids} = \frac{\text{Pulp weight after drying}}{\text{Pulp weight before drying}} \times 100$$

3.6 Soluble solids measurement

The total solids consists of 80 to 90% of water soluble solids. Soluble solids (SS) include sugars, organic acids, amino acids, soluble pectin, and mineral salts. Soluble solids can be determined in the same way as total solids by vacuum drying. The tomato serum is separated by centrifuging and filtering from the insoluble material. In tomato production, natural tomato soluble solids or the °Brix value of the tomato serum is used as a useful index of concentration and an indication of consistency (Barrett *et al.*,1998). The measurement of soluble solids is commonly carried out using a refractometer. The method of soluble solids determination has been performed by many researches some of which are summarised as below.

Luh and Daoud (1971) studied the effect of break temperature (60-115°C) and holding time in pectin and pectic enzymes in the canned tomato pulp. Soluble solids were determined to investigate the effects. A Zeiss-Opton refractometer was used to examine the level of soluble solids in the tomato serum at 20°C. It was reported that the higher the break temperature, the lower the soluble solids. The soluble solids content at 20°C and 115°C were 4.7% and 4.1%, respectively.

Becker *et al.*(1972) studied the effects of acidification on cell walls and cell breakage on the consistency of tomato products. The determination of soluble solids was carried out at 25°C using a refractometer equipped with °Brix scale.

Sherkat and Luh (1976) characterised the quality factors of tomato paste made at different break temperatures. As part of this study, soluble solids were measured using a Zeiss-Opton refractometer. Results were expressed as degrees Brix at 20°C. The soluble solids of tomato paste was reported to be 5°Brix at 20°C.

In this study, after the tomato pulp was prepared, soluble solids of tomato pulp can be determined as follows;

- About 20 g of fresh or microwave-heated tomato pulp at 5 different ripeness was added to a centrifuging tube and centrifuged (BHG Hermle Z320) at 4000 rpm for 20 min.

- The tomato serum was then taken to determine the level of soluble solids by a refractometer (RFM 330, Bellingham+Stanley Ltd.) at 30°C. The result was expressed as °Brix.

3.7 Insoluble solids measurement

Insoluble solids (IS) of tomato pulp can be determined using the vacuum drying oven technique after first washing and centrifuging the pulp to discard supernatant. Most of the literature reports summarised below determined insoluble solids in the tomato paste from the difference in total and soluble solids levels.

Marsh *et al.* (1980) measured the insoluble solids to study the effect of composition upon Bostwick consistency of tomato concentrate. Water-insoluble solids (WIS) were calculated using the following equation.

$$WIS = \frac{(\text{Total solids-Soluble solids}) \times 100}{100 - \text{Soluble solids}}$$

This calculated value is used to determine the ratio of WIS/TS which is usually expressed as a percentage.

Sharma *et al.* (1996) investigated the effect of composition on the rheological properties of tomato thin pulp for six different cultivars. Insoluble solids was determined by the oven drying method. The pulp was separated from the serum fraction by centrifuging tomato thin pulps at 12500 x g for 10 min. The insoluble fraction was washed by resuspending in distilled water, followed by re-centrifugation under the same conditions. The initial weight of tomato thin pulp before centrifugation, and final weight of water-insoluble solids after centrifugation was recorded. The insoluble solids were oven dried at 70°C to determine the dry matter content. It was reported that the water-insoluble solids of the six different cultivars ranged from 0.67 to1.39 %.

Barrett *et al.* (1998) suggested that water-insoluble solids (WIS) content represents the higher cell wall molecular weight and middle lamella components that are important to determine the consistency.

In this study, the determination of insoluble solids was performed by the drying vacuum oven technique as follows;

- About 3.00 g of fresh and microwave-heated tomato pulp at 5 different ripeness were weighed.
- 20 ml of distilled water was added to resuspend the sample. The sample was centrifuged (Sorvall RC5C, Dupont Co., Ltd.) at 12000 rpm at 4°C for 15 min.
- The supernatant was discarded. The insoluble fraction was resuspended in 30 ml distilled water, and recentrifuged at 12,000 rpm for 15 min at 4°C.
- The supernatant was discarded again. The pellet left in the tube was washed out by a small amount of water, and then the pellet was placed into an aluminium dish.
- The dishes were dried in a vacuum oven at 75°C for 48 hr.
- The percentage of insoluble solids in the pulp was determined as the fraction of final dried pellet weight to the original pulp sample weight.

3.8 Pectin measurement

Soluble pectin, insoluble pectin and protopectin significantly contribute to the consistency of tomato juice and play a role to cement the cells together in the form of insoluble compounds. As the tomatoes ripen, more protopectin is changed to pectin which still holds the cells in place but less rigidly so the fruit is no longer hard. The transformation of the pectinous meterials within the tomatoes is brought about by the action of PG and PE enzymes (Barrett *et al.*,1998). The rapid inactivation of pectic enzymes is essential to prevent the losses in viscosity of tomato paste (Foda and McCollum,1970).

The effect of break temperature on the consistency of the canned pastes has been well studied. Researchers stated that an efficient hot break process should be applied to have better retention of consistency and pectin which are in both tomato pulp and tomato serum (Luh and Daoud, 1971, Sherkat and Luh, 1976, Lopez *et al.*,1997, Lopez *et al.*, 1998, Trifiro *et al.*,1998).

Many literatures have determined the level of pectin in the tomatoes. A summary is shown as follows:

Robinson *et al.* (1956) determined the factors influencing the degree of settling in tomato juice when the processing conditions were varied. Viscosity, crude fiber, pectin content, and particle size are the key parameters observed. Pectin content was calculated as calcium pectate. The pectin fractions were prepared for precipitation of calcium pectate as serum pectin, water-soluble pectin on the suspended particles, low methoxyl pectin on the particles, and the protopectin on the particles. The results showed that the distribution of pectin between the serum and particles depends upon the conditions of processing. At low preheating temperature and low speeds of finisher, there is more pectin in the particles than in the serum. At high preheating temperature and high speeds of the finisher, pectin is retained in the serum more than in the particles. In general, when the serum pectin is high, the pectin associated with the suspended particles is also high. In addition, it was assumed that the serum viscosity is proportional to its pectin content.

Sherkat and Luh (1976) reported the quality factors of canned and frozen tomato pastes made at several break temperatures. Pectin, is responsible for the firm texture of fresh fruit and high viscosity in the finished products and was investigated by the versenepectinase carbazole method (McCready and MaComb,1952). Each fraction of pectin was regarded to have unique solubility characteristics. The high-methoxyl pectins are water-soluble. Protopectin was found to be acid soluble and alkali or oxalate dissolves low-methoxyl pectins and pectates. The results were expressed as mg of pectin per 100g sample. It was reported that enzymatic breakdown and thermal degradation of pectin occurred during maceration and also heat processing. The pectin retention decreased as the break temperature decreased. This phenomenon may be explained by the rapid inactivation of polygalacturonase (PG) and pectinesterase (PE) enzymes. Frozen paste contained more total pectin than the canned product made at the same break temperature but pectin levels of both pastes were increased as the break temperature was raised.

Sharma *et al.* (1996) studied the effect of composition obtained from six different cultivars on the rheological and flow behaviour properties of tomato thin pulps. Pectin content, insoluble solids, and total solids were determined. The tomato thin pulp were homogenized and diluted about 100 times for pectin analysis using a modified m-hydroxydiphenyl-sulphuric acid method. The diluted samples (0.5ml) were poured into test tubes placed in an ice-cooled water bath. 4 ml of H_2SO_4/tetraborate was added to 0.5 ml of diluted thin pulp samples in each test tube and mixed carefully on a vortex mixer before heating in a water bath at 100°C for 5 min. The samples were immediately cooled down to room temperature by immersing in an ice bath. 0.1 ml aliquot of 0.15% m-hydroxydiphenyl in 0.5% sodium hydroxide was added to each sample to initiate the reaction. The red colour produced by other carbohydrates present in tomato thin sample during heating was accounted for by running a blank for each individual sample and by replacing the m-hydroxydiphenyl solution with 0.1ml of 0.5%sodium hydroxide. A reagent blank was also prepared by using 0.1 ml of distilled water to zero the instrument. The pink colour of the reactants increased in the first 5 min interval and thereafter decreased to level off after about 30 min at an absorbance reading of 520 nm. The pectin was estimated quantitatively using a standard curve of galacturonic acid (50-200 μg/ml). The kinetics of pectin analysis can be shown as Figure 3.2.

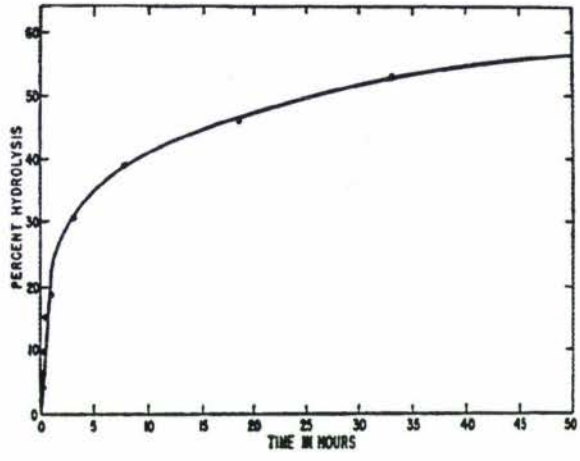

***Figure 3.2** Kinetics of changes in absorbance during pectin analysis when using m-hydroxydiphenyl as a reagent (Sharma et al., 1996)*

The advantage of the Sharma *et al.*(1996) galacturonic acid determination is less interfered by neutral sugars. This method is based on the colour formation which accompanies the addition of m-hydroxydiphenyl to heated solutions of uronic acids in sulfuric acid.

In this study, the method chosen for measuring the rate of pectin hydrolysis was modified from Sharma *et al.*(1996). The procedure is shown as follows;

- 10.00 g of fresh and microwave-heated tomato pulp at 5 different ripeness was pipetted into a centrifuged tube.
- 25 ml of 95% ethanol was added. The mixture was stirred well, left in an ice bin for 30 min, and then centrifuged (Sorvall RC5C, Dupont Co., Ltd.) at 12000 rpm for 15 min at 4°C.
- The supernatant liquid was decanted. The residue was washed again with 25 ml of 95% ethanol and rechilled in the ice bin for 30 min before it was recentrifuged at 12,000 rpm for 15 min at 4°C.
- The supernatant was discarded. The residue was dissolved in a 1 L volumetric flask and made up to the volume to be 1L with distilled water.
- 0.6 ml of each sample was pipetted in the tubes to perform the pectin assay in triplicate. 3.6ml of H_2SO_4/Tetraborate was added and mixed for pectin hydrolysis.
- The tubes were then heated in a water bath at 100°C for 5 min and immersed in the ice bin to cool the samples to room temperature.
- 60 µl of m-hydroxydiphenyl reagent was added and then the samples were left for 30 min to allow the reaction to reach completion.
- A blank of each individual sample was prepared by replacing the tomato pulp with distilled water.
- A UV/visible spectrophotometer (Ultrospec 2000) was used to follow the changes of D-galacturonic acid concentration by measuring absorbance at 520 nm.

3.9 Total solids, insoluble solids, soluble solids and pectin as a function of tomato ripeness

Generally, it is expected that changes in total solids, insoluble solids, soluble solids, and pectins occur when the tomatoes develop from the green to red tomatoes. There are a number of references which discuss these changes as outlined below.

3.9.1 Total solids and insoluble solids as a function of ripeness

Total solids represent the solid components in which the water is removed by drying in a vacuum oven. Water-insoluble solids represent the cell wall and middle lamella components which are not soluble in the water. Generally, there are two methods of the water-insoluble solids determination. Firstly, water-insoluble solids is determined by subtracting the percentage of water-insoluble solids from the percent total solids as mentioned above. The water-insoluble solids is also determined by filtering the samples, washing to remove water-soluble compounds, drying, and weighing the insoluble residue. These two methods should show good agreement but the former method is much faster and easier. Moreover, alcohol-insoluble solids is also a good indication of maturity and texture in some horticultural products. The tomatoes are blended in 80% alcohol, filtered on a vacuum filter, washed with additional 80% alcohol, dried, and the residue weighed. Alcohol-insoluble solids of the tomato pulp contain protein (8%), pectic substances (7%), hemicellulose (4%), and cellulose (6%) dry matter (Davies and Hobson,1981).

Davies and Hobson (1981) described the changes during ripeness by the ratio of the percentage of water-insoluble solids in the total solids. This ratio shows the varietal changes of tomatoes. Water-insoluble solids markedly affect consistency. The higher the ratio, the greater the consistency at any given total solids or soluble solids. Figure 3.3 shows the changes of tomato firmness or ripeness. When the firmness increased, the WIS/TS also increased. This means that the ratio in the green tomatoes is greater than the ratio of the red tomatoes.

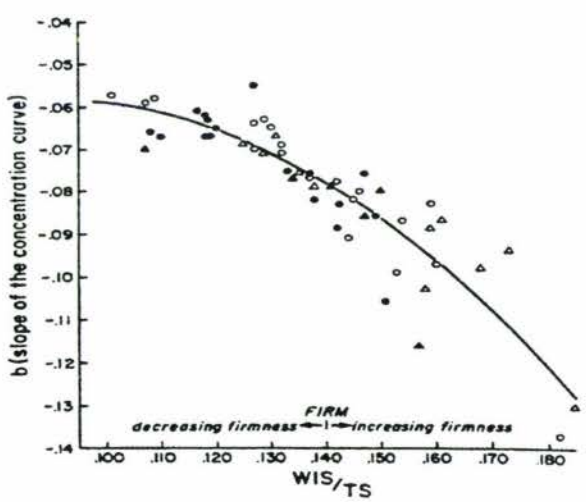

Figure 3.3 *Relationship between slope of concentration curve and WIS/TS ratio (Davies and Hobson,1981)*

3.9.2 Soluble solids as a function of ripeness

The sugar content of the fruits increase when they ripen. Sucrose is the dominant sugar and only small amounts of other reducing sugars are present. Many investigators have studied the changes in sugar content of tomatoes during ripening.

Davies and Hobson (1981) studied the changes in sugar content occurring during ripening. It was concluded that the total sugar content increased as the fruit turned from the green to the red stage of ripeness as shown in Table 3.2.

Table 3.2 *Changes in sugar content of various parts of tomato fruit harvested at five stages of ripeness, expressed as percent fresh weight (Davies and Hobson, 1981)*

Stage of ripeness	*Whole fruit*	*Locular contents*	*Walls*
Green	2.69	2.15	2.87
Green-yellow	3.07	2.58	3.13
Yellow-orange	3.16	2.74	3.28
Orange	3.23	2.72	3.22
Red	3.27	2.79	3.55

3.9.3 Pectin as a function of ripeness

Pectins in the tomatoes are changed during ripening. Huber and Lee (1986) investigated the chemistry and function of pectins. The analysis of total pectins in ethanol powder revealed a trend of increasing pectin in both gel and pericarp when the stages of ripeness change. Table 3.3 shows the amount of total and soluble pectins in pericarp and gel at different stages of ripeness.

Table 3.3 *Total and soluble (acetate-EDTA buffer) pectins in ethanol powder from tomato pericarp and gel (Huber and Lee, 1986)*

Stages of development	*Pericarp*		*Gel*	
	Total pectins μg/mg powder (μg/mg fresh weight)	*Soluble pectins μg/mg powder*	*Total pectins μg/mg powder (μg/mg fresh weight)*	*Soluble pectins μg/mg powder*
Immature green	258.7 (6.9)	61.4	143.8 (2.7)	94.4
Mature green	298.1 (6.9)	91.9	168.2 (1.8)	145.6
Turning	310.9 (5.7)	105.7	196.4 (1.7)	117
Pink	328.4 (5.6)	192.2	188.5 (1.8)	122.8
Ripe	334.6 (6.1)	201.3	211.1 (2.2)	164.9

It is shown that total and soluble pectins in pericarp are higher than in gel at all stages of development. When the tomatoes turn from green to red, the amount of pectin increases. Therefore, it can be expected that the quantity of soluble pectin in this study should increase with ripeness.

Luh and Daoud (1971) and Sherkat and Luh (1976) determined the pectin concentration of tomato puree at the stage of canning ripeness was 1.0 mg/g puree at 60°C and 3 to 4 mg/g puree, respectively.

3.10 Results and discussion

It is known from literature that the viscosity of tomato paste is ultimately dependent on the fraction of solids that are insoluble solids in water after processing. The amount of insoluble solids could be affected by PG enzyme activity in the break process or variation of the level of insoluble solids in the raw material due to using fruit at different stages of ripeness. Each point in Figure 3.4, 3.5, 3.6, and 3.8 represents a pulp sample from a particular tomato ripeness. For each ripeness at least two different tomato fruit were analysed to demonstrate the variability of insoluble solids, total solids, pectin, and °Brix levels between fruit with the same colour. Error bars are included with each point to indicate the variability in the measurement method and were determined by triplicate analysis of each pulp sample. The raw data is included in Appendix 1. Figure 3.4 shows the variation in the ratio of insoluble solids/ fresh tomato pulp at different ripeness.

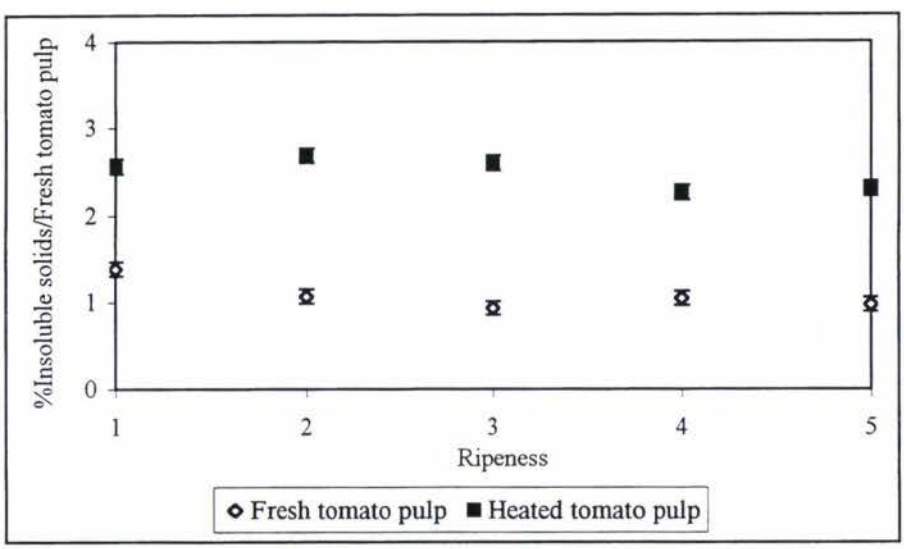

Figure 3.4 *Comparison of % insoluble solids/tomato pulp between the fresh and heated pulp as a function of ripeness (1=Green, 2=Breaker, 3=Turning, 4=Orange, 5=Dark red)*

The fresh (unheated) pulp is consistently lower in insoluble content than microwave-heated pulp from Figure 3.4. This is due to PG enzymes in the fruit being released upon crushing and the subsequent hydrolysis of pectic substances in the fruit during pulp preparation. By heating the intact fruit in a microwave, these enzymes are inactivated prior to pulping to avoid this problem. Therefore, it is necessary for fruit to be treated by heat prior to pulping to get true fruit insoluble solids measurements.

Variability exists between fruit samples insoluble solids level in the range 2-3% in the microwave-heated pulp samples. After allowing for this variation there is no clear trend with respect to ripeness. Some of this variation could be due to differences in pulp moisture content. The measurement of total solids content for the same pulp samples was made to investigate the effect of variation in water content of the fruit. This would allow the more useful comparison of the fraction of total solids in fresh tomato pulp which is insoluble solids in water as a function of ripeness. The total solids levels in the fruit are shown in Figure 3.5.

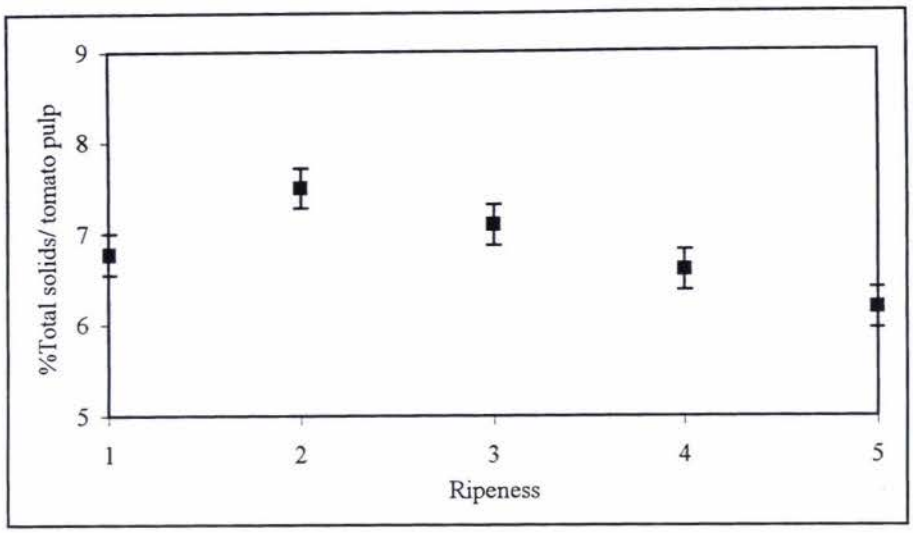

Figure 3.5 *Plot of % total solids/tomato pulp of the heated pulp as a function of ripeness (1=Green, 2=Breaker, 3=Turning, 4=Orange, 5=Dark red)*

The heated pulp sample in Figure 3.5 shows that the total solids content at different ripeness as in the range of 6-8%. There is no clear trend in these results with respect to ripeness. The level of insoluble solids in total solids was then investigated by combining these two measurements. The ratio IS/TS is determined and shown in Figure 3.6.

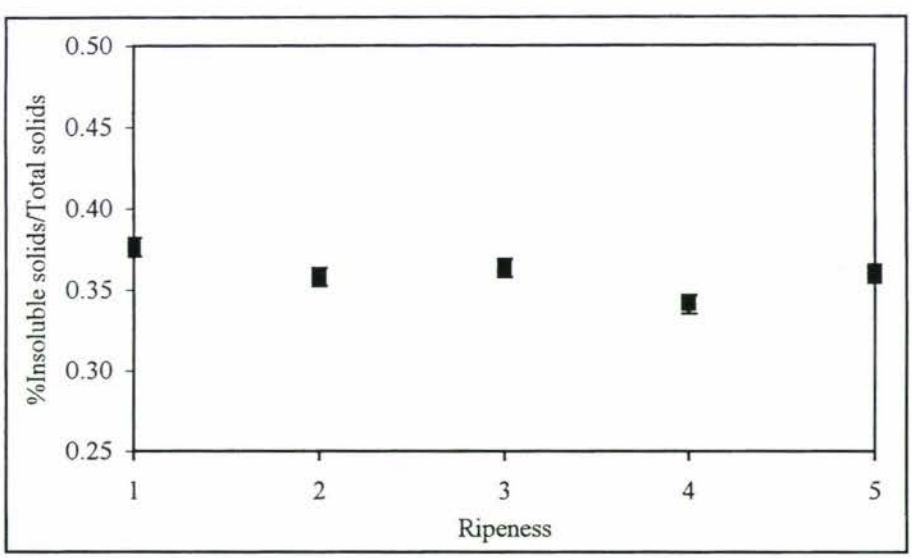

Figure 3.6 *Plot of % insoluble solids/total solids of the heated pulp as a function of ripeness (1=Green, 2=Breaker, 3=Turning, 4=Orange, 5=Dark red)*

Figure 3.6 shows that variation between fruit cannot be explained on the basis of colour. The level of insoluble solids in total solids is between 0.3 to 0.45%. There is no clear trend with respect to ripeness. Therefore, in the model development for the break process, the insoluble solids levels in the feed fruit should be treated as being independent of ripeness.

The levels of pectin in fresh and microwave-heated pulp was also determined to show pectin levels and insoluble solids are correlated. Figure 3.7 shows the differences in pectin level when the pulp is freshly made or heated in the microwave prior to pulping.

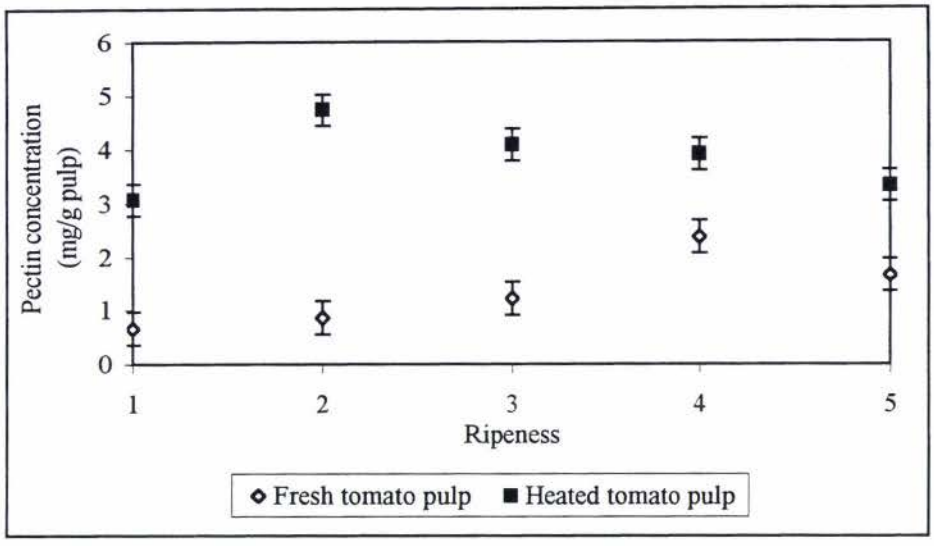

Figure 3.7 *Comparison of pectin concentration between the fresh and heated pulp as a function of ripeness (1=Green, 2=Breaker, 3=Turning, 4=Orange, 5=Dark red)*

It is clear in figure 3.7 that pectin in fresh pulp is lower than heated pulp. This is due to hydrolysis of pectin by PG enzymes. PG enzymes are destroyed by heat in the microwave-heated pulp which results in the level of pectin being higher in each pulp sample. This confirms the hypothesis given above to explain differences in insoluble solids levels between microwave treated and fresh pulp samples.

When the level of pectin from microwave-heated pulp is compared with the level of pectin from literature as shown in Table 3.5, it was found that pectin level of the heated pulp is in the same range of Sherkat and Luh (1976), 3-4 mg/g pulp.

Figure 3.7 also shows that the pectin level is independent on ripeness. There is no trend over the ripeness range studied. Therefore, pectin level could be treated as being independent of ripeness in the break process model development.

The sugar content in the tomato pulp was also investigated at 30°C and is shown in Figure 3.8.

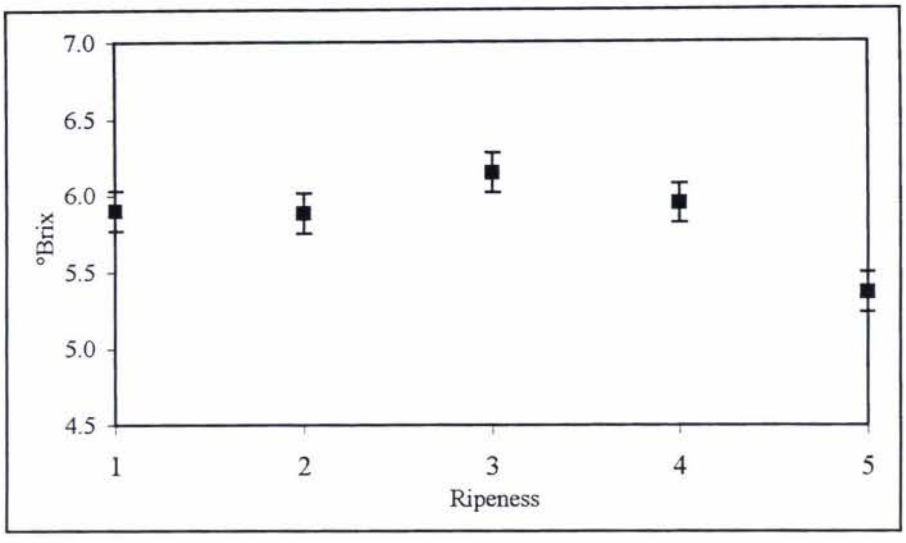

Figure 3.8 *Plot of °Brix for the heated pulp as a function of ripeness (1=Green, 2=Breaker, 3=Turning, 4=Orange, 5=Dark red)*

The °Brix level of the different tomato ripeness in Figure 3.8 is relatively independent on the ripeness of the fruit. This result shows that °Brix of Ferry Morse tomato cultivar is in the range of 5.3 to 6.2.

3.11 Conclusions

In this study, it is clearly shown that heat can destroy PG enzymes which result in a higher level of insoluble solids and pectin content in microwave-heated tomato pulp. These results show that the tomato fruit must be treated before pulping in order to achieve the true value of insoluble solids. A key finding of this work was that there is no trend in total solids, insoluble solids, pectin, and °Brix in heated tomato pulp at different ripeness. Some variability exists between fruits with the same ripeness. This suggests fruit ripeness does not need to be considered when characterising the level of insoluble solids or pectin in raw fruit, and that differences in these values in finished paste must occur during pulp preparation. The effect of break temperature on PG enzyme activity and enzyme inactivation is investigated in the next chapter.

Chapter 4
Characterisation of PG enzymes in tomatoes

4.1 Introduction

After the tomato solids were determined at different ripeness in Chapter 3, work was carried out on characterisation of PG enzymes at different ripeness of the tomatoes and at different break process temperatures. This work is sumarised in this chapter. As tomatoes ripen, the level of PG enzymes increases dramatically. PG enzymes hydrolyse pectin in the cell wall to the monomer, galacturonic acid which is used to measure the rate of PG activity (McColloch and Kertesz,1949).

In tomato processing, there are hot break and cold break processes used for tomato juice or pulp preparation. The tomato product from the cold break process (<60°C for 1-2 minutes) has more natural colour and fresher tomato flavour but separation of solids from the serum might occur in the container. The hot break process (>80°C for 1-2 minutes) produces higher viscosity in the tomato products because of the more rapid inactivation of PG and PE enzymes in the tomato products (Luh and Daoud,1971 and Lopez *et al.*,1997). The viscosity of tomato products is increased when the break temperature is increased. The combination of higher break temperature and longer holding time can achieve the higher consistency of tomato paste because of the rapid inactivation of pectic enzymes and better retention of pectin in the tomatoes (Luh and Daoud,1971).

The aims of this study were to investigate PG enzyme activity at different ripeness of the tomatoes (Green, Breaker, Turning, Orange, and Dark red) and the effect of different break process temperature (from 30 to 80°C) on PG activity.

4.2 Mechanism of tomato ripening

When tomatoes are ripening, the changes in the composition and solubility of polysaccharides in cell wall play a major role in softening. The cell wall of tomatoes consists of three main components, 30% cellulose, 30% hemicellulose, and 35% pectic polysaccharides. During ripening, the quantity of soluble polyuronides increases as a consequence of release from the pectic fraction of the cell wall. This loss of pectin integrity during tomato ripening is the predominant component of softening. Endo-PG enzyme in red tomatoes also appears at the onset of ripening and hydrolyses the link between two adjacent galacturonic residues within a polygalacturonic acid. Exo-PG enzyme has been detected in green tomatoes but comprises only a small fraction of the total PG activity in the dark red tomatoes. It was also reported that the degree of esterification is a critical factor in the solubilization of the cell wall (Barrett *et al.*,1998).

The activity of PG enzymes in the ripe tomatoes is stimulated by ethylene synthesis. Ethylene plays an important role in the initiation and continuation of ripening in all climacteric fruits, including tomatoes. Various environmental stresses such as wounding, water deficiency and chilling temperatures stimulate ethylene formation

through synthase and oxidase enzyme. Synthase and oxidase are enzymes in the tomatoes which play a critical role in ethylene production. When ethylene is supplied, ripening of green tomatoes and the synthesis of PG enzymes occur (Seymour *et al.*,1993).

Pressey (1986) reported that the tomato fruits contain PGI and PGII but that PGII was more effective in breaking down pectin. They also observed that a very low level of exo-PG in green tomatoes could be measured and that there was no presence of endo-PG enzyme present. The optimum pH for PG enzymes is near 4.5.

Seymour *et al.*(1993) reported that polygalacturonase enzyme in tomato can be extracted in three isoenzyme forms, PGI, PGIIa, and PGIIb. They appear only during ripening and no other stage in the life cycle of tomatoes. PGI is thought to be a complex of PGIIa and PGIIb with a further polypeptide known as the β-chain. It is possible that during the early stages of tomato ripening, the β-subunits are insufficient to combine with the initial amounts of smaller forms, PGIIa and PGIIb. Free PGIIa and PGIIb then accumulate and become the dominant form, PGI, as ripening continues. Activity of the larger molecular form of PGI is associated with the rate of pectin solubilization. It was also suggested that PGI is responsible for depolymerisation of the pectin chain. The pathway of PGI, PGIIa, and PGIIb formation is described as Figure 4.1.

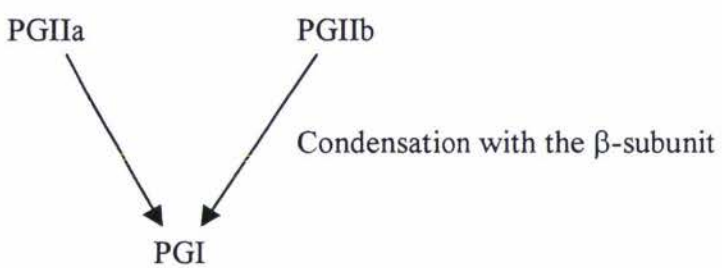

Figure 4.1 *The pathway of PGI, PGIIa, and PGIIb formation (Seymour et al.,1993)*

However, there is no evidence to support the difference between PGIIa+β-subunit and PGIIb+β-subunit. The difference of the molecular weight of PGI, PGIIa, and PGIIb is demonstrated as Table 4.1.

Table 4.1 *Characteristics of the isoforms of tomato polygalacturonase (Seymour et al., 1993)*

Components	***Enzyme molecular weight (kDa)***
PGI	84-115
PGIIa	43
PGIIb	45
β-subunit	38-39

Seymour *et al.*(1993) summarized the possible relationship between physiological and biochemical changes and softening at different ripeness of the tomatoes as follows:

1. **Immature green fruit.** Glycosidase enzyme removes the side-chain from pectic polymers as a possible precursor to a subsequent degradation and solubilization by PG enzymes. Autolysis of the locular gel in tomatoes occurs in the absence of PG enzymes with some softening of the fruit by an unknown mechanism.
2. **Mature green fruit.** At the beginning of ripening, the autocatalytic phase in ethylene production starts. Synthesis of PG, solubilization and depolymerization of pectin occur but are not necessarily linked.

3. **Ripened fruit.** Pectin degradation as a result of PG and PE activity appears quite limited at this stage. The relationship between PG activity and fruit firmness index is not apparent at this stage.

4. **Over-ripening**. PG activity continues rising with the disintegration of cell wall. The depolymerization and degradation of pectic substances are progressive with the breakdown of the control mechanism and a free mixing of enzymes and substrates. The fruits can become infected by fungi and bacteria.

These studies clearly demonstrate large changes in the activity of PG enzymes during the ripening of the fruit. PG activity is very important to the break process.

4.3 Polygalacturonase enzyme activity measurement

As discussed above, PG enzymes in the tomatoes are active when the tomatoes starts ripening. Hobson (1965) investigated the firmness of tomato fruit at various degrees of ripeness and found that pectolytic (PG and PE) enzyme activity is one of the predominant factors governing the firmness of different varieties of ripe tomato fruits. The levels of polygalacturonase enzyme activity in six varieties of tomato fruits were determined for which the results are shown in Table 4.2.

Table 4.2 *Polygalacturonase activity in six varieties of tomato fruit at the commercial picking stage (Hobson, 1965)*

Variety	*Unit of activity (gGA produced/100 g pulp.hr)*
Potentate	3.23
Moneymaker	4.31
JI 68	4.31
E.S.5	4.41
Ailsa Craig	5.01
Harbinger	5.73

The amounts of PG enzymes were different for different cultivars. The numbers ranged from 3.23 to 5.73 units of activity. This suggests that the PG activity in Ferry Morse cultivar in this study are likely to be different from the literature reports for other varieties.

In this study, the methods for PG enzyme assay needed to be developed to suit the Ferry Morse cultivar with the requirements as below.

4.3.1 Method requirements

From the methods for determination of PG enzyme activity reported by many authors, a method had to be selected to investigate PG activity at different ripeness and the temperature range of break process from cold break to hot break (30-80°C). From the literature review, there are a lot of approaches taken to follow the change of PG activity, for example: the acidity changes of tomato paste after the break process (Becker *et al.*,1968 and Becker *et al.*,1972), the viscosity changes after the break process (Luh *et al.*,1954), the changes of volatile acids at the different break temperatures (Sieso and Crouzet,1977), the increase of reducing sugars in different break procedures (Lopez *et al.*,1997, Knegt *et al.*,1988) and the changes of pectin quantity at different ripeness (Luh and Daoud,1971).

The break process temperature and tomato ripeness are two main factors which affect the consistency of tomato paste. Therefore, the possible approaches chosen for use in this work had to be simple, reliable, and accurate enough to carry through the study. Among the scientific approaches in the literature review, three main approaches were chosen for further investigation; viscosity reduction, pectin hydrolysis and formation of reducing sugars.

4.3.1.1 Viscosity reduction

The reduction of viscosity is one approach to determine the PG activity. As the fruit ripens, the pectin in the cell wall is hydrolysed by PG enzymes which results in the softening of the tomatoes. Therefore, the viscosity of tomato paste from green tomatoes is higher than the paste from red tomatoes made under the same conditions because PG enzymes begin to form when the fruit starts ripening.

Luh *et al.*(1954) investigated the pectic enzyme activity by following changes in product viscosity. The decrease in viscosity of pectic acid due to PG activity was followed using Ostwald viscometer at 29.4±0.1°C. It was found that the decrease in viscosity correlated with the increase in hydrolysis of pectic acid.

Luh and Daoud (1971) studied the effect of break temperature (60, 71.1, 82.2, 93.3, 104.4, and 115.6°C) and holding time on the pectin and pectic enzymes in tomato pulp. The activity of PG enzymes was investigated by measuring the decrease in viscosity of polygalacturonic acid. PGA solution was used as the substrate. An Ostwald-Cannon-Fenske viscometer, A.S.T.M (size no.100) was used to follow PG activity as a function of time. The enzyme solution was mixed thoroughly with the PGA solution at 30°C. 20 ml of PGA solution (50 ml of 1% polygalacturonic acid solution at pH 4.5, 20 ml of 0.5M acetate buffer at pH 4.5, and 30 ml of distilled water) was pipetted into a flask in a water bath at 30°C and mixed thoroughly with 10 ml of enzyme solution. The resulting mixture was pipetted immediately into the viscometer and kept at 30°C in a waterbath. Viscosity was measured at various time intervals and expressed as percent loss in viscosity. It was reported that PG activity per gram of tomato pulp can cause 4.09% loss in viscosity of PGA solution per minute at pH 4.5 and there was no PG activity in the tomato pulp samples preheated at 104.5°C for 15 sec.

From the literature above, PG activity can be followed by determining the viscosity changes of the tomato pulp as a function of time. The viscosity determination is very sensitive for random-cleaving enzymes like PG enzymes (Pressey, 1986), therefore, the other methods for determination of PG enzyme activity were also investigated.

4.3.1.2 Pectin hydrolysis

The function of pectin in the tomato is to help the fruit keep firm and to prevent collapse. As pectin is converted to less complex units, there is a decrease in firmness and ultimate collapse of the fruit because polygalacturonase enzyme in the tomato hydrolyses the 1-4 glycosidic bonds between two galacturonic acid residues of protopectin to soluble pectin (Stier *et al.*,1956). The activity of the PG enzymes can be determined from changes to intact pectin levels in the fruit.

Stier *et al.*(1956) determined the changes of pectic substances converted to galacturonic acid during the storage life of tomatoes at 4.4°C for 21 days. The tomatoes from one variety were harvested, washed, air dried and divided into nine one-kilogram samples. Storage was in a natural convection refrigerator. The samples were removed on 0,7,14, and 21 days of storage. The samples were reweighed to determine weight loss which was approximately 10g per week and tests undertaken to determine the changes of pectin, protopectin, methoxyl content and pectate content. Protopectin showed a significant decrease during the storage period. Pectin significantly increased within the first 7 days of storage.

Becker *et al.*(1968) reported the effect of pH adjustment of tomato juice on pectin contents by following the pectin changes described by McCready and McComb (1952). The pH of tomato juice was adjusted during breaking and heating. Tomato juice extracted at both low pH and high pH produced higher pectin contents in the final tomato juice. The extraction of juice at lower pH (1.4-1.6) than the natural tomato pH with hot break temperature (93.3°C) achieved the higher pectin tomato juice. This pectin contained a large proportion of water-soluble, highly esterified pectin, and had a higher viscosity.

Sharma *et al.*(1996) studied the effect of composition on the rheological properties of tomato thin pulp from six different cultivars. Pectin hydrolysis was used to follow the kinetic changes. The tomato thin pulp sample was homogenized and diluted about 100 times. 0.5 ml of the diluted sample was poured into test tubes and place in an ice-cooled waterbath. A reagent of H_2SO_4/tetraborate (4 ml) was added to each test tube and the solution was carefully mixed on a vortex mixer before heating in a waterbath at 100°C for 5 min. After heating, the samples were cooled down in an ice bin until they reached room temperature. 0.1ml of 0.15% m-hydroxydiphenyl in 0.5% sodium hydroxide (m-hydroxydiphenyl solution) was added to each sample to initiate the reaction. A blank for each individual sample was used to determine that the red colour produced from other carbohydrate groups. The m-hydroxydiphenyl solution in the blank was replaced with 0.1 ml of 0.5% sodium hydroxide. The colour of reactants increased in the first minute and levelled off after 30 minutes and absorbance was read at 520 nm. The pectin was estimated quantitatively using a standard curve for galacturonic acid (50-200μg/ml). It is possible by using this technique that changes in pectin after breaking can be used to estimate PG activity.

Pectin hydrolysis by the Sharma *et al.*(1996) procedure is a good method to follow the activity of PG enzymes because the procedure is easy to set up. The relationship between the level of pectin, insoluble solids, and soluble solids can be determined at the same time. Therefore, Sharma *et al.*(1996) analysis could be used as a main procedure to follow PG activity by measuring the level of pectin in this study.

4.3.1.3 Formation of total reducing sugars

Galacturonic acid is normally present in traces in tomatoes. It is formed as a result of enzyme hydrolysis. The absence of galacturonic acid is a sign of total enzymatic inactivation (Porretta, 1991). Therefore, the formation of galacturonic acid could be used as an analysis index. There are many publications that have used the increase of reducing sugar, galacturonic acid, after enzyme hydrolysis to follow the PG activity. Those publications are sumarised below.

Luh *et al.* (1954) investigated the products of pectic acid hydrolysis by PG enzymes. PG activity was determined by following the increase in reducing groups at pH 4.5 and at 29.4±0.1°C. When the pectic acid solution is treated with tomato PG enzymes, the reducing group of the reaction mixture is increased. The hydrolysis was divided into two phases of reaction, (a) an initial rapid stage in which the increase in reducing value is a linear function of time and, (b) a second stage during which the rate of hydrolysis becomes progressively slower. The relation of percent hydrolysis and time is illustrated in Figure 4.2

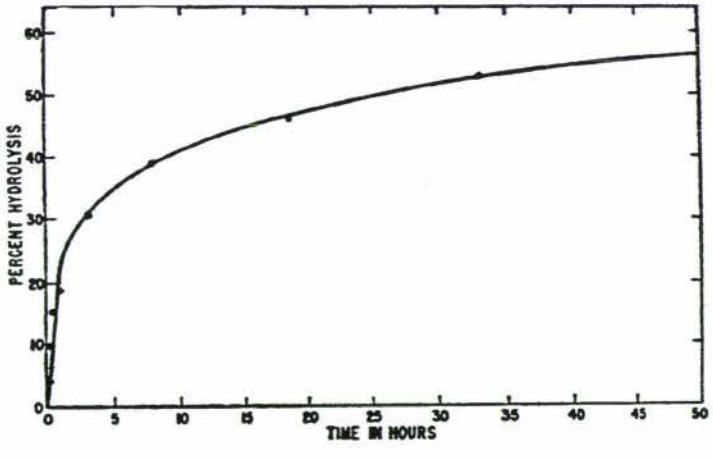

Figure 4.2 *Hydrolysis of 0.5% Sodium pectate to galacturonic acid by PG enzyme (Luh et al.,1954)*

Moshrefi and Luh (1984) studied purification and characterization of two tomato PG isoenzymes. The PG enzyme activity was followed by measuring the formation of reducing groups using the dinitrosalicylic acid procedure with modification. The reaction mixture contained 0.5% polygalacturonic acid, 0.15M NaCl, 0.05M Sodium acetate buffer at pH 4.5 and an appropriate amount of enzyme solution at 35°C in a total volume of 10 ml. The enzyme activity was determined by taking 1 ml aliquot from the reacting mixture at 5 min time intervals (up to 30 min), and heating it in boiling water for 3 min. 0.5 ml of this solution was diluted to 1 ml with distilled water and mixed with 1 ml of dinitrosalicylic acid. The tubes were covered and heated for 5 min

in a boiling water bath and immediately cooled down in tap water. 5 ml of water was added. The absorbance of the reaction mixture at 540 nm was read against a blank which was prepared in the same manner without the enzyme. A standard curve was prepared using ∝-D-galacturonic acid. One PG activity unit was defined as the amount of enzyme producing 1 μmol of reducing groups per minute at 35°C. The optimum pH for PG enzyme activity was found to be pH 4.6. Kinetic constant (k) was determined for the enzyme activity using an Arrhenius plot. The K_m, V_m, and E_a were calculated and shown as Table 4.3.

Table 4.3 *Kinetic constants of PGI and PGII from tomatoes (Moshrefi and Luh, 1984)*

Enzyme	V_{max} ***(U/mg)***	K_m ***(mM)***	E_a	
			kcal/mol	***J/mol***
PGI	27.7	7.5×10^{-2}	16.8	70.3×10^{3}
PGII	58.8	3.8×10^{-2}	14.8	61.9×10^{3}

* All constants were measured at pH 4.6 and 35°C.

The lower K_m value of PGII as compared to PGI indicates that PGII has a higher affinity towards polygalacturonic acid. The data for V_{max} indicates that PGI is almost half as effective as PGII. Therefore, it was assumed that during the later stage of ripening, PGI was converted to PGII.

Knegt *et al.* (1988) studied the roles of PG I and II during tomato ripening by following the appearance of reducing sugar groups upon incubation of PGA with PG enzyme. The incubation medium consisted of 2 ml buffer containing 200 mM Na-acetate and 400 mM NaCl, at pH3.6 for PGI or pH 4.4 for PGII. 2.5 ml of 0.1% PGA and 0.5 ml enzyme solution were diluted or ultradialysed with buffer containing 100 mM Na-acetate and 200 mM NaCl at 35°C. Duplicate samples of 0.5 ml were pipetted into 2.5 ml TBC-buffer which already contained 100 nmol galacturonic acid. The TBC-buffer consisted of 100 mM tetraborate-di-Na and 100 mM boric acid, mixed to give pH 9.0, and 0.1% 2-cyanoacetamide added. 0.5 ml samples were taken every hour and put into 2.5 ml TBC-buffer. The tubes were stoppered with a marble and held for 15 min in a boiling waterbath. After cooling, the absorbance at 270 nm was measured. The activity of PG enzyme was calculated by comparing the absorbance increase during the reaction with the absorbance of 100 nmol galacturonic acid. The unit was expressed as the number of moles of reducing groups produced per litre per sec. It was found that the optimum pH for PG activity varied with substrate size. The PGA, with an average MW of 10 kDa, showed pH optimum for PGI at 3.6 and for PGII at 4.4 in 100 mM Na-acetate buffer and 200 mM NaCl. No activity was detectable in tomatoes at the green stage. At the breaker and turning stages, PGI prevailed, after which PGII increased more than PGI. During ripening, PGI is the first enzyme to appear and is soon surpassed by PGII at the fully ripe stage. The changes of PGI and PGII activities in tomato pericarp during ripening is presented in Figure 4.3.

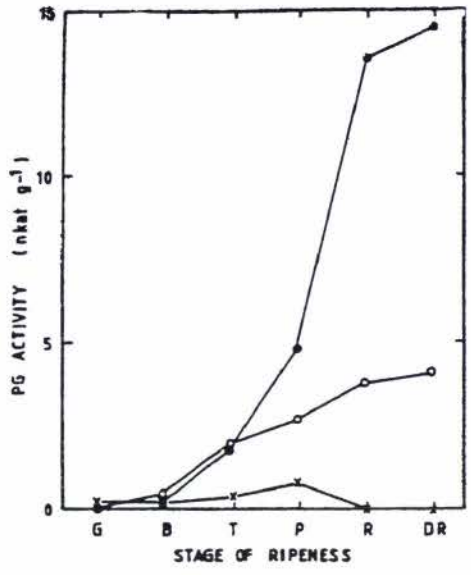

Figure 4.3 *Changes in PGI(o), PGII(•), and free convertor(x) activities in tomato pericarp during ripening (Knegt et al.,1988)*

Lopez *et al.*(1997) investigated thermal resistance of tomato PG and PE enzyme at physiological pH. PG was assayed by measuring the increase in reducing groups of a polygalacturonic acid substrate at 40°C for 1-6 hr. The reaction was started by adding 0.25 ml of the PG enzyme solution (50 mM citrate buffer, pH 4.0, 0.4M NaCl) to 0.25 ml of a 0.4% water solution of polygalacturonic acid. The result was reported that PG activity in tomato extract was inactivated by heat at 72.5°C and the cold break procedure does not destroy PE and PGI activities, and destroys PGII only slightly. The inactivation of PG enzymes followed first-order kinetics. D-values of PGI and PGII were calculated and shown as Table 4.4.

Table 4.4 *Kinetic parameters for PGI and PGII (Lopez et al.,1997)*

Enzymes	***D-values(temperature ranges)***
PGI	15.9 min (87°C) to 0.46 min (95.4°C)
PGII	2.14 min (64°C) to 0.24 min (73°C)

Lopez *et al.*(1998) studied the inactivation of pectic enzymes in tomato using manothermosonication (MTS), a combined treatment of heat and ultrasound under moderate pressure. PG was assayed by measuring the increase in reducing groups of the polygalacturonic acid substrate by Lever's method (Lever,1972). The reaction was performed at 40°C for 10-60 min and was started by adding the PG solution (in 50 mM citrate buffer, pH4.0, 0.4M NaCl) to 0.25 ml of a 0.4% aqueous solution of polygalacturonic acid. Heat at 86°C should be applied to the PG I for more than 40 min while the same effect could be achieved by MTS by heating the enzyme for 30 sec at the same temperature. To reach the same PGI inactivation efficiency during a similar time scale (30 sec), the temperature should be raised to about 97°C. MTS inactivation of PGI and PGII follows first-order kinetics which allows the expression of reaction rates in terms of D-values as Table 4.5.

Table 4.5 D-values for MTS and heating inactivation for PGI and PGII (Lopez et al.,1998)

Enzymes	*MTS (temperature range)*				*Heating*	
	Temp (°C)	*D (min)*	*Temp (°C)*	*D (min)*	*Temp (°C)*	*D (min)*
PGI	37	3.17±0.2	86	0.24±0.02	86	20.6±0.1
PGII	37	2.23±0.3	52.5	1.46±0.05	52.5	38.4±0.1

This method is convenient and applicable for both endo- and exo- PG enzymes to measure the increase of hydrolysis (Fisherman and Jen,1986). It can follow easily and many authors have used this method to investigate the PG activity.

4.3.2 Methodology used in this work for PG activity assay

The determination of the increase in reducing sugar was chosen to measure the change of PG activity. The method of Luh and Daoud (1971) with some modifications was used to determine the level of reducing sugar as below;

- About 2.50 g of tomato pulp was added into 100 ml of 1% Polygalacturonic acid (PGA) solution at 30°C. PGA solution can be prepared from 250 ml 1% polygalacturonic acid, Sodium Polypectate, water-soluble, Sigma Ltd., at pH 4.5, 100 ml 0.5 M acetate buffer at pH 4.5, and 150 ml distilled water in a 500 ml volumetric flask.

- The flask was transferred to a shaking waterbath at 30°C and kept until the temperature of PGA solution reaches 30°C.

- 1 ml of sample was taken at 0,5,10,15,20,25, 30 and 40 min in triplicate and put into a boiling waterbath for 2 min to inactivate PG enzymes in the pulp.

- 10-fold dilution was made. 3 ml of DNS reagent (Appendix 1) was added and the mixture was transferred to boil for 15 min.

- The samples were cooled down for 20 min and absorbance read at 575 nm in a Ultrospec 2000 UV/Visible Spectrophotometer.

A trial with a PG industrial enzyme was made to test the method before it was applied to the tomato pulp samples. Pectinase enzyme was chosen for a preliminary trial. Pectinase is the commercial name of a PG enzyme which is made from *Aspergillus niger*. It was ordered from Sigma Ltd. An experiment was undertaken using similar PG levels as would be found in ripe tomatoes. The calculation of the amount of PG enzyme added is given below.

From a label on the enzyme bottle,

Pectinase consists of 14 units/ mg protein.
1 ml Pectinase consists of 11 mg protein.
The enzyme contatins 209 units per 1 ml Pectinase.
1 unit = liberation of 1 μmol GA/min. at pH 4,25°C

Molecular weight of galacturonic acid = 212.2 µg/µmol

Therefore, PG activity can be calculated from

$$\text{PG activity} = 209 \frac{units}{ml\ Pectinase} x\ 1 \frac{\mu mol\ GA}{min.unit} x\ 212.2\ \frac{\mu g\ GA}{\mu mol\ GA}$$

$$= 44{,}350\ \mu g\ GA/\ ml\ Pectinase.min$$

This means that 1 ml Pectinase enzyme can produce 44,350 µg of galacturonic acid per one minute. For 100 ml of 1% PGA solution to produce 200 µg GA/ml (estimated) in 30 min, therefore, the amount of PG enzyme was calculated as the following.

$$= 200\ x \frac{1}{30} x \frac{100}{44{,}350}\ \frac{\mu g\ GA}{ml\ PGA} x \frac{1}{min} x \frac{ml\ PGA.\ ml\ Pectinase.\ min}{\mu gGA}$$

$$= 0.015\ \frac{ml\ Pectinase\ enzyme}{100\ ml\ 1\%PGA\ solution}$$

$$= 15\ \frac{\mu l\ Pectinase\ enzyme}{100\ ml\ 1\%\ PGA\ solution}$$

The result above could be interpreted that15 microlitre of PG enzyme can hydrolyse 100 ml 1% PGA solution and produce 2 mg/ml/30 min or 200µgGA/ml/30 min. A preliminary trial of 15 µl PG enzyme was done in 1% PGA solution as substrate and the result is shown in Figure 4.4.

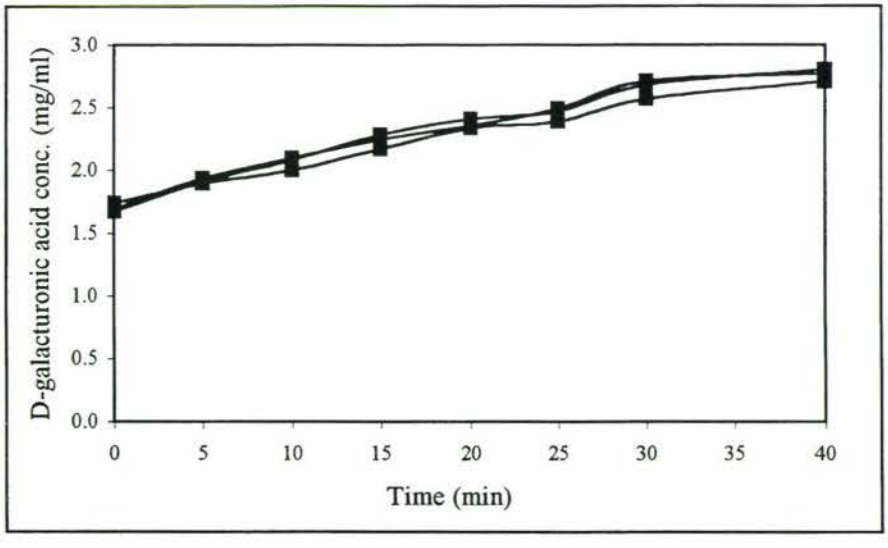

Figure 4.4 *Plot of preliminary trial with15 microlitre PG industrial enzyme on 1% PGA solution*

It is clear that PG industrial enzyme hydrolysed 1% PGA solution and produced an extra 1.2 mg/ml of D-galacturonic acid within 40 minutes. The amount of D-galacturonic acid increased as a function of time from an initial amount of galacturonic acid originally in the polygalacturonic acid solution. The activity (~1000 μg GA/ml/30 min) suggests the activity estimated by the enzyme supplier was conservative.

4.4 Kinetics of PG enzyme activity as a function of ripeness

The activity of pectin hydrolysis caused by the PG enzyme system was measured in this section over a range of 5 stages of fruit ripeness. From this collected data, kinetic models describing the pectin hydrolysis could be developed.

4.4.1 Experimental design

The investigation of PG activity at 5 different levels of tomato ripeness was carried out by considering the following factors.

4.4.1.1 Ripeness scale

The Ferry Morse tomatoes in this study were grown in a greenhouse at Plant Growth Unit, Massey University, Palmerston North. The tomatoes were chosen from the range of 5 different ripeness as described in Chapter 3.

4.4.1.2 Numbers of samples

The samples in this study were prepared in triplicate to ensure the reproducible results. Tomato pulp samples were prepared from four to five of the tomato fruit by blending and immediately chilling in an ice bin to ensure preservation of the PG enzymes in the samples.

4.4.1.3 Sample temperature

To begin with, the effect of tomato ripeness on PG activity at 30°C was determined. This temperature was selected as at this temperature no heat induced inactivation of the enzymes was expected.

4.4.1.4 Total reducing sugar determination

The determination of total reducing sugar level in the tomato pulp was made using DNS reagent. 1 litre of DNS reagent was prepared from dissolving 10g Sodium hydroxide, 182g Potassium Sodium Tartrate (Rochelle salt), 10g Dinitrosalicylic acid (add slowly while stirring), 2g Phenol, and 0.5g Sodium Sulphite in 600 ml water. Then, this solution was transferred to 1 litre volumetric flask and water was added to give 1 litre of solution until reaches the level.

A standard curve was prepared by following the steps below:

1.Make up D-galacturonic acid standard solutions :0.1-1.0 mg/ml in distilled water.
2.Pipette 1 ml of each standard into separate test tubes.
3.Pipette 2 ml of distilled water into a test tube for blank.
4.Add 3 ml of DNS reagent to each test tube and vortex.
5.After capping the tubes, place in boiling water for 15 minutes.
6.Allow to cool in cold water for at least 20 minutes.
7.Read absorbance at 575 nm against the blank.
8.Plot the concentration of D-galacturonic acid versus absorbance. The plot should be linear between 0.1-1.0mg/ml.
9.A new standard curve should be prepared for each batch of DNS reagent.

4.4.1.5 The amount of the tomato pulp in the experiments

PG industrial enzyme was used to investigate of the amount of tomato pulp in this study. From Figure 4.4, it was shown 15 microlitre of PG industrial enzyme hydrolysed 1% PGA solution. The rate and extent of hydrolysis over time were measured following increase in D-galacturonic acid in the sample. The absorbance readings were converted to the concentration of D-galacturonic acid using a standard curve. The standard curve for galacturonic acid was determined using purified D-galacturonic acid (Sigma Ltd.) at the concentrations of 0.2, 0.4, 0.6, 0.8, and 1.0 mg/ml in triplicate. 3 ml of DNS reagent was added and the absorbance of the solution was read at 575 nm after 20 min. the result is shown in Figure 4.5.

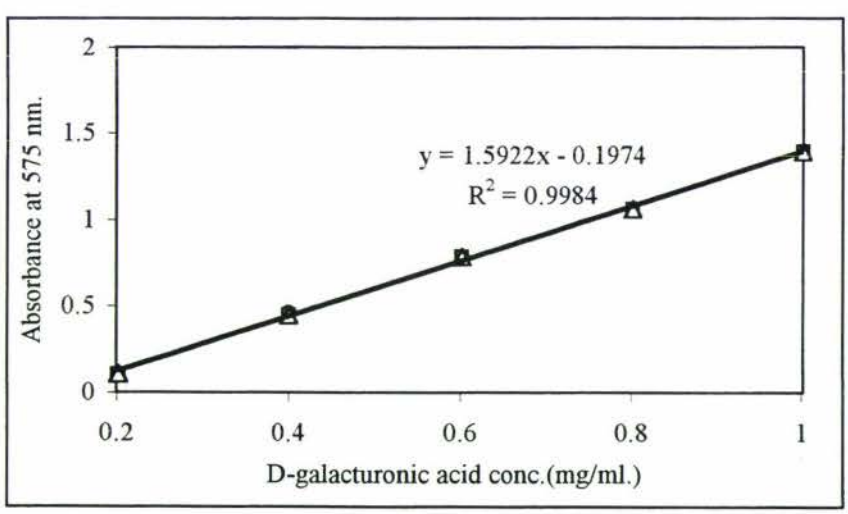

Figure 4.5 *Standard curve of D-galacturonic acid solution (raw data shown in Appendix4)*

From Figure 4.5 the absorbance reading can be converted to the concentration of D-galacturonic acid by using Eq. 4.1.

$$P = \frac{A_{575} + 0.1974}{1.5922} \qquad [4.1]$$

where P = D-galacturonic acid concentration (mg/ml)
A_{575} = Absorbance reading at 575 nm.

Based on literature reports it was estimated that 2.50g to 5.00 g of dark red tomato pulp would achieve a similar observation. It was found that 2.54 g of dark red tomato pulp and 15 microlitre of industrial enzyme produced approximately the same amount of D-galacturonic acid over time, 2.7 mg/ml. Five grams of dark red tomato pulp produced 3.2-3.6 mg/ml in 40 min as shown in Figure 4.6.

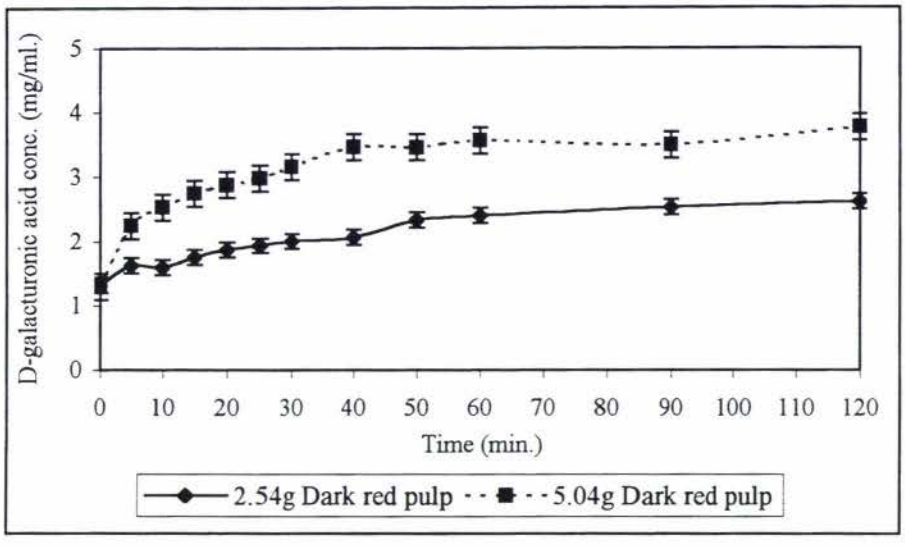

Figure 4.6 *PG activity of 2.54 g and 5.04 g dark red tomato pulp (raw data shown in Appendix5)*

From these results it was decided to use 2.5 g (estimated) of tomato pulp per 100g of 1% PGA solution for further work in this study.

4.4.1.6 Procedures

- About 2.50 and 5.00 g tomato pulp at 5 different ripeness were added into flasks containing 100 ml 1% PGA solution. The flasks were immersed in a waterbath with shaker at 30°C.

- 1 ml of each sample was taken in triplicate and transferred to a test tube every 5 min interval for 40 min.

- These sample tubes were transferred immediately into boiling water for 2 min to inactivate the PG enzymes. After boiling, the samples were cooled down until they reached room temperature.

- The sample tubes were diluted 10-fold using distilled water. 1 ml of each 10-fold dilution sample were then transferred to a test tube and 3 ml DNS reagent was added.

- The mixture was mixed thoroughly using a vortex mixer. The mixture was boiled for 15 min and then cooled in cold water for 20 min.

- The absorbance of the samples was then measured at 575 nm as described above for the GA standards.

4.4.2 Results and discussion

Figure 4.7 shows the formation of D-galacturonic acid after addition of the pulp samples at 5 different ripeness to the PGA solution.

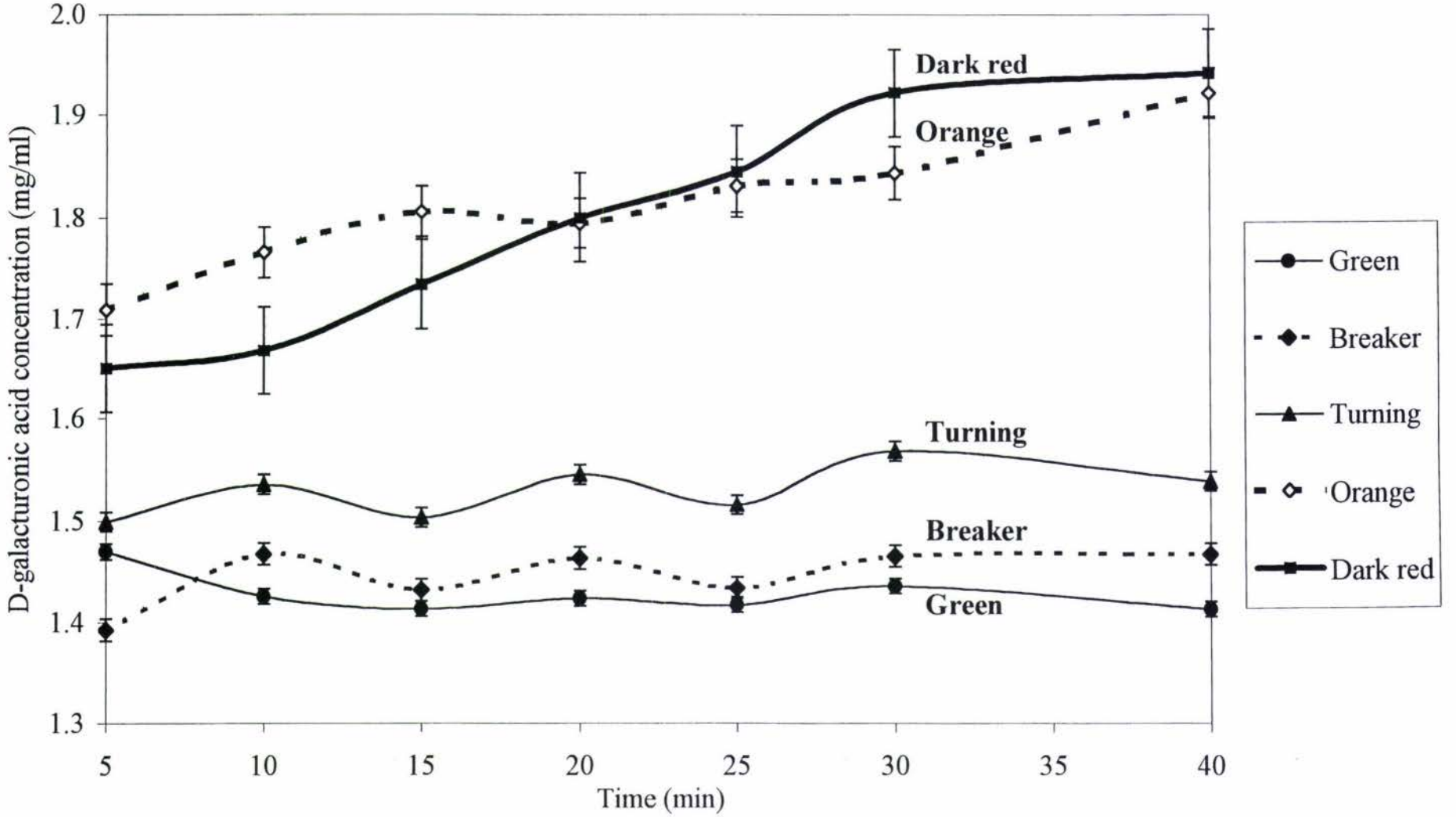

Figure 4.7 *Plot of PG activity at different ripeness (raw data shown in Appendix6)*

Figure 4.7 demonstrates the expected increase of D-galacturonic acid concentration caused by the enzymes in dark red and orange, turning, and breaker tomato pulp. There was no observable activity change from green tomato. This phenomenon is due to the different levels of PG enzymes contained in the cell wall and locular gel of the tomatoes. The high level of PG enzymes in the tomato pulp can hydrolyse the PGA in solution more and produce the high amount of D-galacturonic acid. The dark red tomato pulp can be seen to contain the highest PG enzymes which result in the highest increase of the concentration of D-galacturonic acid. The orange, turning, and breaker pulp contain less PG enzymes than dark red pulp, therefore they produce the lower amount of D-galacturonic acid.

The investigation of PG enzymes at different ripeness showed that the level of PG enzymes in the tomatoes increases with colour from green to dark red as stated in many literature reports. The results show that the orange and dark red tomatoes normally used in tomato processing contain high levels of PG enzymes. As a consequence it is likely that higher break temperatures would be required to retain pectin in the dark red and orange than for green, breaker, and turning fruit. The characterisation of the tomato ripeness from colour before processing is likely to be a good method to control the break process to achieve consistent tomato paste quality.

4.5 Kinetic model for pectin hydrolysis

Michaelis-Menten kinetics are often used to model the kinetics of enzyme reactions. Shuler and Kargi (1992) described how enzyme-substrate interaction can vary from one enzyme-substrate complex to another. Most forces causing the interaction between enzyme (E) and substrate(S) which are responsible for the formation of ES complexes, are Van Der Wals forces and hydrogen bonding. The substrate binds to a specific site on the enzyme known as the active site. One model of the enzyme-substrate complex is the lock and key model, in which the enzyme represents the lock and the substrate represents the key, as shown in Figure 4.8.

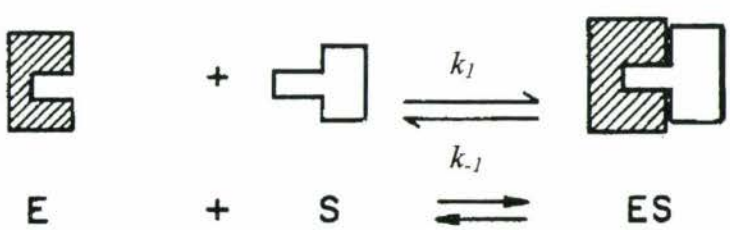

Figure 4.8 *Schematic of the lock and key model of enzyme catalysis (Shuler and Kargi, 1992)*

An enzyme solution has a fixed number of active sites to which substrates can bind. At high substrate concentration, all these sites are occupied by substrates or the enzyme is saturated. The kinetics of this single-substrate-enzyme–catalyzed-reactions involves a reversible step for enzyme-substrate complex formation and a dissociation step for the ES complex (Shuler and Kargi,1992) as shown in Figure 4.9.

$$E + S \underset{k_{-1}}{\overset{k_1}{\rightleftharpoons}} ES \xrightarrow{k_2} E + P$$

Figure 4.9 *The enzyme-substrate complex formation scheme (Shuler and Kargi, 1992)*

The relationship between substrate concentration (S) and rate of an enzyme-catalysed reaction (V) is shown schematically as Figure 4.10.

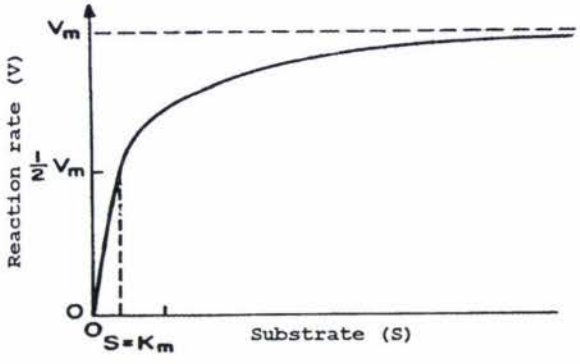

Figure 4.10 *Effect of substrate concentration on the rate of an enzyme-catalyzed reaction (Shuler and Kargi, 1992)*

The enzyme-substrate complex is assumed to be a second order biomolecular reaction and the conversion of enzyme-substrate complex into products is a first order monomolecular reaction (Bailey and Ollis, 1986).

It follows from this that the rate of product formation is given by;

$$v = \frac{dP}{dt} = k_2[ES] \qquad [4.2]$$

where v = the rate of product formation or substrate consumption in moles/l-s

The rate of change in the $[ES]$ complex is given by;

$$\frac{d[ES]}{dt} = k_1[E][S] - k_{-1}[ES] - k_2[ES] \qquad [4.3]$$

Since $[E] = [E_o] - [ES]$ (Because the enzyme is not consumed when the reaction occurs)

At this point, there are two major approaches used to develop a rate expression for the enzyme catalyzed reactions as follows:

4.5.1 The rapid equilibrium assumption

The assumption was made that there is a rapid equilibrium between the enzyme and substrate to form an $[ES]$ complex. The equilibrium coefficient of $[ES]$ can be expressed in terms of $[S]$ as shown in Eq.4.4 and Eq. 4.5.

The equilibrium Michaelis-Menten constant is

$$K'_m = \frac{k_{-1}}{k_1} = \frac{[E][S]}{[ES]} \qquad [4.4]$$

where K'_m = Equilibrium Michaelis-Menten constant.

Since $[E] = [E_o] - [ES]$ if enzyme is conserved, then

$$[ES] = \frac{[E_o][S]}{\frac{k_{-1}}{k_1} + [S]} \qquad [4.5]$$

$$[ES] = \frac{[E_o][S]}{K'_m + [S]} \qquad [4.6]$$

Substituting $K'_m = \frac{k_{-1}}{k_1}$

give; $$v = \frac{dP}{dt} = \frac{k_2[E_o][S]}{K'_m + [S]} = \frac{V_{max}[S]}{K'_m + [S]} \qquad [4.7]$$

where $V_{max} = k_2 [E_0]$ = Maximum forward velocity of the reaction

In this assumption, V_{max} changes if more enzyme is added to the system but the addition of more substrate has no effect on V_{max}. A low value of Michaelis-Menten constant (K'_m) is the high affinity of enzyme for the substrate.

4.5.2 The quasi-steady-state assumption

The quasi-steady-state assumption can be used when the initial substrate concentration greatly exceeds the initial enzyme concentration. From Eq.4.3, the rate of $[ES]$ formation is small because $[E_0]$ is small, $\frac{d[ES]}{dt} = 0$.

After the quasi-steady-state assumption is applied to Eq.4.3, then

$$[ES] = \frac{k_1[E][S]}{k_{-1} + k_2} \qquad [4.8]$$

where $[E]$ = $[E_0]$ - $[ES]$

$$[ES] = \frac{k_1[S]([E_o]-[ES])}{k_{-1}+k_2} \quad [4.9]$$

Solving Eq.4.9 for [*ES*], then

$$(k_{-1}+k_2)[ES] = k_1[S][E_o]-k_1[S][ES] \quad [4.10]$$

$$k_{-1}[ES]+k_2[ES]+k_1[S][ES] = k_1[S][E_o] \quad [4.11]$$

$$[ES] = \frac{k_1[S][E_o]}{k_{-1}+k_2+k_1[S]} \quad [4.12]$$

Dividing R.H.S by k_1 , then

$$[ES] = \frac{[S][Eo]}{\frac{k_{-1}+k_2}{k_1}+[S]} \quad [4.13]$$

From Eq.4.2, the rate of product formation is $v = \frac{dP}{dt} = k_2[ES]$ then, substituted into Eq.4.14.

$$v = \frac{dP}{dt} = \frac{k_2[E_o][S]}{\frac{k_{-1}+k_2}{k_1}+[S]} \quad [4.14]$$

From Eq.4.14, the Michaelis-Menten constant (K_m) and the maximum forward velocity of the reaction (V_{max}) can be determined from $v = \frac{V_{max}[S]}{K_m+[S]}$. Therefore,

From Eq.4.14

$$K_m = \frac{k_{-1}+k_2}{k_1} \quad [4.15]$$

$$V_{max} = k_2[E_o] \quad [4.16]$$

Therefore, $$v = \frac{V_{max}[S]}{K_m+[S]} \quad [4.17]$$

A low value of K_m means a high affinity of enzyme to the substrate. K_m also corresponds to the substrate concentration and gives the half maximal reaction velocity (Shuler and Kargi,1992).

The formation of a product and the consumption of substrate in a simple reaction at steady state can be shown as Figure 4.11.

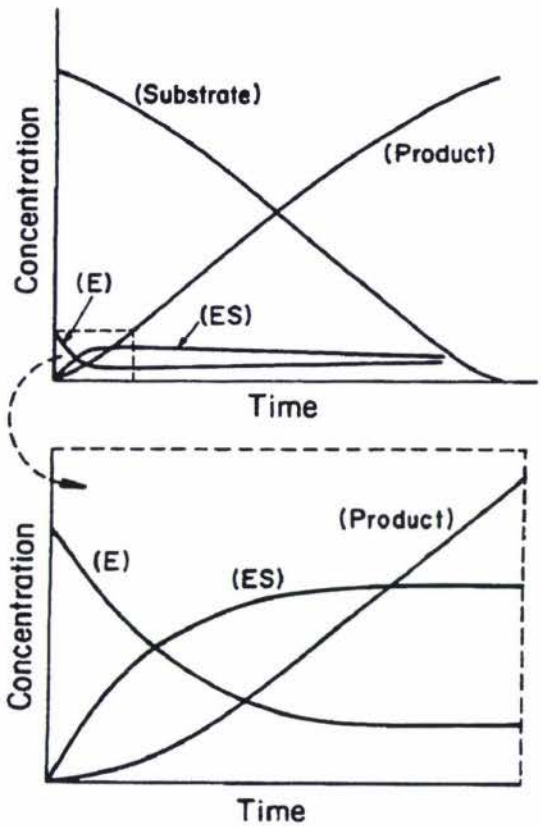

Figure 4.11 *The formation of an enzyme/substrate complex and initiation of steady state (Shuler and Kargi, 1992)*

In conditions where there is an excess of substrate ($K_m << S$), the Michaelis-Menten equation reduces to zero order kinetics.

The plots of Figure 4.7 can then be interpreted to obtain kinetic model of enzyme activity. Zero order kinetics can be expressed as the following.

$$\frac{-dP}{dt} = V_{\max} \qquad [4.18]$$

Separating and integrating, gives

$$\int_{P_i}^{P} dP = V_{max} \int_{0}^{t} dt \qquad [4.19]$$

$$P = P_i + V_{max} t \qquad [4.20]$$

A straight line on a plot of concentration of the product (P) with time will give slope V_{max} (rate constant). Figure 4.7 shows that the change of D-galacturonic acid at different ripeness follows zero order reaction up to at least the 40th minute because the D-galacturonic acid concentration increases linearly.

The value of V_{max} as a function of fruit ripeness is given in Figure 4.12 below.

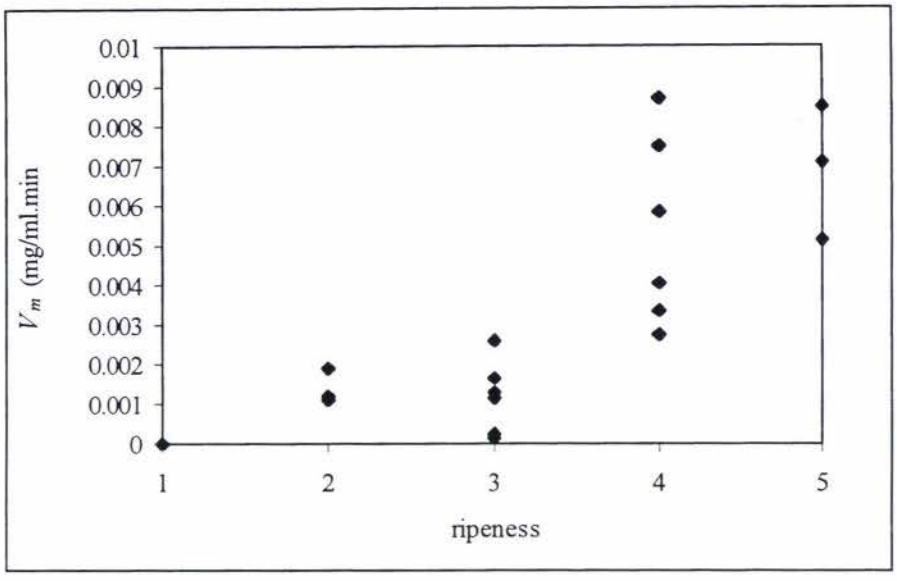

Figure 4.12 *Rate constant as a function of tomato ripeness (1=Green, 2=Breaker, 3=Turning, 4=Orange, 5=Dark red)*

From Figure 4.12, it was found that rate constant (V_{max}) is increasing with ripeness, from green to breaker, turning, orange, and dark red pulp. The higher rate constant represents the faster reaction. Figure 4.12 shows a large difference in PG activity in orange and dark red fruit compared to very low activity at green, breaker, and turning. This has importance when considering the operation of the break process as rapid pectin hydrolysis would occur in feeds of ripe fruit to the process if the enzymes are not inactivated quickly. The results also demonstrate a lot of variability between orange and some variations in dark red fruit. This is likely due to the difficulty in categorising the fruit into different colours by eye, or to natural differences in the fruit.

Figure 4.7 is an indication of the initial levels of galacturonic acid in the PGA solution. It was observed that the intercept also increased for samples with riper fruit. This was due to galacturonic acid being added to the PGA solution in the pulp. The levels of galacturonic acid present in the pulp samples were calculated from the intercept and are shown in Figure 4.13 below.

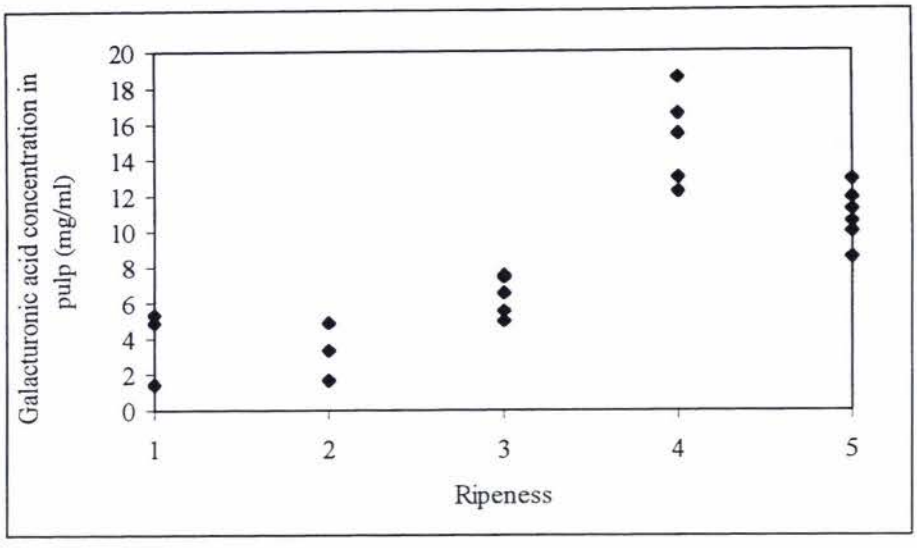

Figure 4.13 *Concentration of D-galacturonic acid in fresh tomato pulp as a function of ripeness (1=Green, 2=Breaker, 3=Turning, 4=Orange, 5=Dark red)*

Figure 4.13 shows that the concentration of D-galacturonic acid present in the fruit increases with ripeness. Orange and dark red pulp contain the higher level of D-galacturonic acid which indicates that the level of PG enzymes is high in the orange and dark red pulp.

4.6 Effect of temperatures on PG enzyme activity

It has been shown that as the ripeness of the tomato fruit increases, the PG activity also increases. The PG enzyme activity of the dark red and orange tomatoes followed zero order at 30°C under the conditions of the experimental work carried out. It was of interest to expand the temperature range of PG activity to higher temperatures.

The experiments were carried out as described below.

4.6.1 Tomato pulp

The dark red pulp of Ferry Morse tomatoes was used in this study. 2.5 g of dark red tomato pulp was added to 100 ml of 1% PGA solution as described previously to investigate the effect of temperatures on PG enzymes in the range of 25-50°C. In this temperature range, enzyme inactivation was not expected to occur.

4.6.2 Numbers of samples

Triplicate samples of one tomato pulp were prepared to ensure reproduceable kinetic data were achieved in the study. Four to five dark red fruit were daily blended and chilled in the ice bin before the assay started.

4.6.3 Reference temperature

The temperature at 30°C was used as a reference temperature. The previous experiment showed that there was a large amount of variation in enzyme activity in dark red fruit. By measuring each pulp sample at 30°C it was possible to account for this variation and determine more accurately, the effect of temperature on enzyme activity.

4.6.4 Total reducing sugar determination

The change of PG activity was determined by following the level of total reducing sugar as done in previous experiments outlined in this chapter.

4.6.5 Procedure

- About 2.50 g dark red fresh tomato pulp was added into a flask of 250 ml 1% PGA solution. Temperature at 25,30,35,40, and 50°C were investigated. 30°C was used as reference sample for every batch of experiment.
- The flask was immersed in a waterbath with a shaker. 1 ml of sample was taken in triplicate every 5 min interval to 40 min.
- The samples were then transferred into boiling water for 2 min to inactivate the PG enzymes. After boiling, the samples were cooled until they reached room temperature.
- The samples were diluted 10-fold before adding 3 ml DNS reagent.
- The mixture was mixed using a vortex mixer, boiled for 15 min and then cooled down for 20 min.
- The absorbance at 575 nm was then measured using a Ultrospec 2000 UV/visible spectrophotometer.

4.6.6 Results and discussion

The studies of PG activity at different pulp temperatures were carried out at 25, 30, 35, 40, and 50°C shown in Figure 4.14.

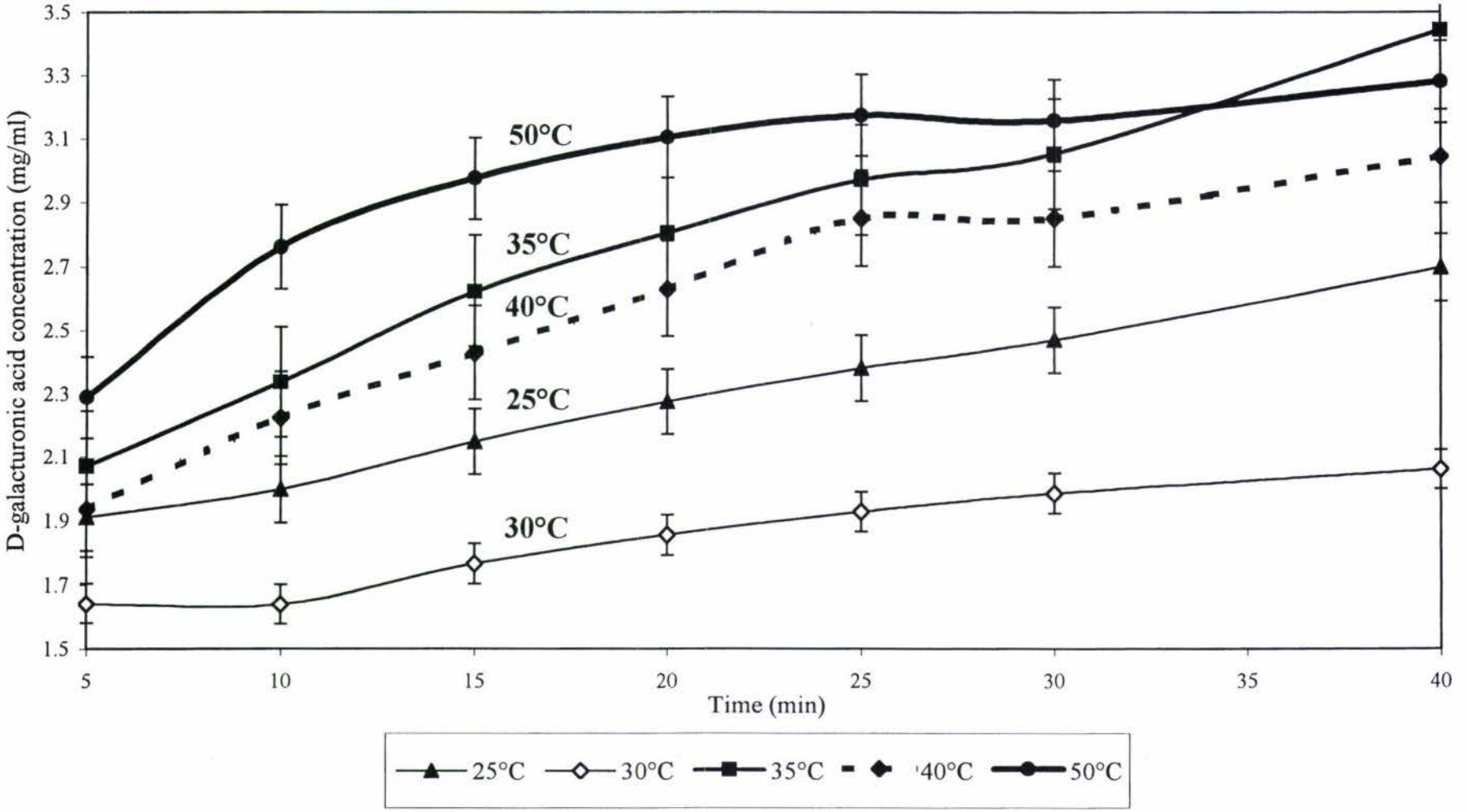

Figure 4.14 *Plot of the effect of temperature (25, 30, 35, 40, and 50°C) on PG enzyme activity (raw data shown in Appendix 7)*

Figure 4.14 shows the result of the study of PG activity at different temperatures. It is clear from the plot that the activity of PG enzymes in the dark red tomato pulp follows zero order kinetics at 25, 30 and 35°C because both plots of the concentration of D-galacturonic acid with time are straight lines. The 30°C data is shown in Figure 4.15 for clarity. The slope of the zero order plot is the rate constant (V_{max}).

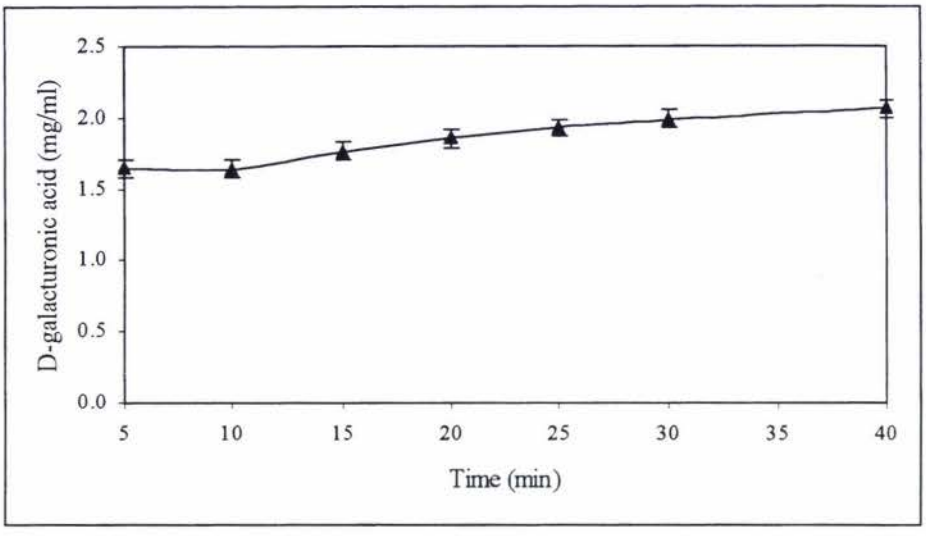

Figure 4.15 *Plot of PG activity in the dark red tomato pulp at 30°C*

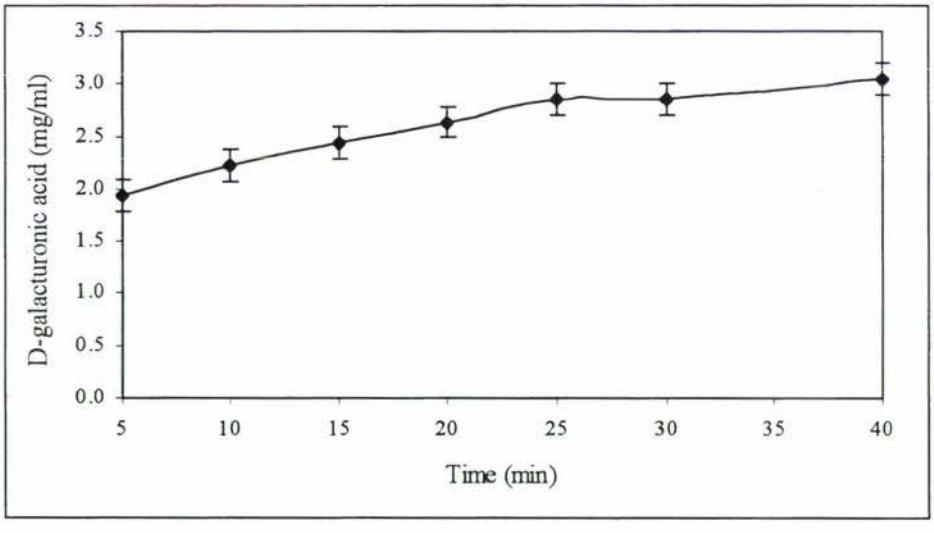

Figure 4.16 *Plot of PG activity in the dark red tomato pulp at 40°C*

It is clearly shown in Figure 4.16 that the plot of PG activity at 40°C is not zero order for all time. Therefore, at longer times substrate can become limiting and Michaelis-Menten kinetics are likely to be a better model to fit the kinetic data at 50°C as described below;

The determination of values for K_m and V_{max} in the batch kinetics of Michaelis-Menten can be analysed and shown below;

The rate of reaction is

$$v = -\frac{d[S]}{dt} = \frac{V_{max}[S]}{K_m + [S]} \qquad [4.21]$$

Integration of the substrate from $[S_o]$ to $[S]$ and time from 0 to t, yields

$$-\int_{S_o}^{S}\left(\frac{K_m + [S]}{V_{max}[S]}\right)d[S] = \int_0^t dt \qquad [4.22]$$

$$\left(\frac{K_m}{V_{max}}\int_{S_o}^{S}\frac{1}{[S]}d[S]\right) + \left(\frac{1}{V_{max}}\int_{S_o}^{S}d[S]\right) = -\int_0^t dt \qquad [4.23]$$

$$\frac{K_m}{V_{max}}(\ln[S] - \ln[S_o]) + \frac{1}{V_{max}}([S] - [S_o]) = -t \qquad [4.24]$$

$$K_m(\ln[S] - \ln[S_o]) + [S] - [S_o] = -V_{max}\,t \qquad [4.25]$$

$$K_m(\ln[S_o] - \ln[S]) - [S] + [S_o] = V_{max}\,t \qquad [4.26]$$

$$\left(K_m \ln\frac{[S_o]}{[S]}\right) + [S_o] - [S] = V_{max}\,t \qquad [4.27]$$

$$\frac{[S_o] - [S]}{t} = \left(-\frac{K_m}{t}\ln\frac{[S_o]}{[S]}\right) + V_{max} \qquad [4.28]$$

A plot of $\frac{1}{t}\ln\frac{[S_o]}{[S]}$ versus $\frac{[S_o]-[S]}{t}$ result in a line of slope $-K_m$ and intercept of V_{max}.

Eq. 4.28 can be divided by $\ln\frac{[S_o]}{[S]}$ to give the Michaelis –Menten equation in a different form as shown in Eq.4.29.

$$\frac{[S_o] - [S]}{\ln\frac{[S_o]}{[S]}} = -K_m + \frac{V_{max}t}{\ln\frac{[S_o]}{[S]}} \qquad [4.29]$$

If this is converted into terms of extent of reaction as shown in Eq. 4.30, rearrange and yield,

$$\frac{[S_o]}{[S]} = \frac{1}{(1-X)} \qquad [4.30]$$

Eq.4.29 can be written as;

$$\frac{[S_o]-[S]}{\ln\frac{1}{(1-X)}} = -K_m + \frac{V_{max}\,t}{\ln\frac{1}{(1-X)}} \qquad [4.31]$$

and $[S_o]-[S]=[S_o]X$, substitute $[S_o]-[S]$ in Eq.4.31,

$$\frac{[S_o]X}{\ln\frac{1}{(1-X)}} = -K_m + \frac{V_{max}t}{\ln\frac{1}{(1-X)}} \qquad [4.32]$$

divide Eq.4.32 by $[S_o]$, therefore,

$$\frac{X}{\ln\frac{1}{(1-X)}} = -\frac{K_m}{[S_o]} + \frac{V_{max}}{[S_o]}\,\frac{t}{\ln\frac{1}{(1-X)}} \qquad [4.33]$$

From Eq.4.33, a plot of $\dfrac{X}{\ln\frac{1}{(1-X)}}$ and $\dfrac{t}{\ln\frac{1}{(1-X)}}$ would produce a straight line of slope $\dfrac{V_{max}}{[S_o]}$ and intercept $-\dfrac{K_m}{[S_o]}$.

Therefore, the data at 50°C was plotted using the linear form of Eq.4.33 as shown in Figure 4.17.

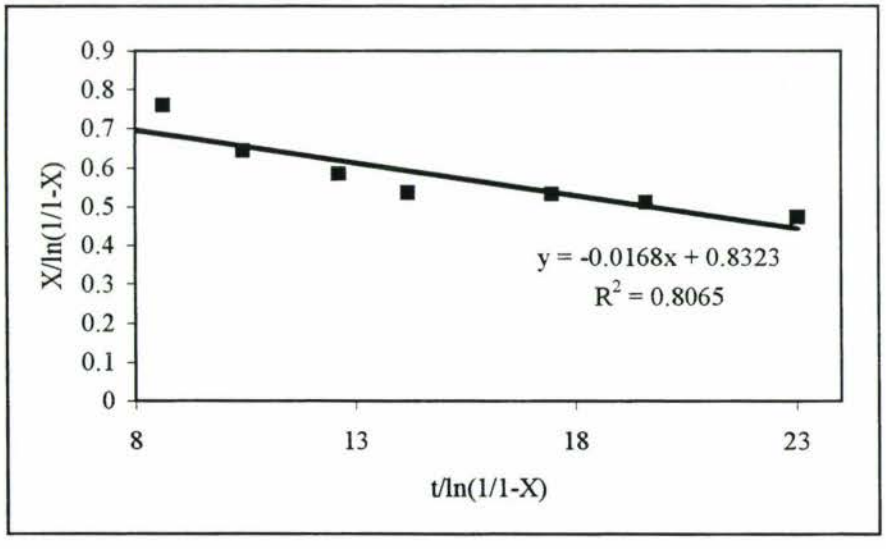

***Figure 4.17** Plot of PG activity in the dark red tomato pulp using Michaelis-Menten model at 50°C*

The plot shown in Figure 4.17 demonstrated that the Michaelis-Menten model fits the data reasonably. The slope of this plot is –0.0168 and the intercept is 0.8323. As it was explained above, the slope of the plot is equal to $\frac{V_{max}}{S_o}$ and the intercept is $-\frac{K_m}{S_o}$. It was difficult to perform this analysis for all the experimental data because the levels of initial substrate, although constant, was not known. In addition the enzyme levels of each pulp sample was not constant. For this reason the integrated form of the Michaelis-Menten equation was fitted to all the data at the same time.

The integrated form of the Michaelis-Menten equation in terms of product concentration is shown as the following;

$$-\frac{d[S]}{dt} = \frac{V_{\max}[S]}{K_m + [S]} \qquad [4.34]$$

where, $P = [S_o] - [S]$

therefore, $[S] = [S_o] - P$ [4.35]

differentiating Eq. 4.35 $\frac{d[S]}{dt} = 0 - \frac{dP}{dt}$ [4.36]

substituting of Eq.4.35 and Eq.4.36 in Eq.4.34 yields,

$$\frac{dP}{dt} = \frac{V_{\max}([S_o] - P)}{K_m + ([S_o] - P)} \qquad [4.37]$$

Integrating, gives $\int_0^P \left(\frac{K_m + 1}{[S_o] - P}\right) dP = \int_0^t dt$ [4.38]

therefore, $\left(-K_m \ln\left(\frac{[S_o] - P}{[S_o]}\right)\right) + P = V_{\max} t$ [4.39]

rearranged, this gives

$$P = [S_o]\left(1 - \exp\left(\frac{-V_{\max} t + P}{K_m}\right)\right) \qquad [4.40]$$

where, $V_{\max} = k_{eo} C_e \exp\left(\frac{-E_e}{R(T + 273)}\right)$

The square residual method was used to fit the model to predict the unknown values. The solver tool in Excel was then used to minimise the sum of square residuals for the model compared with experimental data to achieve the best values of the unknown variables (E_a, K_m, k, C_e, and S_o). The plot of PG activity between the empirical data and the model by the square residue method is shown in Figure 4.18.

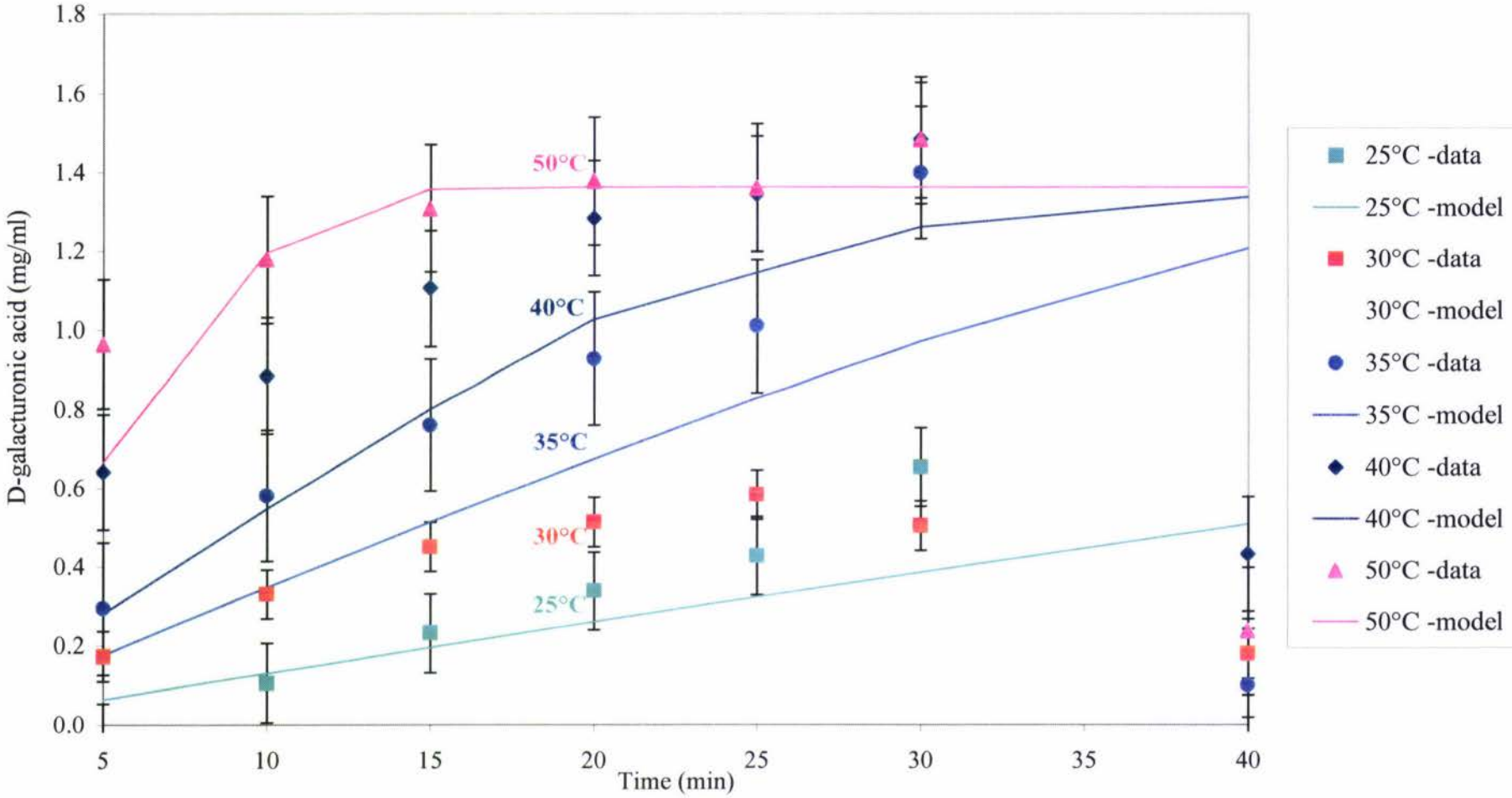

Figure 4.18 *Plot of PG activity as a function of temperatures (25,30,35,40,and 50°C) between empirical data and model using least square residual method*

The fitted parameters resulting from the analysis were;

$$E_e = 75{,}600 \quad \frac{J}{mol}$$

$$K_m = 0.18 \times 10^{-3} \quad \frac{kg}{kg}$$

$$k_{eo}C_{eo} = 4.4 \times 10^{9} \quad \frac{1}{s}$$

$$S_o = 1.364 \times 10^{-3} \quad \frac{kg}{kg}$$

The activation energy of enzyme-catalyzed reactions is generally in the range 17000-84000 J/mol (Shuler and Kargi,1992). The result obtained in the work for PG activity was 75,600 J/mol which is in the range suggested. The high activation energy shows the PG enzymes are quite temperature sensitive. A low value of K_m, 0.18×10^{-3} kg/kg, shows that the enzyme has high affinity to the substrate.

The study of PG enzymes in the temperature range 30 to 50°C revealed a strong temperature dependence of the PG enzymes. In tomato processing, the temperature of break process at 30 to 50°C can not inhibit the activity of PG enzymes. The study of PG inactivation of higher temperatures was then needed. This topic is the subject of the next section.

4.7 Thermal degradation of PG enzyme during break process

When tomato pulp is heated, the rate of PG enzyme inactivation is different depending on the temperature. There are a few authors who have studied the effect of higher temperature on PG enzyme activity as follows.

Lopez *et al.*(1997) investigated the thermostability of PG and PE enzymes in tomatoes at physiological pH (pH 4.0). The heat treatments were performed at cold (60°C) and hot break (90-95°C) temperatures for PGI and PGII. PGI is more thermoresistant than PGII, therefore, higher temperatures were applied to PGI to achieve enzyme inactivation. It was found that the cold break process could destroy PGII only slightly but could not destroy PGI and PE. The kinetic studies on PGI and PGII are shown as Figures 4.19 and 4.20 respectively.

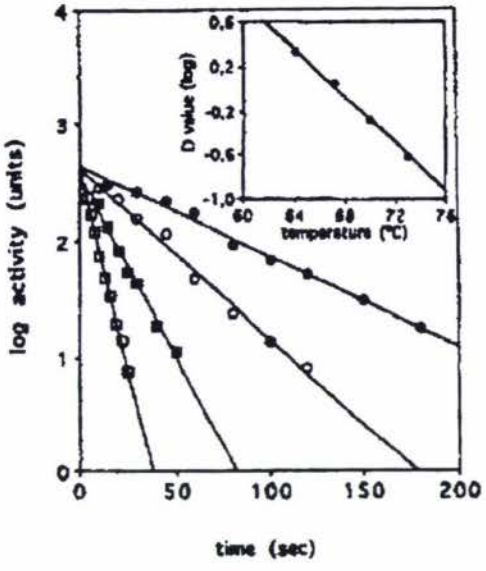

Figure 4.19 *Heat treatment of PG1 at 86°C(•), 90°C(o), 92.9°C(■), and 95.4°C(□) (Lopez et al., 1997)*

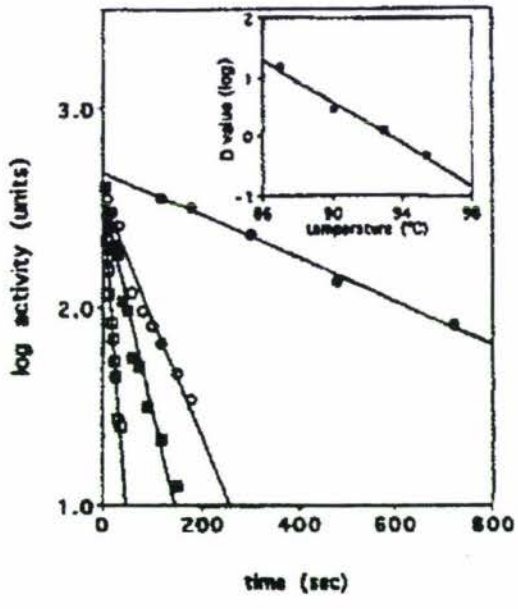

Figure 4.20 *Heat treatment of PG2 at 64°C(•), 67.2°C(o), 70°C(■), and 73°C(□) (Lopez et al., 1997)*

These figures show that the inactivation of PGI and PGII follows first-order kinetics. D and Z value were reported as in Table 4.6.

Table 4.6 *D and Z value for PGI and PGII (Lopez et al.,1997)*

Enzymes	*D-value*	*Z-value*
PGI	15.9 min at 87°C to 0.46 min at 95.4°C	5.6°C
PGII	2.14 min at 64°C to 0.24 min at 73°C	9.4°C

At a break temperature of 82°C, 3.5 sec was required to reduce PGII activity to1% of its original value whereas the time was prolonged to 200 min for PGI to reach 1% activity.

Lopez *et al.*(1998) investigated the inactivation of pectic enzymes by manothermosonication, the combination of heat and ultrasound under moderate pressure. Heat treatment has a negative impact on the characteristics of tomato products, such as colour, flavour, and nutritional value. Manothermosonication can inactivate the enzyme with little heating applied. Figure 4.21 and 4.22 show the inactivation of PGI and PGII by simple heating and by manothermosonication.

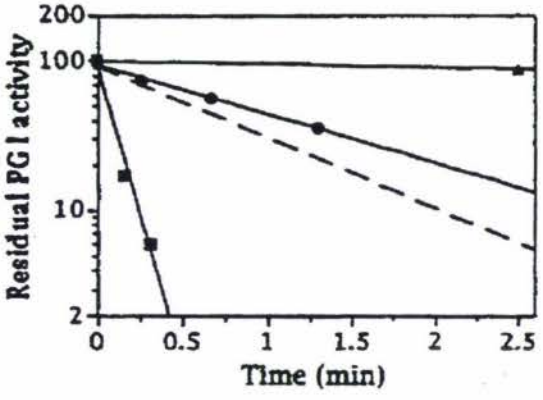

Figure 4.21 *PGI inactivation by: simple heat treatment at 86°C (▲) and MTS at 37°C (•) and 86°C (■). The dashed line represents the theoretical additive effect of enzyme inactivation by MTS at 37°C and heating at 86°C (Lopez et al.,1998)*

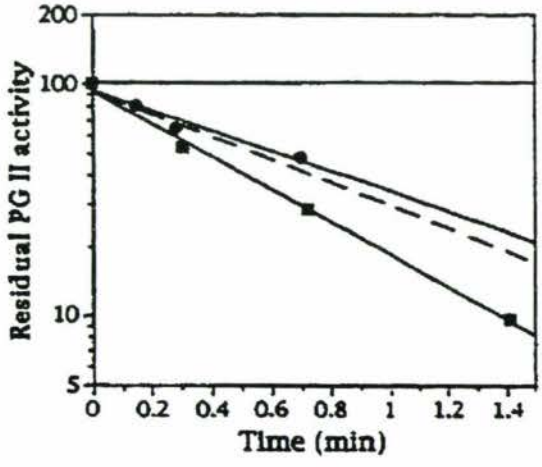

Figure 4.22 *PGII inactivation by: simple heat treatment at 52.5°C (solid line) estimated from experimental data for 50°C, 64°C and 70°C and MTS at 37°C (•) and 52.5°C (■). The dashed line represents the theoretical additive effect of enzyme inactivation by MTS at 37°C and heating at 52.5°C (Lopez et al.,1998)*

The results showed that MTS has a high inactivation efficiency with respect to tomato pectic enzymes. MTS inactivation of both PG enzymes follows first-order kinetics which allows the expression of reaction rates in terms of D values as in Table 4.7.

***Table 4.7** D values for inactivation of PG enzymes by simple heating and manothermosonication at different temperatures (Lopez et al.,1998)*

Enzymes	*MTS*				*Heating*		*D heat/D MTS*	
	Temp(°C)	*D(min)*	*Temp(°C)*	*D(min)*	*Temp(°C)*	*D(min)*	*Temp(°C)*	*Efficiency ratio*
PGI	37	3.17±0.2	86	0.24±0.02	86	20.6±0.1	86	85.8
PGII	37	2.23±0.3	52.5	1.46±0.05	52.5	38.4±0.1	52.5	26.3

It was concluded that manothermosonication can reduce the heating time of PGI, the most thermostable tomato pectic enzyme from 20 min at 86°C to 30 sec at the same temperature. Manothermosonication should be investigated for the future application when ultrasound technology becomes less expensive.

In present study, the effect of thermal degradation of PG enzymes was investigated in the temperature range from 50-80°C. The experiments are quite similar to the previous study on the study of the effect of temperature to PG enzymes. The detail is shown below.

4.7.1 Experimental Design

The experiments were carried out using the following procedures.

Dark red tomatoes selected according to the procedure given in chapter 3 above, were chosen to blend and make the pulp preparation for these experiments. Triplicate samples were prepared to ensure the repeatability of results in the study. Four to five fruits were daily blended and chilled in the ice bin before the assay started.

The change in PG activity was determined by following the level of total reducing sugar after the pulp was added to 100 ml 10% PGA solution. The total reducing sugar assay was described in section 4.1.4 above.

- About 2.5 g of Dark Red tomato pulp was added to 10% polygalacturonic acid solution (PGA) at a range of temperatures (30,50,55,60,65,70, and 80°C). 10% PGA solution was used to ensure the excess of substrate.

- The flask was immersed in a waterbath and the PG activity assay was followed the same procedure as described in 4.6.5.

4.7.2 Results and discussion

It was known that temperature affects the rate of the PG enzyme reaction from the previous study. Above some certain temperature, enzyme activity decreases with temperature because of enzyme denaturation (Shuler and Kargi,1992).

The plot of the PG activity at different temperatures (30,40,50,55,60,65,70, and 80°C) is shown as Figure 4.23.

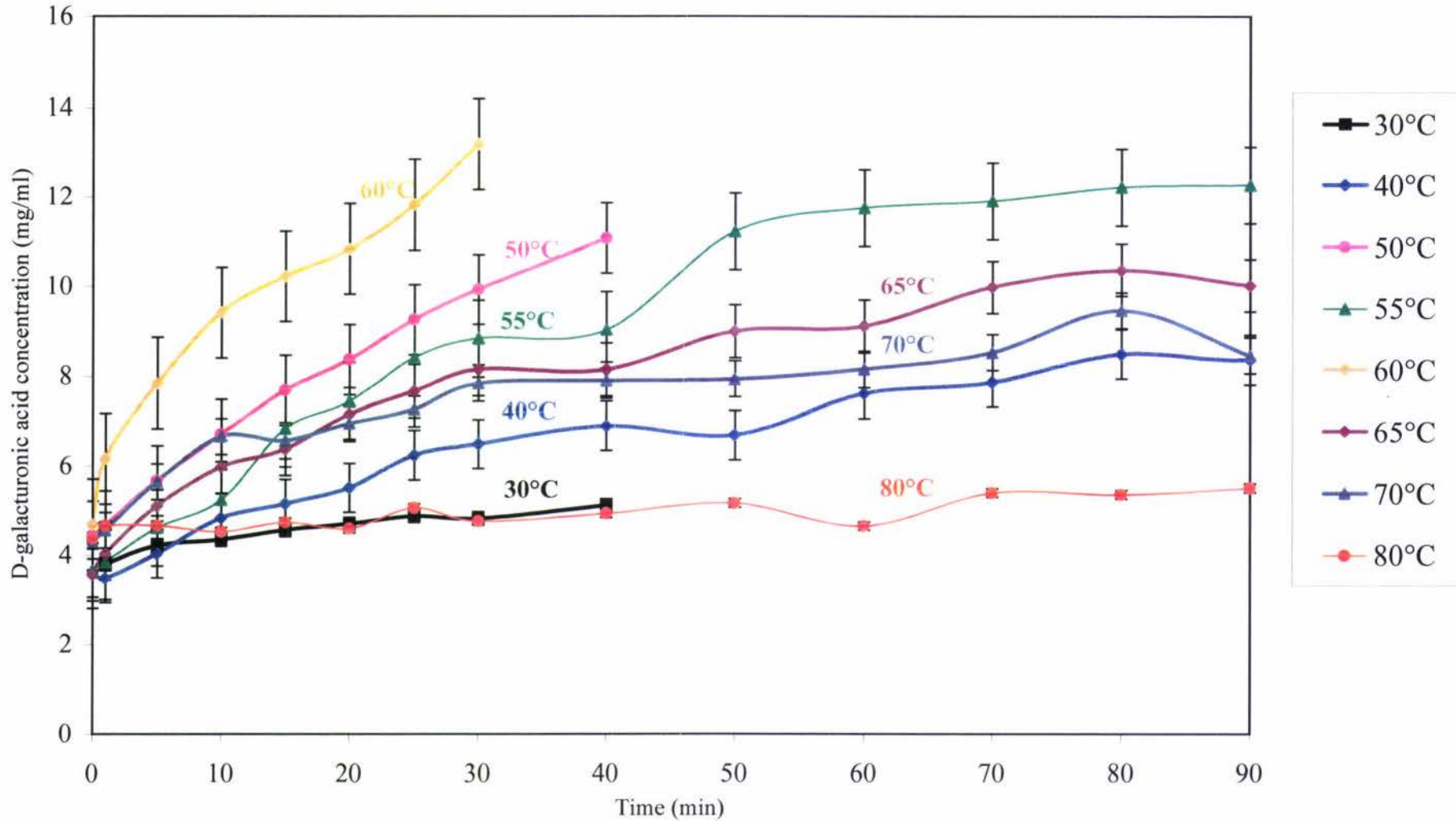

Figure 4.23 *Plot of PG activity at different temperatures (30,40,50,55,60,65,70, and 80°C)(raw data shownin Appendix 8)*

Figure 4.23 shows the increase of D-galacturonic acid does not follow zero order at temperature higher than 60°C. Above this temperature, the concentration of D-galacturonic acid starts to level off because of enzyme denaturation.

At 70 and 80°C, the concentration of D-galacturonic acid increased within the first 15 minutes and leveled off after that. The higher the temperature, the lower the final concentration of D-galacturonic acid.

The experimental data collected was fitted to the Michaelis-Menten model to determine the parameters V_{max} and K_m using the method minimisation of the squared residuals. This method can give the order of the reaction with respect to all components at one time and is not influenced by the experimenter's biases in fitting lines to experimental points (Levenspiel,1992).

To do this we needed an equation describing how the product concentration (P) changes with time. The Michaelis-Menten model is shown as the following;

$$\frac{dP}{dt} = -\frac{dC}{dt} = \frac{V_{\max} C}{K_m + C} \qquad [4.41]$$

Because the experiments were designed so substrate concentration would not be limiting. (ie $C \geq K_m$), this simplifies to zero order kinetics.

$$\frac{dP}{dt} = V_{\max} \qquad [4.42]$$

where V_{max} is dependent on the enzyme level and temperature and can be given as Eq.4.43 for the case of unchanging enzyme level.

$$V_{\max} = k_{eo} C_{eo} \exp\left(-\frac{E_e}{RT}\right) \qquad [4.43]$$

where k_{eo} = Arrhenius constant for enzyme hydrolysis $(\frac{1}{s})$

C_{eo} = Initial enzyme concentration $(\frac{kg}{kg})$

E_e = Activation energy for enzyme hydrolysis $(\frac{J}{mol})$

This model was fitted to experimental data in the previous section for the case where no enzyme inactivation occurred. This provided the following data.

K_m = 0.18×10^{-3} $\frac{kg}{kg}$

E_e = 75,600 $\frac{J}{mol}$

$$k_{eo}C_{eo} = \quad 4.4\text{x}10^{9}\ \frac{1}{s} \quad \text{for dark red pulp}$$

($k_{eo}C_{eo}$ changes with fruit ripeness)

At higher temperature, the enzyme is inactivated. This reaction is known to follow first order kinetics (Lopez *et al.*,1998) and can be written as

$$\frac{dC_e}{dt} = -k_d C_e = -\left(k_{do}\exp\left(-\frac{E_d}{RT}\right)\right)C_e \qquad [4.44]$$

where k_d = Rate constant for enzyme inactivation $\frac{1}{s}$

k_{do} = Arrhenius constant for enzyme inactivation $\frac{1}{s}$

E_d = Activation energy for enzyme degradation $\frac{J}{mol}$

Because all experiments were made at constant temperature it is possible to integrate this equation to give;

$$C_e = C_{eo}\exp\left(-k_d t\right) \qquad [4.45]$$

As a result the rate of product formation under the experimental conditions can be given as;

$$\frac{dP}{dt} = k_{eo}\left(C_{eo}\exp(-k_d t)\right)\exp\left(-\frac{E_e}{RT}\right) \qquad [4.46]$$

where k_d will be dependent on the temperature according to Eq.4.46, gives

$$k_d = k_{do}\exp\left(-\frac{E_d}{RT}\right) \qquad [4.47]$$

If this differential equation (Eq.4.46) is integrated for constant temperature an expression describing the changing concentration of P over time can be obtained.

$$\int_0^P dP = k_{eo}C_{eo}\exp\left(-\frac{E_e}{RT}\right)\int_0^t \exp\left(-k_d t\right)dt \qquad [4.48]$$

$$P = \left(\frac{k_{eo}C_{eo}}{k_d}\exp(-\frac{E_e}{RT})\right)\left(1-\exp(-k_d t)\right) \qquad [4.49]$$

Equations 4.47 and 4.49 were then fitted to the experimental data in Figure 4.24 by minimising the square of the residuals using an Excel spreadsheet. The following parameters were obtained.

$$k_{eo}C_{eo} = \quad 4.4\text{x}10^{9} \ \frac{1}{s}$$ (because it varies with pulp sample and there are not enough degree of freedom to separate k_{eo} from C_{eo})

$$k_{do} = \quad 1.67\text{x}10^{18} \ \frac{1}{s}$$

$$E_d = \quad 136{,}474 \ \frac{J}{mol}$$

The value of E_e calculated in the previous section was used in this process. Figure 4.24 shows a comparison of the fitted model to the experimental data.

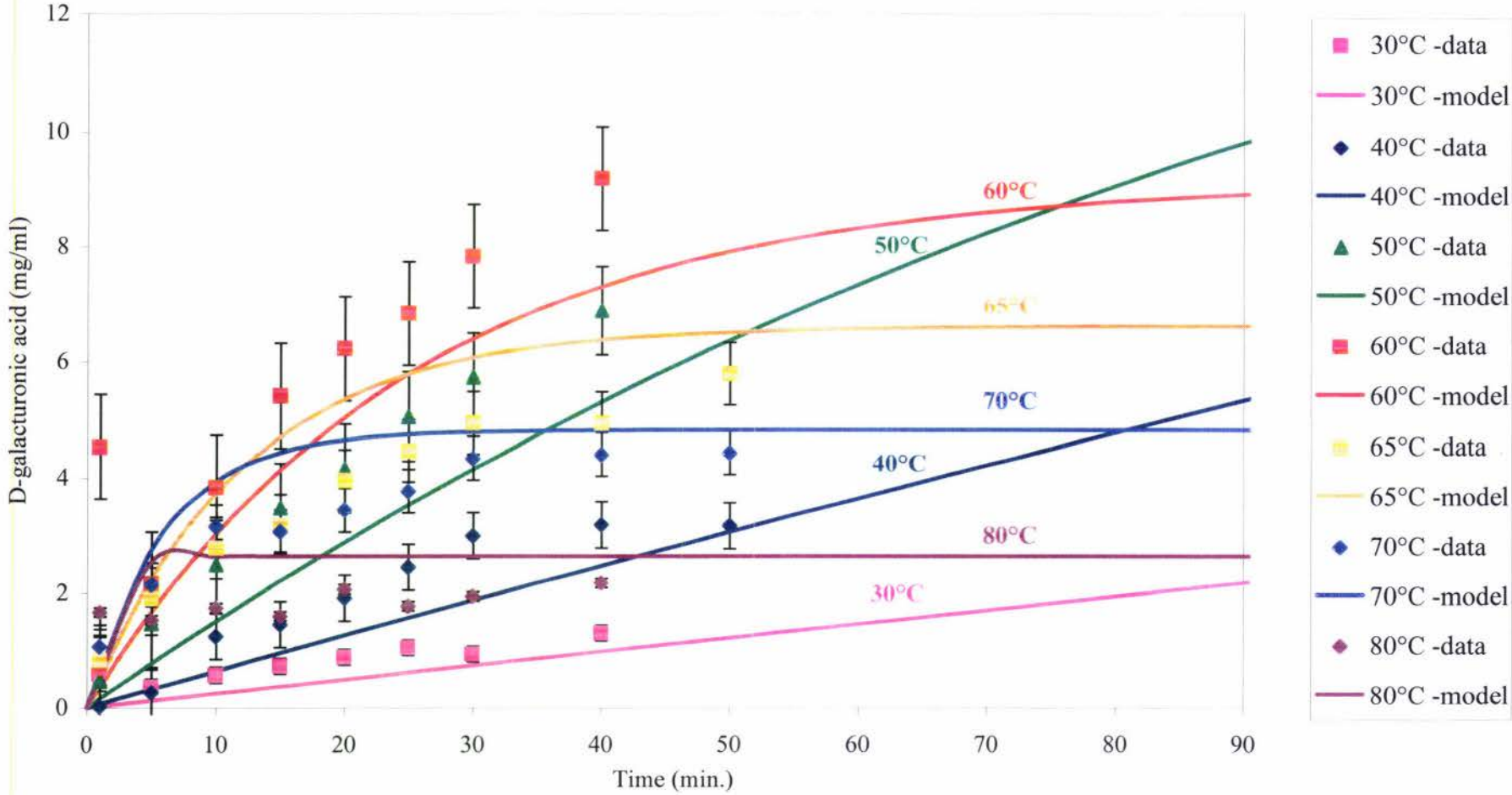

Figure 4.24 *Plot of PG activity as a function of temperature s(30,40,50,60,65,70,and 80°C) between empirical data and model using square residual method*

The activation energy for enzyme degradation is usually in the range 160-500 kJ/mol (Shuler and Kargi,1992). In this study, the activation energy of enzyme degradation was found to be 136 kJ/mol which is slightly less than this range, although it is sensible. The activation energy of enzyme hydrolysis, which is 76 kJ/mol, is lower than the activation energy of enzyme destruction, which is 136kJ/mol, suggesting that the enzyme can be denatured by operating the process at high temperature for a short time.

4.8 Conclusions

From the experiments outlined in this chapter an overall kinetic model for pectin hydrolysis and enzyme destruction in the tomato break process was achieved.

In summary, the kinetic equations for pectin hydrolysis in tomatoes are as follows;

- $$\frac{dC_{pt}}{dt} = -\frac{V_{\max} C_{pt}}{K_m + C_{pt}}$$
- $$V_{\max} = (k_{eo} C_{eo}) \exp \frac{-E_e}{RT}$$

The value for each parameter were shown as follows;

K_m = 0.18×10^{-3} $\frac{kg}{kg}$

E_e = 75,600 $\frac{J}{mol}$

C_{pti} = 4×10^{-3} $\frac{kg}{kg}$

The kinetic equation describing enzyme destruction was modified to the following due to the inability to separate k_{eo} from C_e in the experimental work.

- $$\frac{d(k_{eo} C_e)}{dt} = -k_{do} (k_{eo} C_e) \exp(\frac{-E_d}{RT})$$

where k_{do} = 1.67×10^{18} $\frac{1}{s}$

E_d = 136,474 $\frac{J}{mol}$

The initial concentration of pectic enzymes in fresh pulp ($k_{eo}C_{eo}$) varies with ripeness. Table 4.8 summaries the range of values obtained in this work.

Table 4.8 *Values of $k_{eo}C_{eo}$ at different tomato ripeness at 30°C*

Ripeness	$k_{eo}C_{eo}$ *(1/s)*
Green	0
Breaker	$1.83\text{-}3.5\text{x}10^{8}$
Turning	$1.83\text{-}4.5\text{x}10^{8}$
Orange	$4.5\text{x}10^{8}\text{-}1.42\text{x}10^{9}$
Dark red	$9.83\text{x}10^{8}\text{-}1.42\text{x}10^{9}$

These equations are of a form suitable for inclusion in a mathematical model of the commercial tomato production system which is developed in the next chapter.

Chapter 5
Break process model

5.1 Introduction

In tomato processing, the break process is the process to inactivate enzymes and, as an example, PG enzymes using heat. PG enzyme activity in the cell wall and locular gel of the tomato fruit decreases the consistency of tomato paste after crushing by hydrolysing the long chain of pectin. These results in the decreasing consistency of tomato pulp were discussed in Chapters 3 and 4.

Generally, there are two kinds of break process as carried out in industry, hot break and cold break. Heating above 60°C is applied to hot break processes and to less than 60°C for cold break processes. Hot break is more widely used for tomato processing because heat inactivates PG enzymes rapidly and the consistency of the final products is higher than cold break, although colour and flavour changes can also occur (Luh and Daoud,1971, Lopez *et al.*,1997, and Lopez *et al.*,1998).

In this study, a mathematical model was developed to describe the changes of tomato pulp temperature, pectin concentration, and enzyme concentration in the break tank and heat exchanger during break process operation. This model could then be applied to identify methods to improve control of the paste quality.

5.2 Model formulation

The mathematical model of break process is formulated and shown as the following:

5.2.1 Model purpose

The purpose of the modelling effort was to predict the changes of tomato pulp temperature, pectin and enzyme concentration over the break tank and the heat exchanger in the steady state as a function of time.

5.2.2 Conceptual model development

The break process for tomato pulp is shown in Figure 5.1. The feed at 20°C is pumped into the break tank and then a shell and tube of heat exchanger where the tomato pulp is heated using steam. Tomato pulp is recycled through the heat exchanger into the break tank to achieve the desired temperature. The tomato pulp from the break tank is then sent into the buffer tank to adjust pH and screened by a screener before it is sent to a juice tank. The tomato pulp is evaporated until reaches the required concentration and then sterilised and packaged. In this study, only the break process was considered.

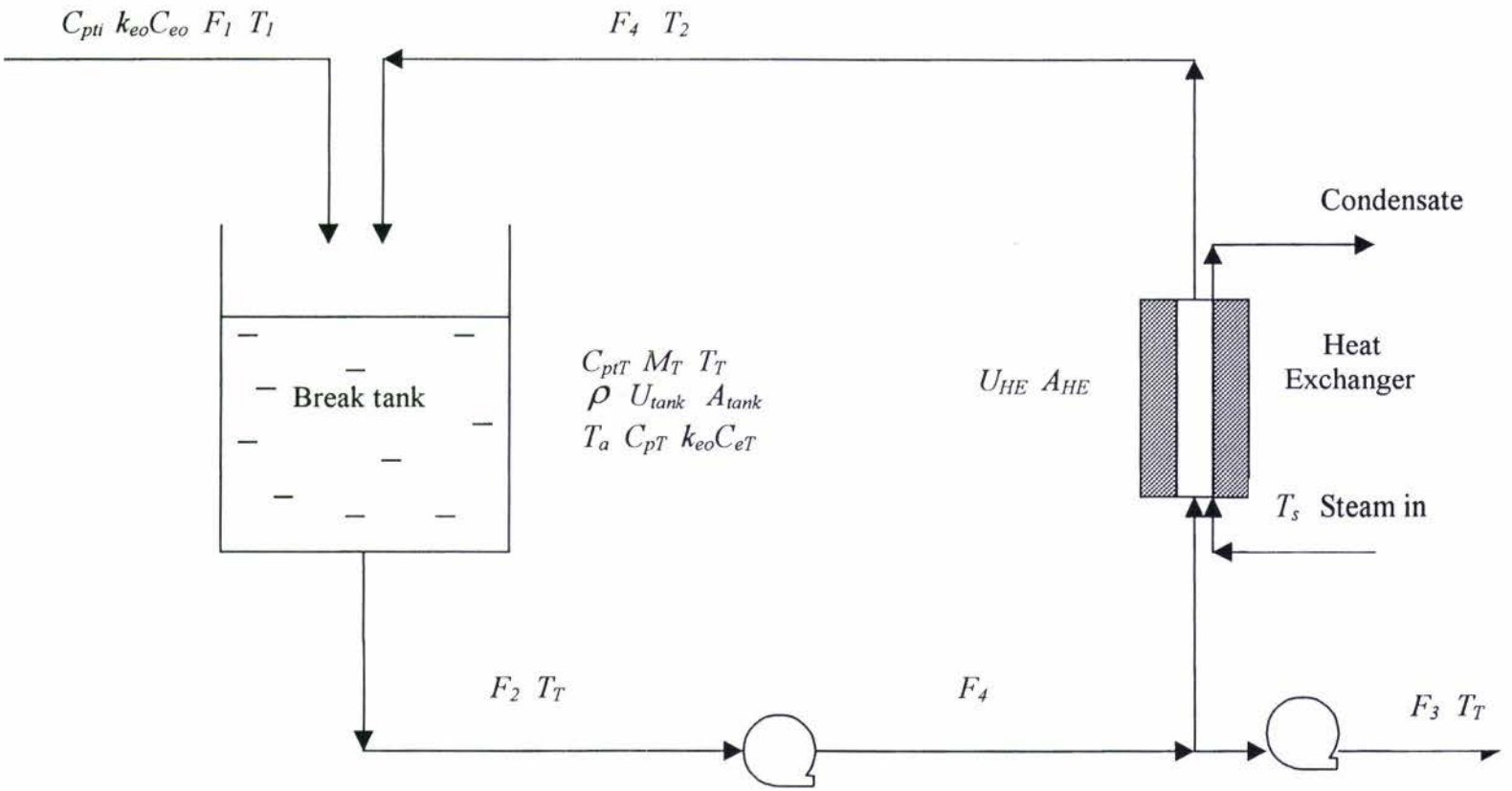

Figure 5.1 *Process diagram of the break tank in tomato processing*

5.2.2 Assumptions

The main assumptions of this model were:

-No evaporation.
-Complete mixing in the break tank.
-Constant thermal properties.
-Negligible tomato pulp hold up in pump or pipes.
-Constant flow rates.
-Constant ambient temperature.
-No heat generated by pump.
-PG enzyme activity and enzyme inactivation follows the kinetics described in chapter 4 above.
-Negligible heat losses

5.2.3 Validity of assumptions

The validity of each assumption used in the break process model is described below.

5.2.3.1 No evaporation

The tomato pulp is heated to 60-90°C in which range evaporation can be important. As a first model it was assumed that evaporation could be ignored because the break tank is a closed system.

5.2.3.2 Constant thermal properties

The tomato pulp can range in temperature from 20-80°C as it is recycled around the heat exchanger and heated up to inactivate enzymes which decrease the consistency of tomato pulp by hydrolysing long-chain pectin. Therefore, the validity of the assumption of constant thermal properties at different temperature should be investigated. Heat capacity of tomato pulp is one thermal properties of importance, so it is necessary to examine the changes that occur in tomato pulp over the temperature range 22 to 80°C.

Table 5.1 *Heat capacity of tomato pulp as a function of temperatures (22-80°C) at* X_w*=0.6410 (Rahman, 1995)*

Temperature (°C)	c_p ***(J/kg°C)***
22	3.2478
30	3.2536
40	3.2610
50	3.2687
60	3.2767
70	3.2849
80	3.2935

From Table 5.1, it is clearly seen that heat capacity of tomato pulp is increased only slightly with temperature. Heat capacity of tomato pulp is raised 1.38 % over the range 22 to 80°C. This change is very small, therefore, the assumption of constant thermal properties could be applied to this model.

5.2.3.3 Complete mixing in the break tank

It is assumed that the tomato pulp in the break tank is a uniform and homogeneous system. The tomato pulp is recycled through the heat exchanger at a high rate, promoting a high degree of mixing. The tank volume is completely turned over in approximately 3 minutes. As a result the pectin and enzyme concentration and temperature in the break tank can be assumed to be uniform.

5.2.3.4 Negligible tomato pulp hold up in the pump and pipeworks

In tomato processing, the tomato pulp is sent from the break tank through the pipe and pumped into the heat exchanger. The volume of the tomato pulp held in the pipe of the heat exchanger can be determined. The pipe is 6 metres long and 46 mm diameter. Therefore, the volume of the pulp in a pipe is 0.15 m^3 whereas the volume the break tank is 3.256m^3. Therefore, the volume of pipes is 5% of the volume of the break tank so can be negligible.

5.2.3.5 Constant flow rate

The flow rates of tomato pulp around the break process were assumed to be constant. A positive displacement pump recycles the tomato pulp around the break process and delivers a constant flow rate. If desired, user defined variable flow rates could be applied to the model.

5.2.3.6 Constant ambient temperature

The break tank is situated outside the plants. Although the ambient temperature changes with day to day climatic changes but it is relatively constant over time in the temperature range 25-30°C.

5.3 Mathematical formulation

The detail of the mathematical model formulation for the break tank during tomato processing are described in Appendix 2 and the nomenclature is shown in Appendix 1. The summary of the models are shown as the following:

An unsteady state total mass balance gives Eq.5.1 for the mass of pulp in the break tank.

$$\frac{dM_T}{dt} = F_1 + F_4 - F_2 \qquad \text{for } t \geq 0 \qquad [5.1]$$

An ordinary differential equations (ODE) describing the change in break tank temperature is given by Eq.5.2.

$$\frac{d(M_T T_T)}{dt} = F_1 T_1 + F_4 T_2 - F_2 T_T - \left(\frac{U_{tank} A_{tank} (T_T - T_a)}{c_{pT}} \right) \qquad \text{for } t \geq 0 \qquad [5.2]$$

The changes to temperature in the heat exchanger can be written as Eq.5.3.

$$\frac{dT}{dt} = \frac{2F_4}{N \rho A_{HE}} \frac{dT}{dx} + \frac{2U_{HE}}{\rho r_{HE} c_{pT}} (T_s - T) \qquad \text{for } t \geq 0,\ 0 < x < L \qquad [5.3]$$

with boundary conditions given by;

$$T = T_T \qquad @x = 0, t \geq 0 \qquad [5.4]$$

$$\frac{dT}{dx} = 0 \qquad @x = L, t \geq 0 \qquad [5.5]$$

and initial conditions;

$$T_T = T_{Ti} \qquad \text{for } t = 0 \qquad [5.6]$$

$$T = T_{Ti} \qquad \text{for } 0 \leq x \leq L, t = 0 \qquad [5.7]$$

The change in pectin levels can be modelled as follows;

In the break tank;

$$\frac{d(C_{ptT} M_T)}{dt} = F_1 C_{pt1} - F_2 C_{ptT} + F_4 C_{pt}(x = L) - \left(\frac{M_T V_{\max} C_{ptT}}{K_m + C_{ptT}} \right) \quad \text{for } t \geq 0 \qquad [5.8]$$

where $$V_{\max} = (k_{eo} C_{eT}) \exp\left(\frac{-E_e}{R(T_T + 273.15)} \right)$$

In the heat exchanger the pectin levels are given by;

$$\frac{dC_{pt}}{dt} = \frac{2F_4}{\rho A_{HE}} \frac{dC_{pt}}{dx} - \frac{V_{\max} C_{pt}}{K_m + C_{pt}} \qquad \text{for } t \geq 0,\ 0 < x < L \qquad [5.9]$$

where $$V_{\max} = (k_{eo} C_e) \exp\left(\frac{-E_e}{R(T_T + 273.15)} \right)$$

with boundary conditions;

$$C_{pt} = C_{ptT} \qquad @x = 0, t \geq 0 \qquad [5.10]$$

$$\frac{dC_{pt}}{dx} = 0 \qquad @x = L, t \geq 0 \qquad [5.11]$$

and initial conditions;

$$C_{ptT} = C_{pti} \qquad @t = 0 \qquad [5.12]$$

$$C_{pt} = C_{pti} \qquad for\, 0 \leq x \leq L, t \geq 0 \qquad [5.13]$$

The active enzyme levels were modelled using the following equations.

In the break tank;

$$\frac{d((k_{eo}C_{eT})M_T)}{dt} = F_1(k_{eo}C_{eo}) - F_2(k_{eo}C_{eT}) + F_4 k_{eo}C_e(x = L) - M_T k_{do}(k_{eo}C_{eT})\exp\left(\frac{-E_d}{R(T_T + 273.15)}\right) \quad \text{for } t \geq 0 \quad [5.14]$$

In the heat exchanger;

$$\frac{dk_{eo}C_e}{dt} = \frac{2F_4}{\rho A_{HE}}\frac{dk_{eo}C_e}{dx} - k_{do}(k_{eo}C_e)\exp\left(\frac{-E_d}{R(T + 273.15)}\right) \text{for } t \geq 0, 0 < x < L \quad [5.15]$$

with boundary conditions;

$$k_{eo}C_e = k_{eo}C_{eT} \qquad @x = 0, t \geq 0 \qquad [5.16]$$

$$\frac{dk_{eo}C_e}{dx} = 0 \qquad @x = L, t \geq 0 \qquad [5.17]$$

and initial conditions;

$$k_{eo}C_{eT} = k_{eo}C_{eo} \qquad @t = 0 \qquad [5.18]$$

$$k_{eo}C_e = k_{eo}C_{eo} \qquad @0 \leq x \leq L, t = 0 \qquad [5.19]$$

5.4 System input determination

There are many input parameters required in the break tank model. They were determined as described in the following sections.

5.4.1 Specific heat capacity of tomato pulp

The specific heat capacity of food products depends on the composition and temperature. Rahman (1995) reported a model relating specific heat capacity to product components as Eq. 5.20.

$$c_p = \sum_{i=1}^{N} c_{pi} X_i \qquad [5.20]$$

where c_{pi} = Specific heat capacity of component phase $\frac{J}{kg°C}$

X_i = Mass fraction of component i

It is shown in Eq. 5.20 that three main components in tomato pulp, water (87%), carbohydrate (8.9%), and fiber (0.4%), are required. The specific heat capacity of each component of food in the temperature range at –40°C to 150°C is shown as Eq.5.21-5.23, from Table 4.33 on p.264 of Rahman (1995). They are sumarised as the following.

For water,

$$c_w = 4.1762 - (9.0864x10^{-5}(T)) + (5.4731x10^{-6}(T^2)) \qquad [5.21]$$

For carbohydrates,

$$c_{ca} = 1.5488 + (1.9625x10^{-3}(T)) - (5.9399x10^{-6}(T^2)) \qquad [5.22]$$

For fiber,

$$c_{FI} = 1.8459 + (1.8306x10^{-3}(T)) - (4.6509x10^{-6}(T^2)) \qquad [5.23]$$

where T = Temperature (°C)

After the specific heat capacity of tomato pulp was optimised the results are shown as Table 5.2.

Table 5.2 *Calculated specific heat capacity of tomato pulp as a function of temperatures (22-80°C) and water contents*

Temperature (°C)	***c_p(kJ/kgK)***			
	X_w=0.641	***X_w= 0.748***	***X_w=0.816***	***X_w=0.945***
22	3.248	3.525	3.701	4.035
30	3.254	3.529	3.704	4.037
40	3.261	3.535	3.710	4.040
50	3.269	3.542	3.716	4.045
60	3.277	3.549	3.722	4.051
70	3.285	3.557	3.729	4.057
80	3.294	3.565	3.737	4.065

Table 5.2 shows that specific heat capacity is higher when the water fraction and temperature are higher. Actual experimental values of specific heat capacity of tomato pulp at 20 to 40°C were also given by Rahman (1995) as shown in Table 5.3. These literature values were plotted against the predictions from Table 5.2 and are shown in Figure 5.2.

Table 5.3 *Specific heat capacity of tomato pulp as a function of water fractions From Rahman's model (Rahman, 1995)*

X_w	***c_p (kJ/kgK)***
0.641	2.93
0.748	3.18
0.816	3.48
0.945	3.94

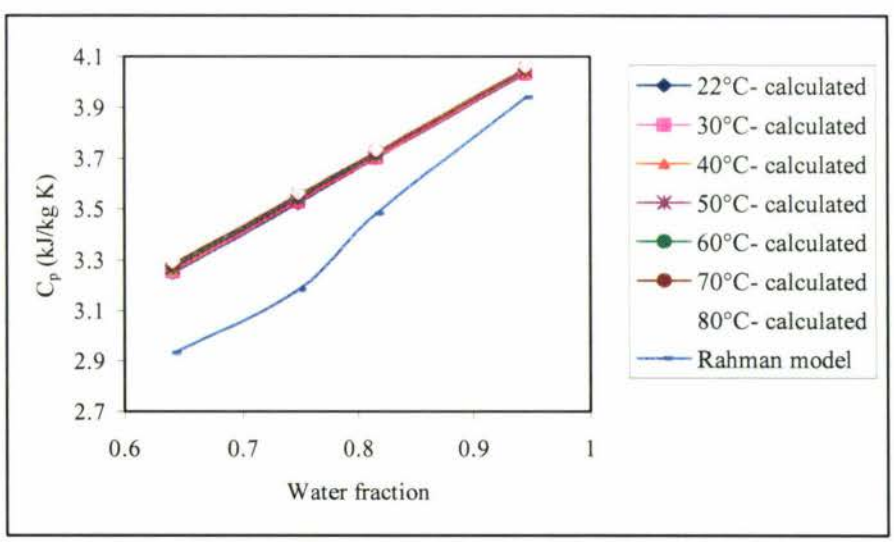

Figure 5.2 *Comparison of specific heat capacity of tomato pulp as a function of water fractions and temperatures between calculated values and experimental predictions based on Rahman's work*

Figure 5.2 demonstrates that the specific heat capacity from calculation and Rahman's experimental data are different. It is obvious that specific heat capacity for both calculated and Rahman's experimental values increases when water fraction is higher. The water content of pulp in the break tank is relatively constant (typically 87%). It can be seen from the model predictions, that the effect of temperature is very small and can be negligible. This suggests a single value of 3.7 kJ/mol should be used for model application in later work.

5.4.2 Thermal conductivity of tomato pulp

The thermal conductivity of tomato pulp can be predicted from the Parallel model. The equation is shown as Eq.5.24 (Rahman,1995).

$$\lambda = \sum_{i=1}^{n} \in_i \lambda_i \qquad [5.24]$$

where $\in_i$ = Volume fraction of ith component phase.

λ_i = Thermal conductivity of i phase.

The fractions of the main components of tomato pulp consist of water (87%), carbohydrate (8.9%), and fiber (0.4%). From Table 5.33 on p.327 of Rahman (1995), the equations for thermal conductivity of each food component were taken and used to predict thermal conductivity using Eq.5.25-5.27.

For water,

$$\lambda_w = 5.71x10^{-1} + 1.76x10^{-3}(T) - 6.70x10^{-6}(T^2) \qquad [5.25]$$

For carbohydrates,

$$\lambda_{ca} = 2.01x10^{-1} + 1.39x10^{-3}(T) - 4.33x10^{-6}(T^2) \qquad [5.26]$$

For fiber,

$$\lambda_{Fi} = 1.83x10^{-1} + 1.25x10^{-3} - 3.17x10^{-6}(T^2) \qquad [5.27]$$

where T= Temperature (°C)

These equations above used to predict thermal conductivity in the temperature range 20 to 80°C. Thermal conductivity of tomato pulp increases when the temperature is increased as shown in Table 5.4.

Table 5.4 *Calculated thermal conductivity of tomato pulp as a function of temperatures (20 to 80°C)*

Temperature (°C)	***Thermal conductivity (W/m K)***
20	0.5491
30	0.5613
40	0.5766
50	0.5919
60	0.6072
70	0.6225
80	0.6378

It is clearly shown that thermal conductivity increases with the temperature. These calculated values can be compared with the Rahman's experimental values sumarised in Rahman (1995) and shown in Table 5.5.

Table 5.5 *Thermal conductivity of tomato pulp as a function of temperatures and water contents from the Rahman model (Rahman,1995)*

Temperature (°C)	***Thermal conductivity (W/mK)***		
	X_w***=0.538***	X_w***=0.708***	X_w***=0.87***
30	0.4556	0.5904	0.7189
40	0.4601	0.6264	0.7849
50	0.4778	0.6538	0.8215

The calculated and Rahman's experimental values are compared in Figure 5.3.

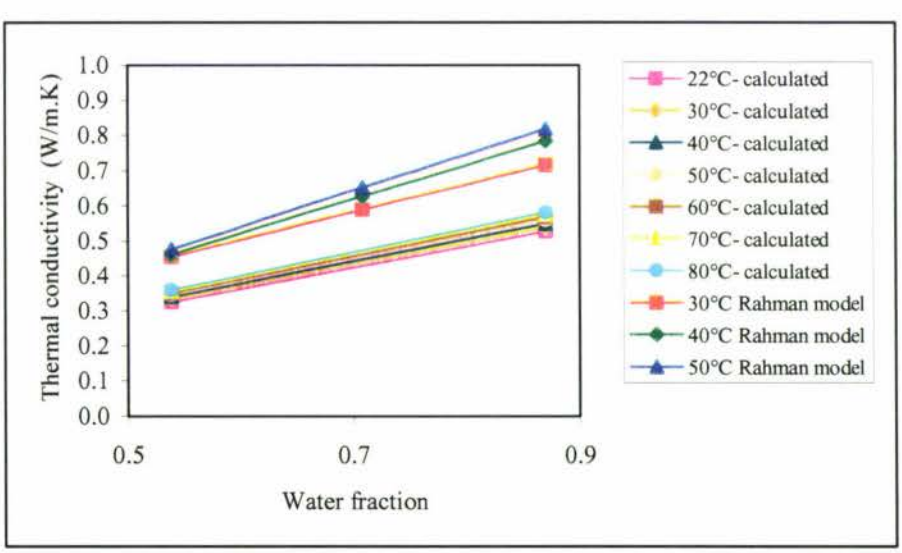

Figure 5.3 *Comparison of thermal conductivity of tomato pulp as a function of temperatures and water fractions between calculated values and experimental predictions based on Rahman's work*

It was found that thermal conductivity determined from Rahman's model is higher than the calculated values. The difference of thermal conductivity between Rahman's model and calculated values is quite high. As a result, the calculated data were used in this work.

5.4.3 Density of tomato pulp

The density of food materials is different, depending on the kind of food. Rahman (1995) reported how the density of major food components changes as a function of temperature and composition. From p.206 of Rahman (1995), the density of foods can be written as Eq.5.28.

$$\frac{1}{\rho_T} = \sum_{i=1}^{m} \frac{X_i}{(\rho_T)_i} \qquad [5.28]$$

where X_i = Mass fraction of each component

ρ_i = True density of component i.

Therefore, the fractions of main compositions of tomato pulp which are carbohydrates, fiber and water are needed. From the literature in Chapter 2, the composition of tomato paste consists of water (87%), carbohydrate (8.9%), and fiber (0.4%).

The equations of tomato food component densities are illustrated as Eq.5.29-5.31 (Rahman,1995).

For water,

$$\rho_w = 9.9718x10^2 + 3.1439x10^{-3}(T) - 3.7574x10^{-3}(T^2) \qquad [5.29]$$

For carbohydrates,

$$\rho_{ca} = 1.5991x10^3 - 0.31046(T) \qquad [5.30]$$

For fiber,

$$\rho_{FI} = 1.3115x10^3 - 0.36589(T) \qquad [5.31]$$

where T = Temperature (°C)

These equations were used to determine the density of tomato pulp in the temperature range 25 to 80°C. It was found that the density of tomato pulp decreases when the temperature is increased as shown in Table 5.6 and Figure 5.4.

Table 5.6 *Density of tomato pulp at different temperature (25-80°C)*

Temperature (°C)	***Density of tomato pulp (kg/m^3)***
25	1072
30	1070
40	1067
50	1064
60	1060
70	1055
80	1049

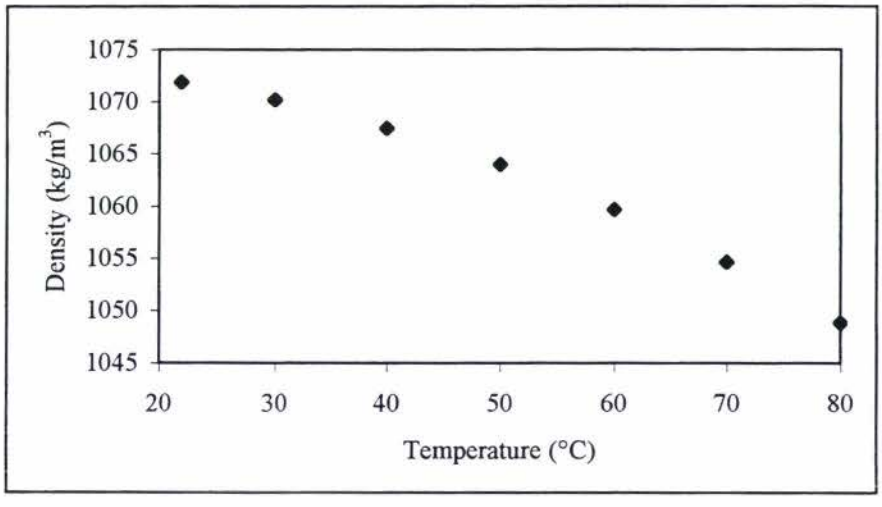

Figure 5.4 *Density of tomato pulp at different temperatures (25-80°C)*

The uncertainty introduced by assuming constant density of tomato pulp could be determined as the following.

$$Error = \frac{1074 - 1048}{1048} x100$$

$$= 2.5\%$$

It is clear that the error in assuming constant tomato density over the temperature range 20 to 80°C is very small. Therefore, an average value of 1060 $\frac{kg}{m^3}$ was used for the purposes of this work.

5.4.4 Ambient temperature

The ambient temperature of the break process in this study is approximately 15-25°C.

5.4.5 Surface area of break tank

The surface area of the break tank is required in the model to predict heat losses from the tank. The area of the break tank was calculated from the geometry of the tank at Heinz-Watties, King Street and was found to be 10.7m^2.

5.4.6 Maximum mass of tomato pulp in the break tank

When the break tank is full, the mass of tomato pulp was determined from density of tomato pulp and volume of the break tank. The maximum pulp mass in the break tank was found to be 3,500 kg.

5.4.7 Feed temperature

The temperature of tomato feed into the break tank was measured during a typical processing day at Heinz-Watties, Hastings and found to be approximately 20°C.

5.4.8 Steam temperature

The steam temperature into the heat exchanger was 140°C.

5.4.9 Flow rate to the break tank and through the heat exchanger

Typically a tomato feed (F_1) to the process is 2.3 kg/s as determined by observation at Heinz-Watties during a typical processing day. The flow rate (F_4) from the heat exchanger to the break tank was determined using a heat balance over the heat exchanger at steady state as follows.

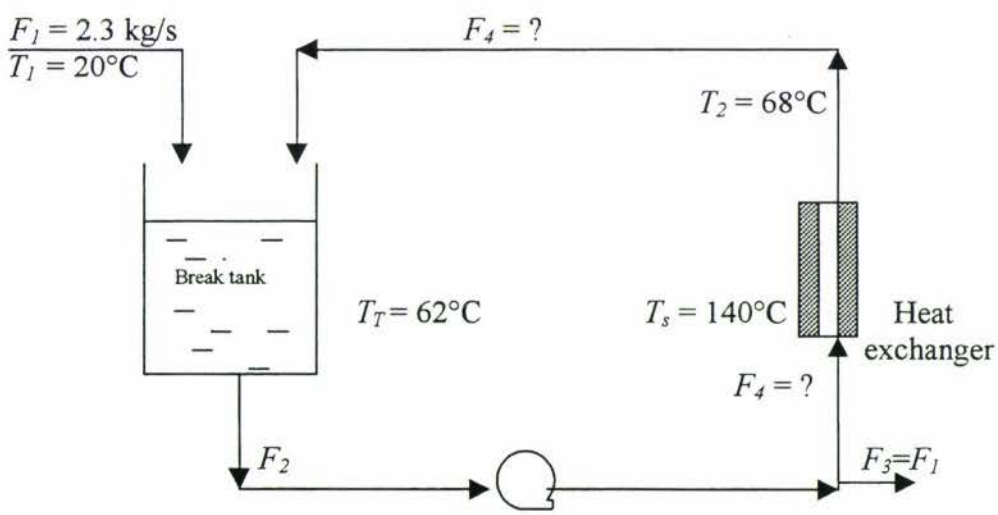

***Figure 5.5** Break process diagram over the break tank and the heat exchanger at steady state*

At steady state,

Rate of heat gain by the break tank content = Rate of heat transfer from the heat exchanger

$$F_1 c_{pT}(T_T - T_1) = F_4 c_{pT}(T_2 - T_T) \qquad [5.35]$$

$$F_4 = \frac{F_1(T_T - T_1)}{(T_2 - T_T)}$$

where parameters were measured as;

$$F_1 = 2.3\frac{kg}{s}$$
$$T_T = 62°C$$
$$T_1 = 20°C$$
$$T_2 = 68°C$$

Therefore, the flow rate could be calculated as;

$$F_4 = 16.1 kg/s$$

At steady state, $F_2 = F_1 + F_4$

$$F_2 = 2.3 + 16.1$$

$$= 18.4\frac{kg}{s}$$

The overall heat transfer capacity of the heat exchanger ($U_{HE}A_{HE}$) could be calculated in a similar way.

Rate of heat gain by tomato pulp in the break tank = Rate of heat transfer from the heat exchanger

$$F_1 c_{pT}(T_T - T_1) = U_{HE}A_{HE}\Delta T_{lm} = U_{HE}A_{HE}\left(\frac{(T_s - T_T) - (T_s - T_2)}{\ln\left(\frac{T_s - T_T}{T_s - T_2}\right)}\right) \qquad [5.36]$$

Therefore,

$$U_{HE}A_{HE} = \frac{F_1 c_{pT}(T_T - T_1)}{\frac{(T_2 - T_T)}{\ln\left(\frac{T_s - T_T}{T_s - T_2}\right)}}$$

Giving,

$$U_{HE}A_{HE} = 4972\frac{W}{K}$$

5.4.10 Convective heat transfer coefficient between tank and air

The heat transfer coefficient for losses to ambient air were as follows:

The temperature difference between the tomato pulp and air was typically 58°C. The heat transfer coefficient for natural convection from various surfaces could be developed from Table 4.7 – 2, p.256. Geankoplis (1993) for which Prandlt and Grasshoff numbers are required. The Prandlt number is shown as Eq.5.32.

For Prandt number,

$$N_{Pr} = \frac{c_{pair}\mu_{air}}{\lambda_{air}} \qquad [5.32]$$

where c_{pair} = Heat capacity of air $\frac{J}{kg°C}$

μ_{air} = Viscosity of air $\frac{kg}{m.s}$

λ_{air} = Thermal conductivity $\frac{W}{m.K}$

Average temperature = $\frac{22+80}{2}$ = 51°C

Geankoplis (1993) p.866, the physical properties of air were calculated as

c_{pair} = 1.007 $\frac{kJ}{kg.K}$

μ_{air} = 1.962×10^{5} $\frac{kg}{m.s}$

λ_{air} = 1.068×10^{-3} $\frac{W}{m.K}$

giving the value of N_{Pr} = 1.850×10^{11}

The Grasshoff number is given as

$$N_{Gr} = \frac{L\rho_{air}^{2} g\beta\Delta T}{\mu_{air}^{2}} \qquad [5.33]$$

From Table A.3-3 Physical Properties of Air at 1Atm,p.866 (Geankoplis,1993)

$\frac{g\beta\rho^{2}}{\mu_{air}}$ @ 51.0°C = 1.1638×10^{7} $\frac{1}{m^{3}}$

The length of break tank (L) was 2 m and the temperature difference was on average 58°C.

The Grasshoff number is given as,

$$N_{Gr} = 2^3 \times 1.638 \times 10^7 \times 51$$
$$= 6.683 \times 10^9$$

From Table 4.7 – 2, p. 256 Geankiplis (1993) with $N_{pr}\,N_{Gr}$ 1.236×10^{21}, the heat transfer coefficient could be found;

$$\text{Heat transfer coefficient } (U) = 1.24(\Delta T)^{1/3} \qquad [5.34]$$
$$= 1.24(51)^{1/3}$$
$$= 5 \quad W/m^2.K$$

The prediction is sensible for relatively stagnant air flows and was used in the prediction of heat loss in the break tank which is negligible as shown below;

Heat loss from the break tank to surroundings $= U_{\tan k} A_{\tan k} (T_T - T_a)$

$= 5x10.7x(62 - 15)$

$= 2514 \frac{J}{s}$

Heat gain from the heat exchanger $= F_4 c_{pT} (T_2 - T_T)$

$= 16.1x3874x(68 - 62)$

$= 374228 \frac{J}{s}$

When heat loss was compared with heat gain from the heat exchanger, it is 0.67%. Therefore, heat loss can be ignored.

5.4.11 Heat transfer coefficient of heat exchanger

Heat transfer coefficient of the heat exchanger could be determined from the equations of Geankoplis (1993) which depend on the fluid flow inside pipes (laminar, transitional, or turbulent flow). Dimensionless numbers such as Reynolds and Prandtl numbers are used to characterise the flow inside pipes.

The Reynolds number of tomato pulp could be determined as follows:

$$N_{Re} = \frac{Dv\rho}{\mu}$$

whereas D = Diameter of the tube inside the heat exchanger m
= 0.024 m

v = Velocity of tomato pulp inside the tube of the heat exchanger $\frac{m}{s}$

whereas Volumetric flow rate = 16000 $\frac{L}{hr}$

Number of tubes = 5

Length of each tube = 10 m

Area of each tube = πr^2

= $\pi \times 0.012^2$

= 4.526×10^{-4} m^2

$$v = \frac{16000}{3600x5x1000x4.526x10^{-4}}$$

$$= 1.964 \ \frac{m}{s}$$

ρ = Density of tomato pulp $\frac{kg}{m^3}$

$$= 1071 \ \frac{kg}{m^3} \ @ \ 20 \ ^\circ C$$

μ = Viscosity of tomato pulp $\frac{kg}{m.s}$

$$= 0.23 \ \frac{kg}{m.s}$$

$$N_{Re} = \frac{0.024x1.964x1071}{0.23}$$

$$= 219.49$$

From Geankoplis (1993), the flow inside pipes is laminar when N_{Re} below 2100, transition when N_{Re} between 2100 and 10^4, and turbulent when N_{Re} above 10^4.

Therefore, the flow in this work is laminar because N_{Re} is below 2100. Geankoplis (1993) reported that the following equation can be used to determine the heat transfer coefficient for laminar flow inside horizontal tubes or pipes.

$$\frac{UD}{\lambda} = 1.86(N_{Re}N_{Pr}\frac{D}{L})^{\frac{1}{3}}(\frac{\mu_b}{\mu_w})^{0.14} \qquad [5.37]$$

$$h_a = \frac{\lambda}{D}1.86(N_{Re}N_{Pr}\frac{D}{L})^{\frac{1}{3}}(\frac{\mu_b}{\mu_w})^{0.14}$$

whereas λ = Thermal conductivity $(\frac{W}{mK})$

$$= 0.6378 \ \frac{W}{mK}$$

N_{Pr} = Prandtl number

$$N_{Pr} = \frac{c_p\mu}{\lambda}$$

Previously the heat capacity was shown to be, c_p is 3.8743 $\frac{kJ}{kgK}$ when X_w= 0.87

$$N_{Pr} = \frac{3.8743x0.23x1000}{0.6378}$$

$$= 1397.13$$

Therefore, heat transfer coefficient of the heat exchanger could be determined from

$$U = \frac{\lambda}{D} 1.86 (N_{Re} N_{Pr} \frac{D}{L})^{\frac{1}{3}} (\frac{\mu_b}{\mu_w})^{0.14} \qquad [5.38]$$

where $\mu_b \cong \mu_w$

$$U_{HE} = \frac{0.6378}{0.024} x1.86x(219.49x1397.13x\frac{0.024}{10})^{\frac{1}{3}}$$

$$U_{HE} = 443 \ \frac{W}{m^2 K}$$

5.5 Numerical solution of the model

The temperature of tomato pulp, the pectin and enzyme concentration over the heat exchanger, formulated in the form of Partial deifferential equations (PDE) in section 5.3 were converted into ODE's in order to use Matlab to solve them. The length of heat exchanger was divided to 21 nodes (J=20). One ODE was then used to describe the change in heat, pectin, enzyme in each node in the heat exchanger. The transformation from PDE to ODE's is shown in the following.

The PDE's describing the temperature in the heat exchanger were transformed into the following ODE's.

For node j =1

$$\frac{dT_1}{dt} = \frac{2F_4(T_T - T_1)}{\rho\pi r^2 \Delta x} + \frac{2U_{HE}(T_s - T_1)}{\rho r c_{pT}} \qquad \text{for } t \geq 0 \qquad [5.39]$$

For nodes j = 2 to J

$$\frac{dT_j}{dt} = \frac{F_4(T_{j-1} - T_j)}{\rho\pi r^2 \Delta x} + \frac{2U_{HE}(T_s - T_j)}{\rho r c_{pT}} \qquad \text{for } t \geq 0 \qquad [5.40]$$

For node j = J+1

$$\frac{dT_{J+1}}{dt} = \frac{2F_4(T_J - T_{J+1})}{\rho\pi r^2 \Delta x} + \frac{2U_{HE}(T_s - T_{J+1})}{\rho r c_{pT}} \qquad \text{for } t \geq 0 \qquad [5.41]$$

Similarly for pectin in the heat exchanger;

For node j=1

$$\frac{dC_{pt}(1)}{dt} = \frac{2F_4(C_{ptT} - C_{pt}(1))}{\rho\pi r^2 \Delta x} - \frac{V_{\max} C_{pt}(1)}{K_m + C_{pt}(1)} \qquad \text{for } t \geq 0 \qquad [5.42]$$

$$\text{whereas} \quad V_{\max} = (k_{eo} C_e(1)) \exp\left(\frac{-E_e}{R(T(1) + 273.15)}\right)$$

For nodes j =2 to J

$$\frac{dC_{pt}(j)}{dt} = \frac{F_4(C_{pt}(j-1) - C_{pt}(j))}{\rho\pi r^2 L} - \frac{V_{\max} C_{pt}(j)}{K_m + C_{pt}(j)} \qquad \text{for } t \geq 0 \qquad [5.43]$$

$$\text{whereas} \quad V_{\max} = (k_{eo} C_e(j)) \exp\left(\frac{-E_e}{R(T(j) + 273.15)}\right)$$

For node j =J+1

$$\frac{dC_{pt}(j)}{dt} = \frac{2F_4(C_{pt}(J) - C_{pt}(J+1))}{\rho\pi r^2 \Delta x} - \frac{V_{\max} C_{pt}(J+1)}{K_m + C_{pt}(J+1)} \qquad \text{for } t \geq 0 \qquad [5.44]$$

$$\text{whereas} \quad V_{\max} = (k_{eo} C_e(J+1)) \exp\left(\frac{-E_e}{R(T(J+1) + 273.15)}\right)$$

And for the enzyme concentration in the heat exchanger

For node j = 1

$$\frac{dk_{eo}C_e(1)}{dt} = \frac{2F_4(k_{eo}C_{eT} - k_{eo}C_e(1))}{\rho\pi r^2 \Delta x} - \left(k_{do}(k_{eo}C_e(1)) \exp\left(\frac{-E_d}{R(T(1) + 273.15}\right)\right)$$

$$\text{for } t \geq 0 \qquad [5.45]$$

For node j = 2 to J

$$\frac{dk_{eo}C_e(j)}{dt} = \frac{F_4(k_{eo}C_e(j-1) - k_{eo}C_e(j))}{\rho\pi r^2 L} - \left(k_{do}(k_{eo}C_e(j)) \exp\left(\frac{-E_d}{R(T(j) + 273.15}\right)\right)$$

$$\text{for } t \geq 0 \qquad [5.46]$$

For node $j = J+1$

$$\frac{d(J+1)}{dt} = \frac{2F_4(k_{eo}C_e(J) - k_{eo}C_e(J+1))}{\rho\pi r^2 \Delta x} - \left(k_{do}(k_{eo}C_e(J+1))\exp\left(\frac{-E_d}{R(T(J+1)+273.15}\right)\right)$$

for $t \geq 0$ [5.47]

These mathematical models were solved numerically using Matlab's Runga Kutta, ode-solver 45. The Matlab files are shown in Appendix 3.

5.6 Model checking

After the formulation of the model was solved in Matlab, the correctness of Matlab programme and programming errrors was checked, for numerical accuracy.

5.6.1 Numerical error checking

To check for numerical errors in the Matlab solution, the tolerance value in the ode solver was altered to see if the effect of step size (characterised by Relative Tolerance (Rel. Tol.) in Matlab) occured. The Relative Tolerance was changed by running with the default telerance 1e-6 and run again with 1e-7. The results were checked for the tank temperature, pectin fraction and enzyme fraction as shown in figure 5.6, 5.7, and 5.8.

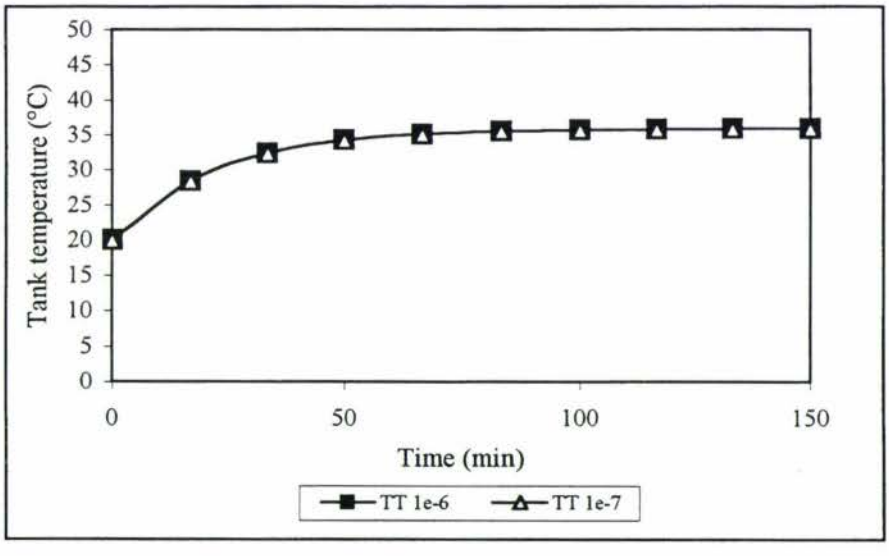

***Figure 5.6** Tank temperature at Rel. Tol. number of 1e-6 and 1e-7*

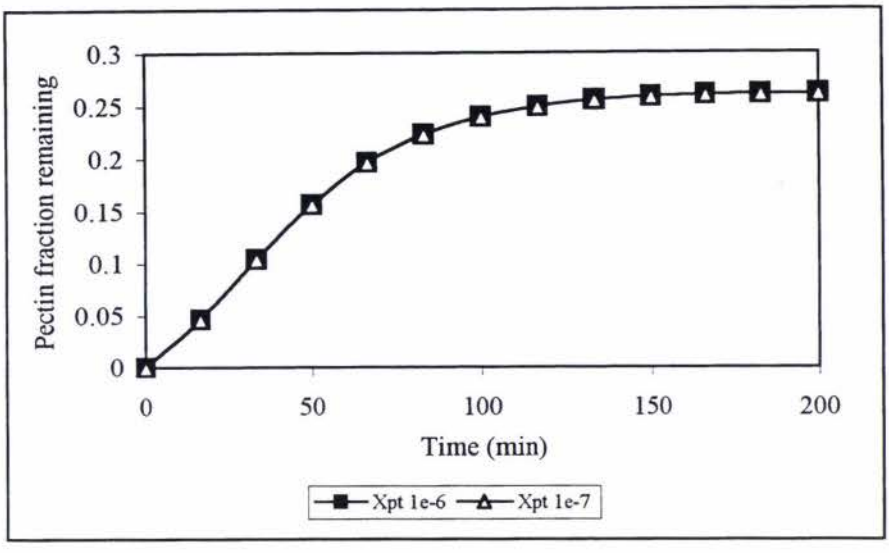

Figure 5.7 *Pectin fraction remaining at Rel. Tol. number of 1e-6 and 1e-7*

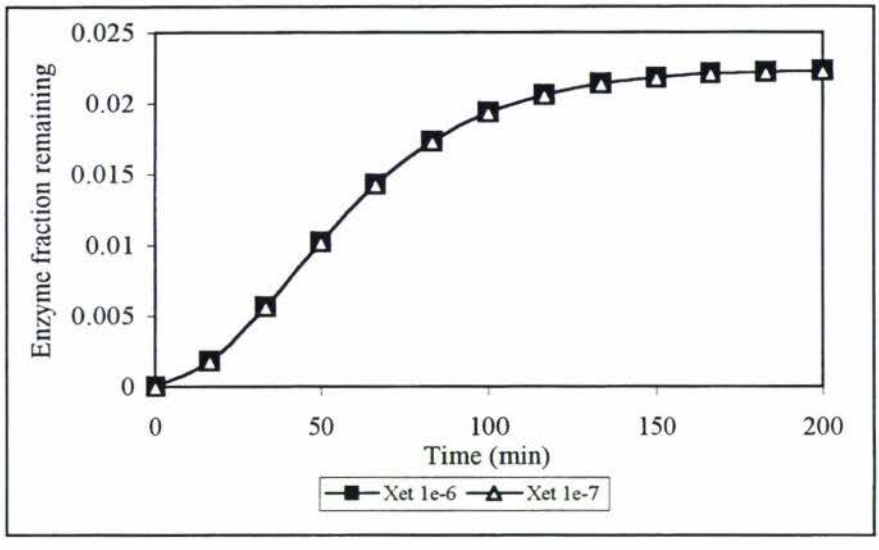

Figure 5.8 *Enzyme fraction remaining at Rel. Tol. number of 1e-6 and 1e-7*

It is clearly that there is no numerical error was present between different Rel. Tol. numbers of 1e-6 and 1e-7 for tank temperature, pectin and enzyme fractions. This indicated that time step control was acceptable for model use. In a similar way the effect of number of nodes (J) was checked. It was found that running the solution with 20 nodes was sufficient to avoid numerical errors.

5.6.2 Analytical checking

After numerical error checking confirmed that there were no errors in the Matlab solution, the model was simplified to allow comparison of the results with an analytical solution. Such checks were carried out to demonstrate confidence in the model solution before applying it to the break process.

The tank temperature and mass of tomato pulp were investigated. The unsteady state heat balance for the break tank could be simplified and solved analytically as shown below.

5.6.2.1 Tank temperature

From the unsteady state heat balance of the break tank:

$$\frac{d(M_T T_T)}{dt} = F_1 T_1 + F_4 T_2 - F_2 T_T - \frac{U_{\tan k} A_{\tan k} (T_T - T_a)}{c_{pT}} \qquad \text{for } t \geq 0 \qquad [5.48]$$

The model was simplified to give Eq.5.49 by setting the feed and recycle rate to zero.

$$M_T \frac{(dT_T)}{dt} = -\frac{U_{\tan k} A_{\tan k} (T_T - T_a)}{c_{pT}} \qquad \text{for } t \geq 0 \qquad [5.49]$$

This problem can be solved analytically as follows.

$$\int_{T_{Ti}}^{T_T} \frac{1}{T_T - T_a} dT_T = \frac{-U_{\tan k} A_{\tan k}}{M_T c_{pT}} \int_0^t dt \qquad \text{for } t \geq 0 \qquad [5.50]$$

$$\ln\left(\frac{T_T - T_a}{T_{Ti} - T_a}\right) = \frac{-U_{\tan k} A_{\tan k} t}{M_T c_{pT}}$$

$$T_T = \left((T_{Ti} - T_a) \exp\left(\frac{-U_{\text{tank}} A_{\tan k} t}{M_T c_{pT}} \right) \right) + T_a$$

Matlab was then run using the system inputs as below.

$$F_1 = F_2 = F_4 = 0$$

The results are compared with the analytical solution in Figure 5.9 as below.

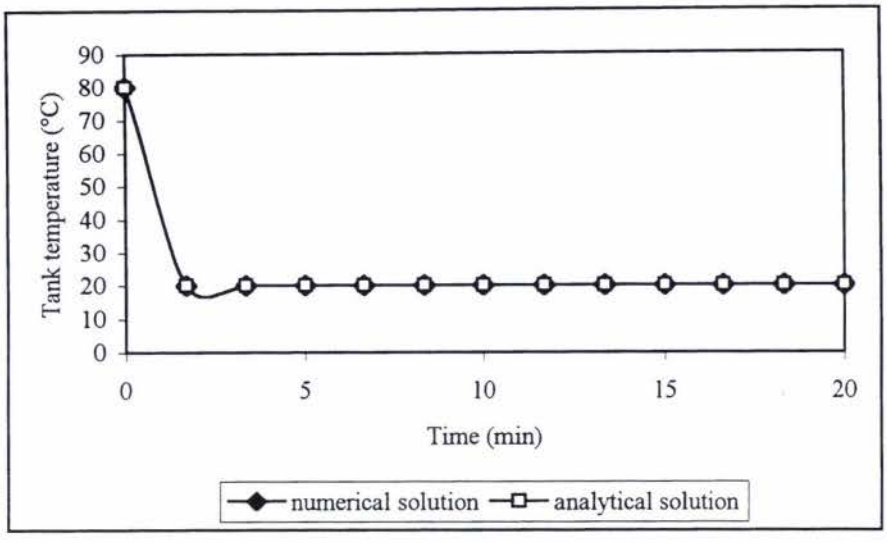

***Figure 5.9** Numerical and analytical solution of break tank temperature*

Figure 5.9 shows that there is no difference between the analytical and numerical solutions.

5.6.3 Model validation

After the successful formulation and solution of the break tank process, the models should be validated. Because the time did not permit collection of data to validate the model, this should be done in the future before application of the model for process optimisation purposes.

5.7 Conclusion

The model of break tank was formulated in the mathematical equations to predict the changes of tank temperature and the pectin and enzyme concentration when the temperature of the break tank is changed. The assumptions of the model were justified and the system inputs of the break model were also determined. These numbers were then used in the Matlab model to predict the changes occurring during processing. Although the model was not validated due to time limitations in the project, it can be used to gain some understanding of the factors affecting pulp consistency and potential control strategies that could be employed to improve performance.

Chapter 6
Model Application

6.1 Introduction

After the mathematical model for the break tank was formulated in Chapter 5, the model was used to investigate how the break process behaves and responds to varying processing conditions, determine which variables affect process the most and determine how the process could be better controlled. However, time constraints did not allow this to be done comprehensively, therefore, the model applications presented below are included to show how the model could be used in optimising tomato processing in future work.

6.2 Application of the model to tomato processing

In tomato processing, there are many factors affecting the quality of tomato paste. The mathematical equations formulated are used to predict these changes and determine the results. The effects are shown in the following sections.

6.2.1 Effect of residence time on break tank temperature

The effect of residence time on the temperature and changes of pectin and PG enzyme concentration in the break tank was studied. The temperature of tomato pulp in the break process was determined from a steady state heat balance over the break tank and the heat exchanger as shown in Figure 6.1 below.

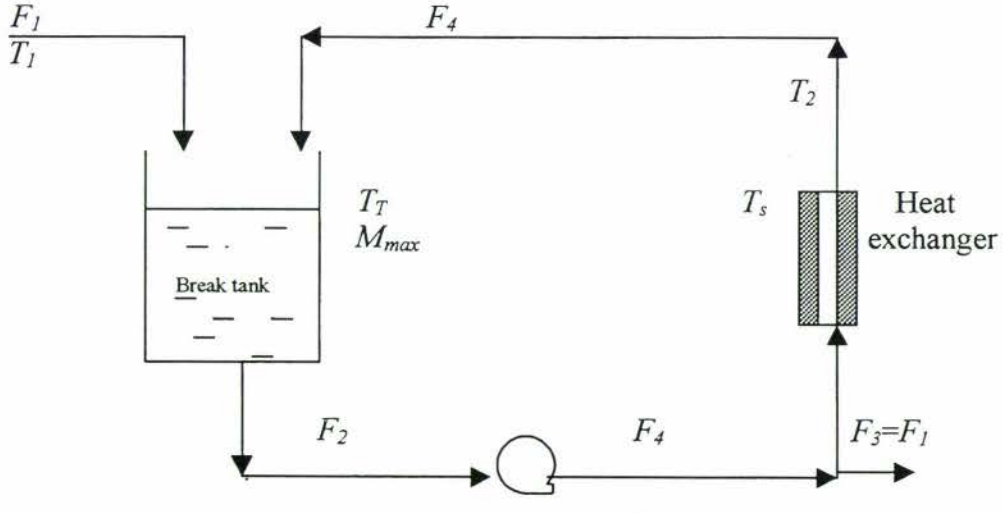

***Figure 6.1** Break process diagram over the break tank and the heat exchanger*

The flow rates of F_1, F_2, F_3 and F_4 were established. The flow rate of the feed (F_1) and the flow rate from pump to the buffer tank (F_3) were made the same and they are varied from 2.3-10 kg/s to achieve a range of different residence times (M_{max}/F_1).
Tank temperature and the pectin and enzyme fractions remaining were then determined using a steady state component balance over the break tank.

A steady state heat balance over the break process can be expressed (assuming no heat losses) as below.

At steady state,

Rate of heat gain by tomato pulp over the break process	=	Rate of heat gain by tomato pulp through the heat exchanger	=	Rate of heat transferred from condensing steam to tomato pulp in the heat exchanger

$$F_1 c_{pT}(T_T - T_1) = F_4 c_{pT}(T_2 - T_T) = U_{ex} A_{ex} \left(\frac{(T_s - T_T) - (T_s - T_2)}{\ln(\frac{T_s - T_T}{T_s - T_2})} \right) \qquad [6.1]$$

dividing by $(T_2 - T_T)$, gives

$$F_4 c_{pT} = \frac{U_{ex} A_{ex}}{\ln\left(\frac{T_s - T_T}{T_s - T_2}\right)}$$

$$\ln\left(\frac{T_s - T_2}{T_s - T_T}\right) = -\frac{U_{ex} A_{ex}}{F_4 c_{pT}}$$

$$T_s - T_2 = (T_s - T_T)\exp\left(-\frac{U_{ex} A_{ex}}{F_4 c_{pT}}\right)$$

Therefore,

$$T_2 = T_s - (T_s - T_T)\exp\left(-\frac{U_{ex} A_{ex}}{F_4 c_{pT}}\right) \qquad [6.2]$$

To determine the break temperature (T_T), a steady state heat balance of the break process could be shown as Eq.6.3,

Rate of heat gained by tomato pulp over the break process	=	Rate of heat gained by tomato pulp through the heat exchanger

$$F_1 c_{pT}(T_T - T_1) = F_4 c_{pT}(T_2 - T_T) \qquad [6.3]$$

Substituting T_2 from Eq. 6.2 into Eq. 6.3,gives;

$$F_1 T_T - F_1 T_1 = F_4 T_s - F_4 T_s \exp\left(-\frac{U_{ex} A_{ex}}{F_4 c_{pT}}\right) + F_4 T_T \exp\left(-\frac{U_{ex} A_{ex}}{F_4 c_{pT}}\right) - F_4 T_T$$

$$F_1T_T + F_4T_T - F_4T_T \exp\left(-\frac{U_{ex}A_{ex}}{F_4c_{pT}}\right) = F_4T_s + F_1T_1 - F_4T_s \exp\left(-\frac{U_{ex}A_{ex}}{F_4c_{pT}}\right)$$

$$T_T\left(F_1 + F_4\left(1-\exp\left(-\frac{U_{ex}A_{ex}}{F_4c_{pT}}\right)\right)\right) = F_1T_1 + F_4T_s\left(1-\exp\left(-\frac{U_{ex}A_{ex}}{F_4c_{pT}}\right)\right)$$

$$T_T = \frac{F_1T_1 + F_4T_s\left(1-\exp\left(-\frac{U_{ex}A_{ex}}{F_4c_{pT}}\right)\right)}{F_1 + F_4\left(1-\exp\left(-\frac{U_{ex}A_{ex}}{F_4c_{pT}}\right)\right)} \qquad [6.4]$$

Therefore, the temperature of tomato pulp in the break tank (T_T) could be determined using Eq.6.4 for a range of steam temperatures and residence times. The results of tank temperature when residence time is varied shown in Figure 6.2.

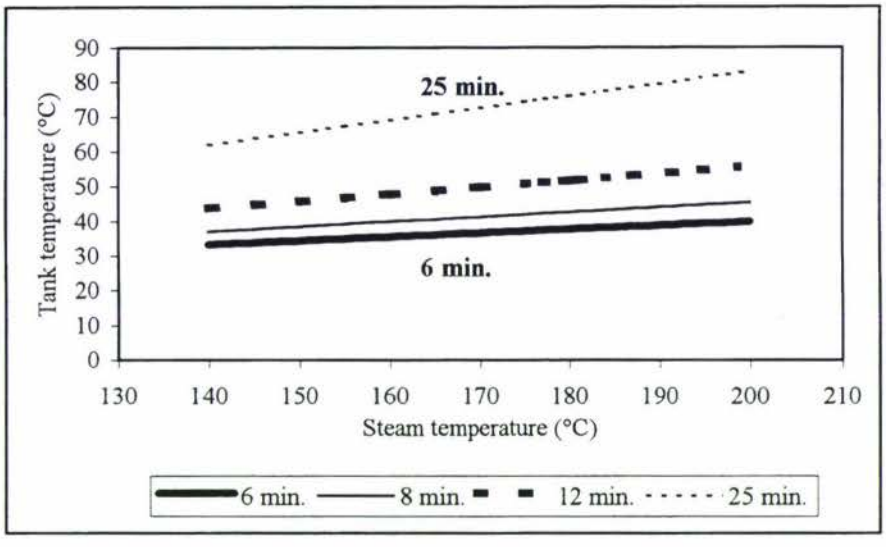

***Figure 6.2** Effect of residence times on steam temperature and tank temperature*

It is clear that tank temperature increases as a function of steam temperature as shown in Figure 6.2. The higher residence time increases the tank temperature because the longer time in the break process allows more heating of the tomato pulp. The effect of residence time on the change of pectin and enzyme concentration was also investigated. A steady state enzyme balance in the break tank was taken over the system shown in Figure 6.3.

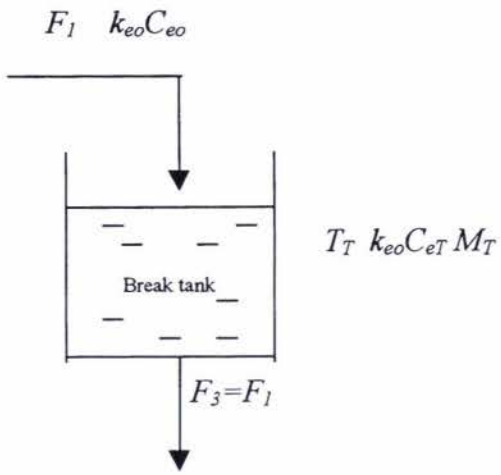

Figure 6.3 *Break tank diagram of the change of enzyme concentration at steady state*

The steady state enzyme balance over the break tank is shown in Eqs.6.5 and 6.6.

At steady state,

Rate of enzyme entering in feed	-	Rate of enzyme leaving the break tank	-	Rate of enzyme destruction in the break tank	=	0

$$F_1 k_{eo} C_{eo} - F_1 k_{eo} C_{eT} - k_{do} \exp\left(\frac{-E_d}{R(T_T + 273.15)}\right) k_{eo} C_{eT} = 0 \qquad [6.5]$$

$$k_{eo} C_{eT} = \frac{F_1 k_{eo} C_{eo}}{F_1 + k_{do} \exp\left(\frac{-E_d}{R(T_T + 273.15)}\right)} \qquad [6.6]$$

And the extent of reaction could be determined from Eq.6.7,

$$X_e = \frac{k_{eo} C_{eo} - k_{eo} C_{eT}}{k_{eo} C_{eo}} \qquad [6.7]$$

The change of enzyme concentration over the break tank from Eq.6.6 and the enzyme fraction remaining at different residence time over the break tank were calculated for different residence times in the break tank. The results of these simulations are shown in Figure 6.4.

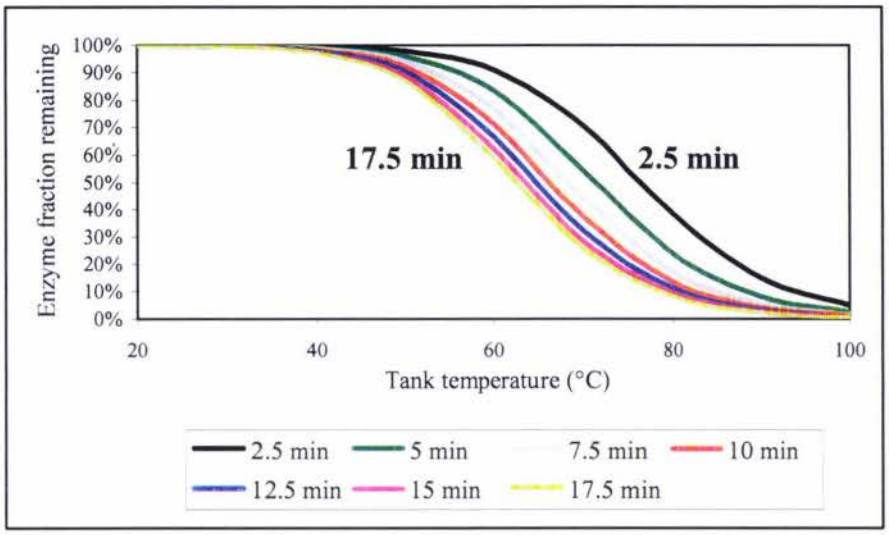

Figure 6.4 *Effect of residence time on the break tank temperature and enzyme fraction remaining*

It is clear in Figure 6.4 that the enzyme fraction remaining decreases as a function of tank temperature. When residence time is higher, the enzyme fraction remaining is lower since more enzyme reaction can occur. In the range of hot break processes, 60-80°C, the remaining enzyme concentration is decreased dramatically when the residence time is higher. At 80°C the enzyme fraction remaining is 90% when the residence time is 17.5 min whereas the enzyme fraction remaining is 40% when the residence time is 2.5 min. The enzyme inactivation is 100% at every residence time when the tank temperature is above 100°C.

Longer residence time is required to minimise the enzyme concentration with low break temperature. The enzyme fraction remaining reaches zero when tank temperature is at 100°C at 17.5 min of residence time. Therefore, Figure 6.4 could be a guideline to select time and temperature of the hot break process.

An alternative way of presenting this information is by placing the requirement of the break process at 90% enzyme inactivation. The same result could be achieved with the different process conditions indicated in Table 6.1.

Table 6.1 *Summary of residence time and tank temperature at 90% enzyme inactivation*

Residence time (min.)	***Tank temperature (°C)***
2.5	93
5.0	87
7.5	83
10.0	82
12.5	80
15.0	78
17.5	77

Table 6.1 shows the range of temperature and residence times that could achieve 90% enzyme inactivation. However, the change of pectin concentration is also an important consideration so as to find a good combination between residence time and tank temperature to which will give a low enzyme residual and a high level of pectin from the break process.

A break process diagram for the system for which a steady state pectin balance was carried out is shown in Figure 6.5.

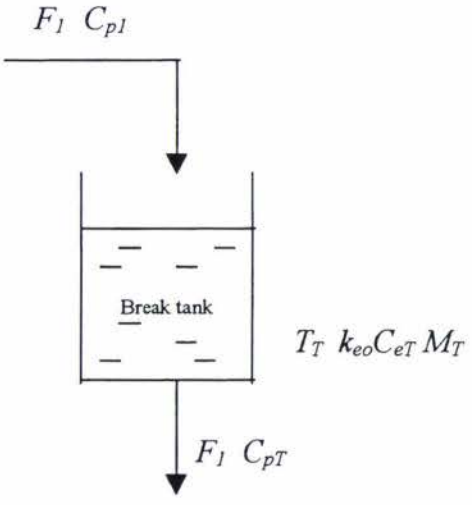

Figure 6.5 *Break tank diagram of the change of pectin concentration at steady state*

The change of pectin concentration in the break tank in Figure 6.5 could be determined by carrying out mass balance at steady state, as shown in Eq.6.8, 6.9, 6.10, and 6.11 below.

At steady state,

Rate of pectin entering in the feed	-	Rate of pectin eaving the break tank	-	Rate of pectin hydrolysis in the break tank	=	0

$$F_1 C_{pt1} - F_1 C_{ptT} - \frac{V_{\max} C_{ptT} M_T}{K_m + C_{ptT}} = 0 \qquad [6.8]$$

where $V_{\max} = k_{eo} C_{eT} \exp\left(\frac{-E_e}{R(T_T + 273.15)}\right)$

rearranging gives;

$$F_1 C_{pt_1} - \frac{F_1 C_{ptT} k_m - F_1 C_{ptT}^{\ 2} - V_{\max} C_{ptT} M_T}{K_m + C_{ptT}} = 0$$

$$F_1 C_{pt_1}(k_m + C_{ptT}) = F_1 C_{ptT} K_m + F_1 C_{ptT}^{\ 2} + V_{\max} C_{ptT} M_T$$

$$F_1 C_{pt_1} K_m + F_1 C_{pt_1} C_{ptT} = F_1 C_{ptT} K_m + F_1 C_{ptT}^{\ 2} + V_{\max} C_{ptT} M_T$$

$$C_{ptT}(F_1 C_{pt1} - F_1 K_m - V_{\max} M_T) - F_1 C_{ptT}^{\ 2} + F_1 C_{pt_1} K_m = 0$$

$$F_1 C_{ptT}^{\ 2} - (F_1 C_{pt1} - F_1 K_m - V_{\max} M_T) C_{ptT} - F_1 C_{pt1} K_m = 0 \quad [6.9]$$

Equation 6.9 is arranged in the form of $ax^2+bx+c=0$ which a, b, c, and C_{ptT} could be determined from Eq.6.10 (the quadratic equation).

$$C_{ptT} = \frac{-b \pm \sqrt{b^2 - 4ac}}{2a} \quad [6.10]$$

where $a = F_1$

$b = F_1 C_{pt_1} - F_1 K_m - V_{\max} M_T$

$c = -F_1 C_{pt1} K_m$

The extent of reaction could be determined from Eq.6.12.

$$X_{pt} = \frac{C_{pt_1} - C_{ptT}}{C_{pt1}} \quad [6.11]$$

The pectin fraction remaining could then be determined for a range of temperatures and break tank residence times, as shown in Figure 6.6.

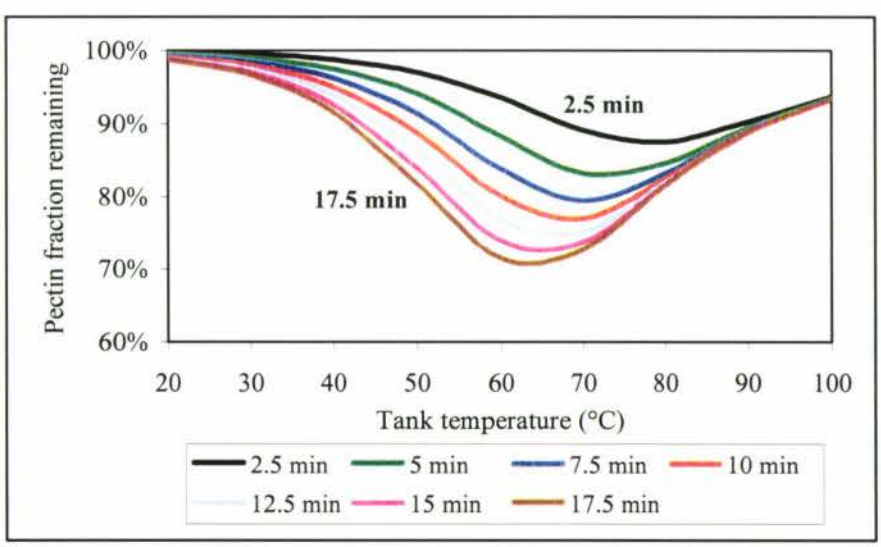

Figure 6.6 *Effect of residence time on the break tank temperature and pectin fraction remaining*

It is shown in Figure 6.6 that the pectin fraction remaining decreases when the tank temperature is between 30 and 60°C. This is due to PG enzyme being active at low temperatures and so pectin hydrolysis results in lower levels of pectin remaining in the break tank. When the temperature of tomato pulp in the break tank is heated above 60°C, the pectin fraction remaining is increased because PG enzyme is inactivated, reducing pectin hydrolysis. The effect of residence time on the concentration of pectin in the break tank shows a trend with the pectin fraction remaining is higher when the residence time is decreased. At 80°C the pectin fraction remaining is 90% when the residence time at the break tank is 2.5 min, whereas the pectin fraction remaining is 80% when the residence time is 17.5 min. The pectin fraction residual is 95% at every residence time when the tank temperature reaches 100°C. This shows that there is no effect of residence time on pectin hydrolysis at 100°C.

Therefore, the model allows selection of the combination of residence time and tank temperature required to achieve a high pectin fraction and a low enzyme fraction remaining in the break process. The application of this model would be very helpful to design a hot break process and to develop high viscosity tomato paste by maximising the pectin fraction remaining and minimising the enzyme fraction remaining in the pulp.

6.2.2 Effect of ripeness combination

From chapter 4, it is clear that PG enzyme activity in dark red tomatoes is higher than in green tomatoes. In tomato processing, dark red tomato is usually used to produce tomato paste. However, green tomatoes or another ripeness of tomato fruits might come into the process along with the dark red tomatoes. Therefore, the effect of the ripeness combination of tomato fruits coming into the process must be considered when attempting to optimise the break process. The steam temperature used in this section was 140°C. The initial concentration of PG enzyme in each ripeness used in this investigation is given chapter 4 and shown in Table 6.2.

Table 6.2 *Summary of initial enzyme concentration at different ripeness*

Ripeness	$k_{eo}C_{eo}$ ***(1/s)***
Green	0
Breaker	1.83×10^{8}
Turning	3.33×10^{8}
Orange	8.33×10^{8}
Dark red	1.42×10^{9}

The simulation of these initial numbers showing on the effect of ripeness on the pectin destruction has been calculated on a spreadsheet and the results are shown in Figure 6.7.

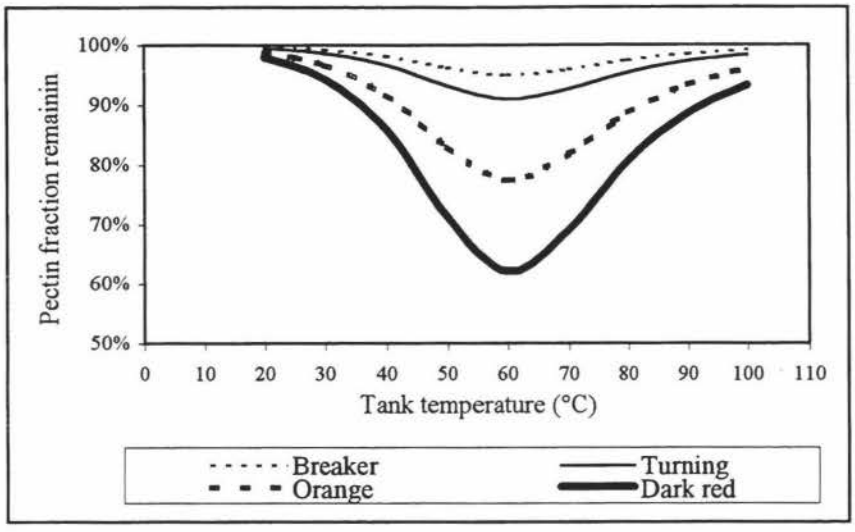

***Figure 6.7** Effect of ripeness on the break tank temperature and pectin fraction remaining*

Figure 6.7 shows that the dark red tomato pulp had the highest hydrolysis of pectin because of the lowest pectin fraction remaining in the break tank in the temperature range 20 to 100°C. It is clear that the hydrolysis of pectin at every ripeness is greatest when tank temperature reaches 60°C and the pectin fraction remaining increased when tank temperature is raised above 60°C. This is due to the high pectin hydrolysis in the temperature range 20 to 60°C and the inactivation of PG enzyme which results in low pectin hydrolysis above 60°C. Higher level of pectin concentration at every ripeness can be achieved when the tank temperature is above 60°C. At lower levels of ripeness (Breaker, Turning, and Orange) pectin fraction remaining is higher than the dark red tomato because lower pectin hydrolysis which is due to lower amount of PG enzyme presented in these unripe fruit.

Therefore, when the orange and dark red tomatoes coming into the process are mixed with another ripeness (Green, Breaker or Turning), it would have a positive affect on the amount of pectin. Lower break temperature could be used to achieve the same extent of pectin hydrolysis as for feeds with high levels of ripe tomatoes. Operation of the process in this way may allow better control over both viscosity and colour of the finished paste.

6.2.3 Effect of feed interrupted from external

In this application of the model, the effect of feed interruption was investigated. The dynamic model was used and allowed to reach steady state (33mm.). The feed was then stopped for 9 minutes and then restored to its initial value. This was done to see the likely effect of halting the process to allow change of tomato truckload at the start of the process. In Matlab simulation, the change in feed rate was achieved using two logic statements in a function file as below.

```
if    t>2000
      F1=0;
end

if   t>2500
      F1=F1set;
end
```

The initial mass of tomato pulp was 1500 kg. The change of mass of tomato pulp, tank temperature and the pectin and enzyme fraction remaining in the break tank are shown in Figures 6.8, 6.9, 6.10, and 6.11 below.

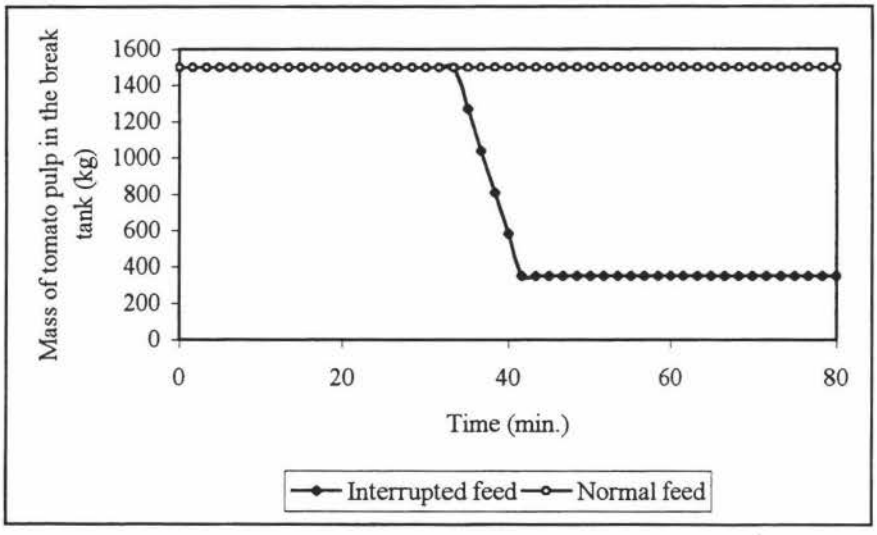

Figure 6.8 *Effect of feed interruption on mass of tomato pulp in the break tank*

Figure 6.8 shows that the mass of tomato pulp in the break tank was changed when the feed was stopped for 9 minutes. The initial mass is decreased from 1500 kg to 380 kg during the time interrupted and reaches steady state again after 42th minute. The change of tank temperature is shown in Figure 6.9.

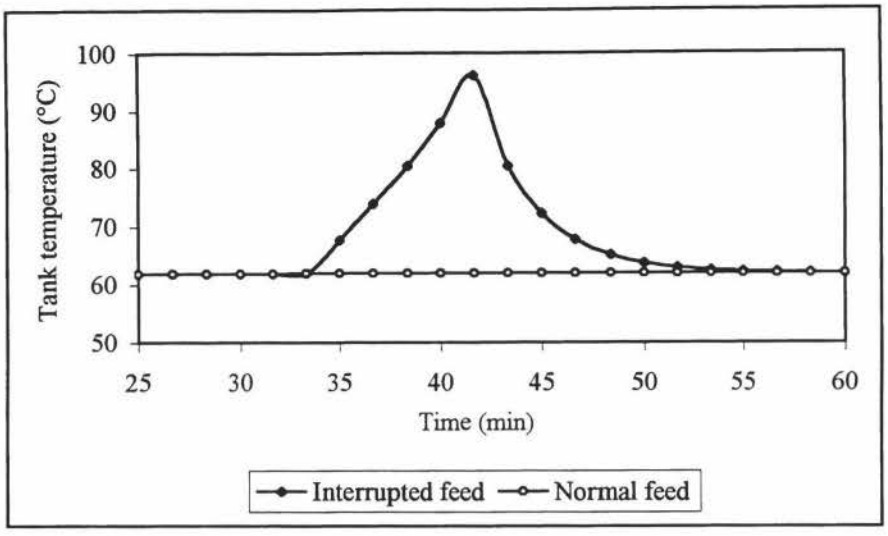

***Figure 6.9** Effect of feed interruption on the break tank temperature*

It is clearly shown in Figure 6.9 that when the feed is interrupted at 33rd minute, the tank temperature, initially at 62°C, experienced a sudden sharp increase and reached 96°C at 40th minute. After the 40th minute, when the feed was turned back on, the tank temperature decreases and reaches steady state at 62°C again. This is due to the cooling effect of tomato pulp entering the break tank being stopped over this period. In normal operation a feedback control on the steam supply to the heat exchanger would help to minimise this effect.

The effect of this temperature change on pectin and enzyme fractions remaining in the pulp are also shown in Figures 6.10 and 6.11.

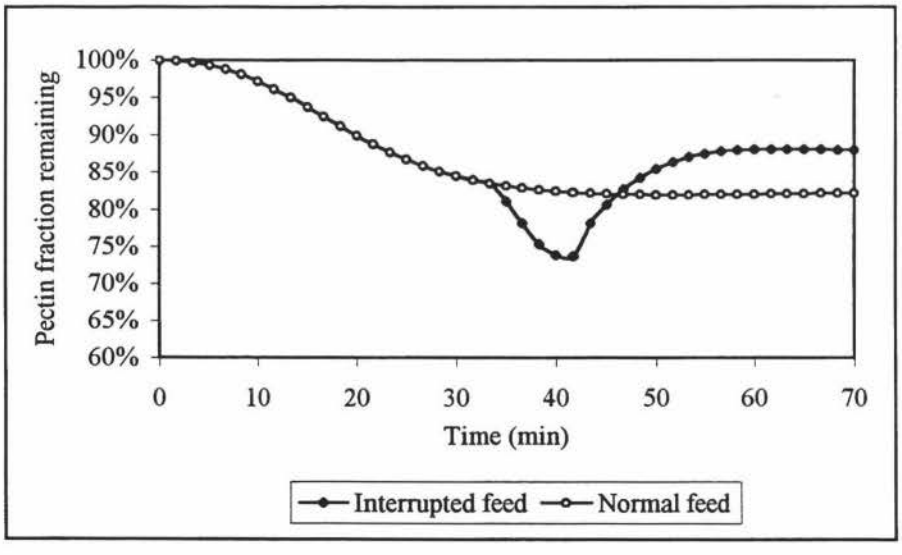

***Figure 6.10** Effect of feed interruption on pectin fraction remaining in the break tank*

During the interruption to the feed, the pectin fraction remaining was reduced from 0.85 to 0.75 as shown in Figure 6.10. This is due to that the pectin in the break tank was hydrolysed by the PG enzymes in the tomato pulp when the feed was stopped. When the feed is turned on at the 42nd minute, the pectin fraction remaining in the break tank increased from the feed coming into the break tank and reached steady state again with the higher level of pectin fraction remaining when the tank temperature is constant as shown in Figure 6.9. This effect shows that if the feed is interrupted, the amount of residual pectin in the break tank decreased for a short time due to PG enzyme activity. The new steady state pectin level is brought about by the decreased residence time in the break tank due to lower pulp mass.

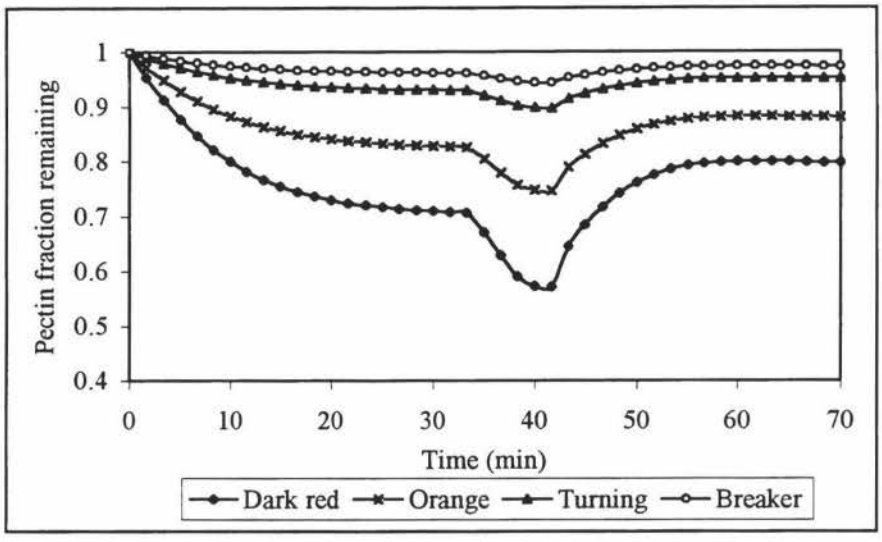

Figure 6.11 *Effect of ripeness on pectin fraction remaining in the break tank when the feed was interrupted*

The effect of ripeness on pectin fraction remaining in the break tank when the feed interrupted was also studied. It is clear from Figure 6.11 that the level of pectin remaining in the break tank decreases with increasing ripeness. It can be seen from this figure that the process is less affected by the changes to the system for fruit with lower ripeness (PG levels).

The enzyme fraction remaining in the break tank when the feed is interrupted was also determined and the results are shown in Figure 6.12.

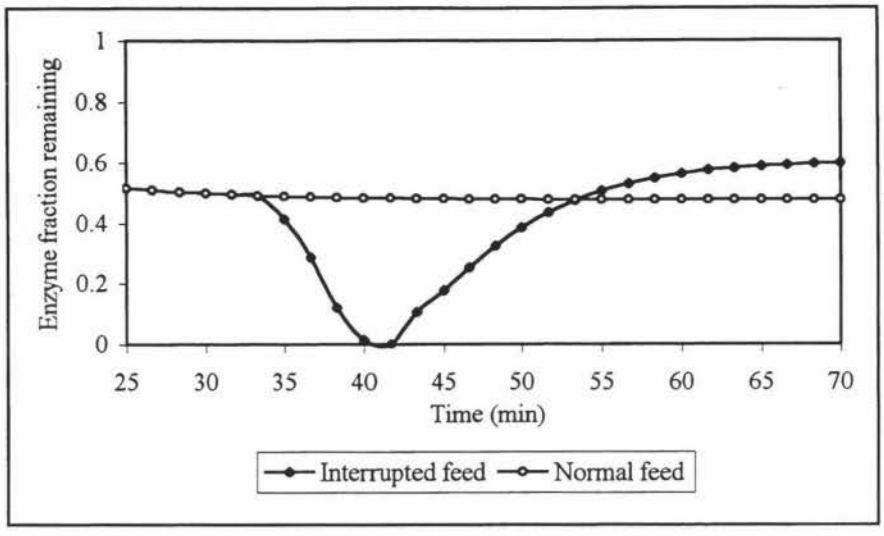

***Figure 6.12** Effect of feed interruption on enzyme fraction remaining in the break tank*

The enzyme fraction remaining in the break tank decreased from 0.5 to 0 during the interruption to the feed as demonstrated in Figure 6.12. This is due to the entire amount of enzyme in the break tank being inactivated in the elevated temperatures. After the 42nd minute, the enzyme fraction remaining increased again because the feed was turned on providing fresh PG enzymes to the break tank.

It can be concluded from this study that an interrupted feed could significantly affect tank temperature, pectin and enzyme concentration in the break tank. The quantitaive understanding provided by the model could allow alternative operation of the process to avoid or minimise changes to final paste viscosity.

6.3 Conclusions

Examples of the applications of the break process model have been demonstrated both qualitatively and quantitatively. First, The effect of residence time on tank temperature and pectin and enzyme concentration shows that a longer residence time in the break tank result in high tank temperature, lower pectin fraction remaining, and higher enzyme inactivation. The model allows a combination of tank temperature, pectin and enzyme fraction remaining to be selected to optimise the process.

The second application of the model was to investigate the effect of ripeness on break process performance. The simulation showed that if Green, Breaker, and Turning tomatoes are mixed with Orange and Dark red fruit in tomato processing, the level of pectin leaving the break process would increase due to the lower levels of enzyme present in unripe fruit. These simulations also showed that lower break temperatures can be used for feeds with higher proportions of unripe fruit, to achieve the same extent of pectin hydrolysis leaving the break process.

The last scenario studied was the effect caused by an interruption to the feed. It was found that feed disruptions affect tank temperature, pectin and enzyme concentration. Tank temperature shows a sharp increase if not controlled and the pectin and enzyme

concentrations also demonstrated significant changes during the interrupted feed period.

Although, time does not allow the full investigation of how to best control the process, this chapter shows clearly how the process responds to the disruptions to the process and how the model can be useful in optimising the operation of tomato paste production.

Chapter 7
Conclusion

7.1 Conclusions

The effect of fruit variation was characterised in terms of levels of insoluble solids, total solids, pectin levels, and °Brix in Ferry Morse tomatoes and found that tomato solids were independent of tomato ripeness.

The change of D-galacturonic acid concentration produced from pectin hydrolysis can be used to determine the level of PG enzyme activity in tomatoes. The results of pectin hydrolysis showed that PG enzyme activity increased as a function of ripeness from green to dark red and the level of PG enzyme activity was high in orange and dark red tomatoes.

The rate of PG activity increased as a function of time and temperature over the temperature range 25 to 80°C. Heat did not inhibit the activity of PG enzymes in temperature range 30 to 60°C but the PG enzyme started to be denatured at 65°C and to be completely inactivated at 80°C.

A kinetic model of enzymatic pectin hydrolysis and enzyme inactivation was formulated in a form suitable for inclusion in a mathematical model of the break tank. A mathematical model of the break process was simulated using Matlab to study the dynamic changes of the break temperature and time on pectin hydrolysis and PG enzyme destruction for any inputs of residence time, feed rate, and ripeness variation of feed.

When the tank temperature was above 80°C, pectin fraction remaining was higher than 80% at every residence time and enzyme fraction remaining was lower than 7% at 17.5 minute residence time. Therefore, this model application can be used as a guide to achieve the desired viscosity of tomato paste. A good combination of residence time and steam temperature in the break tank for high level of pectin fraction remaining and low level of enzyme fraction remaining can result in thick tomato paste.

The effect of mixed unripe fruit coming into the break process can result in the change of pectin level. When tank temperature was above 80°C, pectin fraction remaining in the break tank was in the range 80-100% which was high because the low level of PG enzymes. Lower break temperature can be used to inactivate low level of PG enzymes. This result showed that the unripe tomatoes came into the process can result in the positive effect to the viscosity. However, the effect of colour losses, vitamin losses, flavour change, and browning reaction are needed to be optimised.

The interruption of feed can increase the tank temperature dramatically and decreased the pectin and enzyme fraction remaining significantly in the first five minutes. During 5^{th} to 9^{th} minute, the tank temperature dropped and reached the same steady state again and the pectin fraction remaining and enzyme fraction remaining increased at a new steady state. This effect showed that the feed interruption can affect on the process significantly. The alternative operation can be chosen to minimise changes to final tomato products.

7.2 Suggestions for future work

Although the break process model could predict the changes of tank temperature, pectin and enzyme concentration in the system, some future work to improve the model is suggested;

- The model should be validated against the real data from the process to ensure its accuracy.

- The kinetics for colour losses, vitamin losses, flavour changes and browning reaction in the tomatoes during heating are needed to be optimised.

- The break process may be optimised using the model to produce high tomato paste quality in real tomato processing.

References

Adam, J.B. 1991: Review:enzyme inactivation during heat processing of food-stuffs. *International Journal of Food Science and Technology 26*:1-20.

Arias, R.; Lee, T.; Logendra, L.; Janes, H. 2000: Correlation of lycopene measured by HPLC with the *L,a,b* colour readings of a hydroponic tomato and the relationship of maturity with colour and lycopene content. *Journal of Agricultural and Food Chemistry 48*:1697-1702.

Bailey, J.E.; Ollis, D.F. 1986: Biochemical Engineering Fundamentals. New York, McGraw-Hill, 984p.

Barreiro, J.A.; Milano, M.; Sandoval, A.J. 1997: Kinetics of colour change of double concentrated tomato paste during thermal treatment. *Journal of Food Engineering 33*:359-371.

Barrett, D.M.; Garcia, E.; Wayne, J.E. 1998: Textural modification of processing tomatoes. *Critical review in Food Science and Nutrition 38 (3)*:73-258.

Becker, R.; Miers, J.C.; Nutting, M.D.; Dietrich, W.C.; Wagner, J.R. 1972: Consistency of tomato product (7.Effects of acidification on cell walls and cell breakage). *Journal of Food Science 37*:118-125.

Becker, R.; Wagner, J.R.; Miers, J.C.; Sanshuck, D.W.; Dietrich, W.C. 1968: Consistency of tomato products (III.Effect of pH adjustment during tomato juice preparation on pectin contents and characteristics. *Food Technology 22*:159-162.

BeMiller, J.N. 1986: An introduction to Pectins: Structure and Properties. Pp2-12 *in*: Chemistry and Function of Pectins, Fishman, M.L.; Jen, J.J. *ed.* Washington D.C., American Chemical Society.

Bontovits, L. 1981: The effect of processing technologies on colour changes in tomato. *Acta Alimentaria 10*:215-228.

Boskovic, M. 1979: Fate of lycopene in dehydrated tomato products: Carotenoid isomerization in food system. *Journal of Food Science 44(1)*:84-86.

Broeck, I.V.; Ludikhuyze, L.R.; Loey, A.M.; Hendrickx, M.E. 2000: Effect of temperature and/or pressure on tomato pectinesterase activity. *Journal of Agricultural and Food Chemistry 48*:551-558.

Buescher, R.W. 1979: Influence of high temperature on physiological and compositional characteristics of tomato fruits. *Lebensmittel-Wissenschaft Technologie 12(3)*:2-4.

Campbell, C. 2002: Characterisation of tomato paste. Unpublished Masters thesis, Massey University, Palmerston North, New Zealand.

Caradec, P.L.; Nelson, P.E.; Takada, N. 1985: Tomato products:A new serum separation measurement. *Journal of Food Science 50*:1493-1494.

Chin, H.B.; Kimball, J.R.; Hung, J.; Allen, B. 1985: Microwave oven drying determination of total solids in processed tomato products. *Journal. Association of Official Analytical Chem*ists *68(6)*:1081-1083.

Davies, J.N.; Hobson, G.E. 1981: The constitutents of tomato fruit-The influence of environment, nutrition , and genotype. *Coordinating Research Council Critical Reviews in Food Science and Nutrition 11*:205-280.

Foda, Y.H.; McCollum, J.P. 1970: Viscosity as affected by various constituents of tomato juice. *Journal of Food Science 35*:333-338.

Gancedo, M.C.; Luh, B.S. 1986: HPLC analysis of organic acids and sugars in tomato juice. *Journal of Food Science 51(3)*:571-573.

Gaonkar, A.G. 1995: Food processing (Recent development). Amsterdam, Elsevier Science B.V. 315 p.

Giovannoni, J.J.; Penna, D.D.; Bennett, A.B.; Fischer, R.L. 1992: Polygalacturonase and Tomato Fruit Ripening Pp 67-103 *in*:Horticultural Reviews, Janick, J. *ed.* New York, John Wiley & Sons, Inc.

Goose, P.G.; Binsted, R. 1973: Tomato paste and other tomato products. London, Food Trade Press. 270 p.

Gould, W.A. 1992: Tomato production, processing&technology. Maryland, CDI Publications, Inc. 535 p.

Hayes, W.A.; Smith, P.G.; Morris, A.J. 1998: The production and quality of tomato concentrates. *Critical Reviews in Food Science and Nutrition 38(7)*:537-564.

Hobson, G.E. 1965: The firmness of tomato fruit in relation to polygalacturonaseactivity. *Journal of Horticultural Science 40*:66-72.

Huber, D.J.; Lee, J.H. 1986: Comparative Analysis of Pectins from Pericarp and Locular Gel in Developing Tomato Fruit. Pp141-156 *in*: Chemistry and Function of Pectins, Fishman, M.L.; Jen, J.J. *ed.* Washington D.C., American Chemical Society.

Knegt, E.; Vermeer, E.; Bruinsma, J. 1988: Conversion of the polygalacturonase isoenzymes from ripening tomato fruits. *Physiologia Plantarum 72*:108-114.

Laratta, B.; Fasanaro, G.; Sio, F.D., Castaldo, D. 1995: Thermal inactivation of pectin methylesterase in tomato puree:Implications on cloud stability. *Process Biochemistry 30(3)*:251-259.

Lee, Y.C.; Kirk, J.R.; Bedford, C.L.; Heldman D.R. 1977: Kinetics and computer simulation of ascorbic acid stability of tomato juice as functions of temperature, pH and metal catalyst. *Journal of Food Science 42(3)*:640-648.

Levenspiel, O. 1972: Chemical reaction engineering. New York, John Wiley&Sons. 578 p.

Lever, M. 1972: A new reaction for colorimetric determination of carbohydrates. *Analytical Biochemistry 47*:273-279.

Lopez, P.; Sanchez, A.C.; Vercet, A.; Burgos, J. 1997: Thermal resistance of tomato polygalacturonase and pectinmethylesterase at physiological pH. *Zeitschrift Fuer Lebensmittel-Untersuchung Und Forschung 204*:146-150.

Lopez, P.; Verset, A.; Sanchez, A.C.; Burgos, J. 1998: Inactivation of tomato pectic enzymes by manothermosonication. *Zeitschrift Fuer Lebensmittel-Untersuchung Und Forschung 207*:249-252.

Lovric, T.; Sablek, Z.; Boskovic, M. 1970: Cis-trans isomerisation of lycopene and colour stability of foam-mat dried tomato powder during storage. *Journal of the Science of Food and Agriculture 21*:641-647.

Luh, B.S.; Daoud, H.N. 1971: Effect of break temperature and holding time on pectin and pectic enzymes in tomato pulp. *Journal of Food Science 36*:1039-1043.

Luh, B.S.; Lonard, S.J.; Phaff, H.J. 1954: Hydrolysis of pectic materials and oligosaccharides by tomato polygalacturonase. *Annual Meeting of the Institute of Food Technologists 14*:448-455.

Marsh, G.L.; Leonard, S.J.; Buhlert, J.E. 1979: Yield and quality of catsup produced to a standard solids and consistency level : II.Influence of handling practices, break temperature and cultivar. *Journal of Food Processing and Preservation 3*:195-212.

Martha, P. 1986-87: Flavor of tomato and tomato products. *Food Reviews International 2(3)*: 309-351.

McColloch, R.J.; Kertesz, Z.I. 1949: Recent development of practical significance in the field of pectic enzymes. *Food Technology 3*:94-96.

McColloch, R.J.; Rice, R.C.; Underwood, J.C. 1956: Storage stability of canned concentrated tomato juice. *Food Tech*nology *11*:568-570.

McCready, R.M.; McComb, E.A. 1952: Extraction and determination of total pectic materials in fruits. *Analytical Chemistry 24(12)*:1986-1988.

Miladi, S.S.; Gould, W.A.; Clements, R.L. 1969: Heat processing effect on starch, sugars, proteins, amino acids, and organic acids of tomato juice. *Food Technology 23 (691)*:93-95.

Miller, G.L. 1959: Total reducing sugar assay. *Analytical Chem*istry *31(3)*:426-8.

Moshrefi, M.; Luh, B.S. 1984: Purification and characterization of two tomato polygalacturonase isoenzymes. *Journal of Food Biochemistry 8*:39-54.

Nguyen, L.; Schwartz, S.J. 1999: Lycopene:chemical and biological properties. *Food Tech*nology *2*:38-45.

Nguyen, M.L.; Schwartz, S.J. 1998: Lycopene stability during food processing. *Proceedings of Society for Experimental Biology and Medicine 218(2)*:101-105.

Okitani, A.; Kim, S.Y.; Hayase, F.; Chung, T.; Kato, H. 1983: Heat-induced changes in free amino acids on manufacturing heated pulps, purees and pastes from tomatoes. *Journal of Food Science 48*:1366-1367.

Porretta, S. 1991: Nonenzymatic browning of tomato products. *Food Chemistry 40*:323-335.

Porretta, S.; Sandei, L. 1991: Determination of 5-(Hydroxymethyl)-2-Furfural (HMF) in tomato products:Proposal of a rapid HPLC method and its comparison with the colorimetric method. *Food Chemistry 39*:51-57.

Porretta, S.; Birzi, A.; Ghizzoni, C.; Vicini, E. 1995: Effects of ultra-high hydrostatic pressure treatments on the quality of tomato juice. *Food Chemistry 52*:35-41.

Pressey, R. 1986: Polygalacturonases Pp157-174 *in*: Chemistry and Function of Pectins, Fishman, M.L.; Jen, J.J. *ed.* Washington D.C., American Chemical Society.

Rahman, S. 1995: Food Properties Handbook. Florida, CRC Press, Inc. 500 p.

Robinson, W.B.; Kimball, L.B.; Ransford, J.R.; Moyer, J.C.; Hand, D.B. 1956: Factors influencing the degree of settling in tomato juice. *Food Tech*nology *10*:109-112.

Rodrigo, M.; Martinez, A.; Sanchis, J.; Trama, J.; Giner, V. 1990: Determination of Hot-Fill-Hold-Cool process specifications for crushed tomatoes. *Journal of Food Science 55*:1029-1032.

Sandoval, A.J.; Barreiro, J.A.; Mendoza, S. 1992: Thermal resistance of *Bacillus* coagulans in double concentrated tomato paste. *Journal of Food Science 57(6)*:1369-1370.

Seymour, G.B.; Taylor, J.E.; Tucker, G.A. 1993: Biochemistry of Fruit Ripening. London, Chapman&Hall.

Sharma, S.K.; Maguer, M.L. 1996: Kinetics of lycopene degradation in tomato pulp solids under different processing and storage conditions. *Food Research International 29(3-4)*:309-315.

Sherkat, F.; Luh, B.S. 1976: Quality factors of tomato pastes made at several break temperatures. *Journal of Agricultural and Food Chemistry 24(6)*:1155-1158.

Shi, J.; Maguer, M.L. 2000: Lycopene in Tomatoes:Chemical and Physical Properties Affected by Food Processing. *Critical Reviews in Food Science and Nutrition 40(1)*:1-42.

Shuler, M.L.; Kargi, F. 1992: Bioprocess Engineering Basic concepts. New jersey, Prentice-Hall, Inc. 479 p.

Sieso, V.; Crouzet, J. 1977: Tomato volatile components: Effect of processing. *Food Chemistry 2*:241-252.

Sio, F.D.; Dipollina, G.; Villari, G.; Loiudice, R.; Laratta, B.; Castaldo, D. 1995: Thermal resistance of pectin methylesterase in tomato juice. *Food Chemistry 52*:135-138.

Siviero, P.; Trifiro, A.; Sandei, L.; Franceschini, M. 1996: Importance of raw material characteristics for the production of high-viscosity tomato products. *Industria Conserve 71*:139-146.

Stier, E.F.; Ball, C.O.; Maclinn, W.A. 1956: Changes in pectic substances of tomato during storage. *Food Technology 10*:39-42.

Tanglertpaibul, T.; Rao, M.A. 1987a: Rheological properties of tomato concentrates as affected by particle size and methods of concentration. *Journal of Food Science 52(1)*:141-145.

Tanglertpaibul, T.; Rao, M.A. 1987b: Flow properties of tomato concentrates:Effect of serum viscosity and pulp content. *Journal of Food Science 52(2)*:318-321.

Thakur, B.R.; Singh, R.K.; Nelson, P.E. 1996a: Quality attributes of processed tomato products:A review. *Food Reviews International 12(3)*:375-401.

Thakur, B.R.; Singh, R.K.; Tieman, D.M.; Handa, A.K. 1996b: Tomato product quality from transgenic fruits with reduced pectin methylesterase. *Journal of Food Science 61(1)*:85-87.

The Association of Official Analytical Chemists International 1975: Vegetable products, processed. 12nd edition. Washington D.C., Association of Official Analytical Chemists International Suite.

The Association of Official Analytical Chemists International 2000: Vegetable products, processed. 17th edition. Maryland, Association of Official Analytical Chemists International Suite.

Trifiro, A.; Gherardi, S.; Zoni, C.; Zanotti, A.; Pistocchi, M.; Paciello, G.; Sommi, F.; Arelli, P. L.; Antequera, M.A. 1998: Quality changes in tomato concentrate production: Effects of heat treatments. *Industria Conserve 73*:30-41.

Tucker, G.A.; Robertson, N.G.; Grierson, D. 1982: Purification and changes in activities of tomato pectinesterase isoenzymes. *Journal of the Science of Food and Agri*culture *33*:396-400.

Villari, P.; Costabile, P.; Fasanaro, G.; Sio, F.D.; Laratta, B.; Pirone, G.; Castaldo, D. 1994: Quality loss of double concentrated tomato paste: Evolution of the microbial flora and main anlytical parameters during storage at different temperatures. *Journal of Food Processing and Preservation 18*:369-387.

Wagner, J.R.; Miers, J.C. 1967: Consistency of tomato products (I.The effects of tomato enzyme inhibitor by additives). *Food Technology 21*:114-117.

Wiese, K.L.; Dalmasso, J.P. 1994: Relationships of colour, viscosity, organic acid profiles and ascorbic acid content to addition of organic acids and salt in tomato juice. *Journal of Food Quality 17*:273-284.

Xu, S.; Shoemaker, C.F.; Luh, B.S. 1986: Effect of break temperature on rheological properties and microstructure of tomato juices and pastes. *Journal of Food Sci*ence *51(2)*:399-402.

Appendix A1
Nomenclature

A_{575}	Absorbance reading at 575 nm.	
A_{ex}	Area in the heat exchanger	m^2
A_{tank}	Area of the break tank	m^2
C_e	Enzyme concentration	kg/kg
C_{eo}	Initial enzyme concentration	kg/kg
C_{eT}	Enzyme concentration in the break tank	kg/kg
C_{pt}	Pectin concentration	kg/kg
c_{pT}	Heat capacity of tomato puree in the break tank	J/kg°C
C_{pti}	Initial pectin concentration	kg/kg
C_{ptT}	Pectin concentration in the break tank	kg/kg
D	Diameter of the tube in the heat exchanger	m
E_d	Activation energy for enzyme inactivation	J/mol
E_e	Activation energy for pectin hydrolysis	J/mol
F_1	Flow rate of tomato pulp in the break tank	kg/s
F_2	Flow rate of tomato pulp from the break tank to the heat exchanger	kg/s
F_3	Flow rate of tomato pulp from the break tank to the buffer tank	kg/s
F_4	Flow rate of tomato puree into the heat exchanger	kg/s
G	Standard acceleration of gravity = 9.8	m/s^2
J	General node number	
J	Number of nodes	
k_d	Rate constant for enzyme inactivation	1/s
k_{do}	Arrhenius constant for enzyme degradation	1/s
k_{eo}	Arrhenius constant for enzyme hydrolysis	1/s
K_m	Michaelis-Menten constant	kg/kg
L	Length of tubes in the heat exchanger	m
M_{max}	Maximum mass of tomato pulp in the break tank	kg
M_T	Mass of tomato pulp in the break tank	kg
M_{Ti}	Initial mass of tomato puree in the break tank	kg
N	Number of tubes in the heat exchanger	
N_{Gr}	Grasshoff number	
N_{Pr}	Prandlt number	
N_{Re}	Reynold number	
P	Product concentration	kg/kg
R	Radius of the tube in the heat exchanger	m
R	Ideal gas constant = 8.314	J/molK
R_{ex}	Radius of the tube in the heat exchanger	m
T	Time	s
T_1	Temperature of feed	°C
T_2	Temperature of tomato pulp from the heat exchanger to the break tank	°C
T_a	Ambient temperature	°C
T_s	Steam temperature	°C
T_T	Temperature of the break tank	°C
T_{Ti}	Initial tomato puree temperature in the break tank	°C

U_{ex}	Heat transfer coefficient of the heat exchanger	$W/m^2°C$
U_{tank}	Heat transfer coefficient of the break tank	$W/m^2°C$
V_{max}	Maximum forward velocity of the reaction	1/s
X	Position in the heat exchanger	m
X_w	Water fraction	

Greek letters

λ	Thermal conductivity	W/mK
ρ	Density of tomato pulp	kg/m^3
μ	Viscosity of air	kg/ms
v	Velocity of tomato pulp inside the pipe	m/s
β	Volumetric coefficient of expansion	1/K
π	Dimensionless number = 3.142	
Δ	Change	
ρ_{air}	Density of air	kg/m^3
μ_b	Fluid viscosity at bulk average temperature	kg/ms
ΔT_{lm}	Log mean temperature difference	
μ_w	Viscosity at the wall temperature	kg/ms

Appendix A2

Model Formulation

1.Word balance

1.1 Unsteady state heat balance in the break tank

Rate of heat accumulation in the break tank = Rate of heat flow into the break tank - Rate of heat flow out of the break tank - Heat losses

$$\frac{d(M_T T_T)}{dt} = F_1 T_1 + F_4 T_2 - F_2 T_T - \frac{U_{\tan k} A_{\tan k} (T_T - T_a)}{c_{pT}} \qquad \text{for } t \geq 0$$

1.2 Unsteady state mass balance in the break tank

Rate of mass accumulation in the break tank = Rate of tomato puree flow into the break tank - Rate of tomato puree flow out of the break tank

$$\frac{dM_T}{dt} = F_1 + F_4 - F_2 \qquad \text{for } t \geq 0$$

1.3 Unsteady state heat balance over the heat exchanger

The tubes in the heat exchanger are cylinder, therefore, the model is shown as below:

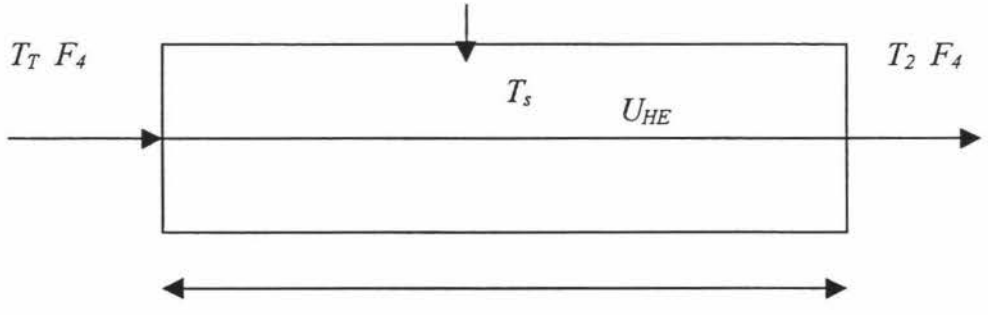

For a generalised region, j

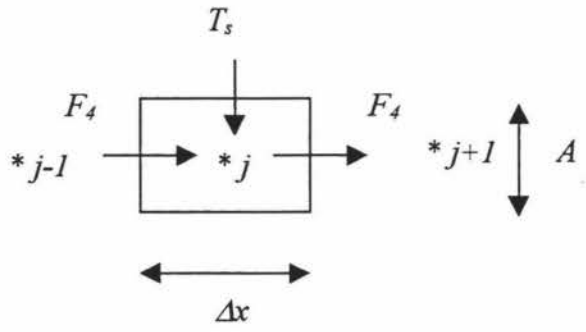

Rate of heat accumulation in generalised region j	=	Rate of heat flow into the region from j-1	-	Rate of heat flow into the region j+1	+	Rate of heat flow from steam

$$\pi r^2 \Delta x c_{pT} (\frac{dT_T}{dt})_j = F_4 c_{pT} T_{j-1} - F_4 c_{pT} T_j + U_{HE} 2\pi r \Delta x (T_s - T_j) \qquad for t \geq 0$$

$$(\frac{dT_T}{dt})_j = \frac{F_4}{\pi r^2} (\frac{T_{j-1} - T_j}{\Delta x}) + \frac{2U_{HE}}{r c_{pT}} (\frac{T_s - T_j}{\Delta x}) \qquad for t \geq 0$$

From Taylor series, $\frac{dT_T}{dx} = (\frac{T_j - T_{j-1}}{\Delta x})$

$$(\frac{dT_T}{dt})_j = -\frac{F_4}{\pi r^2} (\frac{dT_T}{dx}) + \frac{2U_{HE}}{r c_{pT}} (T_s - T_j) \qquad for 0 < x < L, t \geq 0$$

At boundaries

$$T = T_T \quad @ \; x = 0, \; t > 0$$

$$\frac{dT_T}{dx} = 0 \quad @ \; x = L, \; t > 0$$

For node j =1

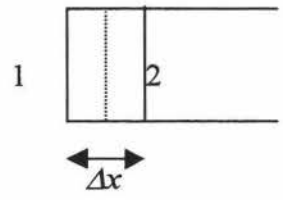

Rate of heat accumulation in generalised region j	=	Rate of heat flow across the the region j =1	+	Rate of heat flow from steam

$$\rho\pi r^2 \frac{\Delta x}{2} c_{pT} \left(\frac{dT_1}{dt}\right) = F_4 c_{pT} (T_T - T_1) + U_{HE} \pi r \Delta x (T_s - T_1) \qquad for t \geq 0$$

$$\frac{dT_1}{dt} = \frac{2F_4}{N\rho\pi r^2 \Delta x}(T_T - T_1) + \frac{2U_{HE}}{\rho r c_{pT}}(T_s - T_1) \qquad for t \geq 0$$

From Taylor series, $\frac{dT_T}{dx} = \left(\frac{T_j - T_{j-1}}{\Delta x}\right)$

$$\frac{dT_1}{dt} = \frac{2F_4}{N\rho\pi r^2}\left(\frac{dT}{dx}\right) + \frac{2U_{HE}}{\rho\, r\, c_{pT}}(T_s - T_1) \qquad for 0 < x < L, t \geq 0$$

For node j = 2:J

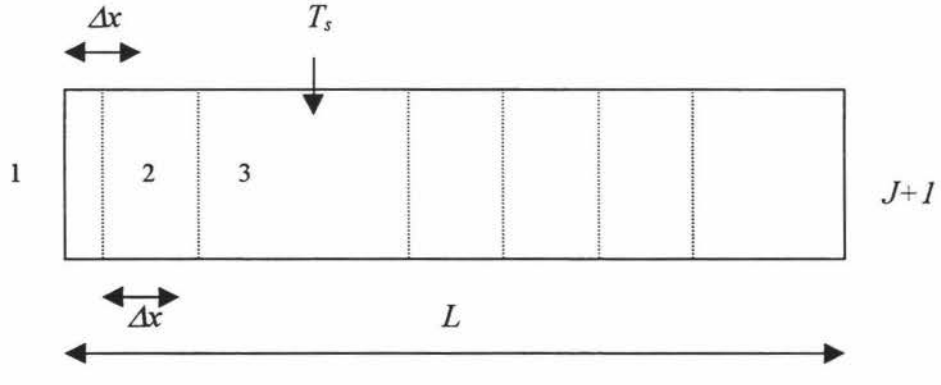

J = Number of space steps = $L/\Delta x$
No. of node = J+1 nodes

Rate of heat accumulation in generalised region j = Rate of heat flow into the region from j-1 to j + Rate of heat flow from steam to region j

$$\rho\pi r^2 \Delta x c_{pT}\left(\frac{dT_j}{dt}\right) = \frac{F_4 c_{pT}}{N}(T_{j-1} - T_j) + U_{HE} 2\pi r \Delta x (T_s - T_j) \qquad for\, t \geq 0$$

$$\frac{dT_j}{dt} = \frac{F_4}{N\rho\pi r^2}\left(\frac{T_{j-1} - T_j}{\Delta x}\right) + \frac{2U_{HE}(T_s - T_j)}{\rho\, r\, c_{pT}} \qquad for\, 0 < x < L, t \geq 0$$

From Taylor series, $\frac{dT_T}{dx} = \left(\frac{T_j - T_{j-1}}{\Delta x}\right)$

$$\frac{dT_j}{dt} = \frac{F_4}{N\rho\pi r^2}\left(\frac{dTj}{dx}\right) + \frac{2U_{HE}(T_s - T_j)}{\rho\, r\, c_{pT}} \qquad for\, 0 < x < L, t \geq 0$$

For node $j = J$+1

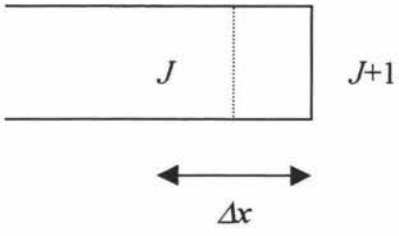

Rate of heat accumulation in generalised region J+1 = Rate of heat flow into the region from J to J+1 + Rate of heat flow from steam to region J

$$\rho\pi r^2 \frac{\Delta x}{2} c_{pT}\left(\frac{dT_{J+1}}{dt}\right) = \frac{F_4 c_{pT}}{N}(T_J - T_{J+1}) + U_{HE}\pi r \Delta x (T_s - T_J) \qquad for\, t \geq 0$$

$$\frac{dT_{J+1}}{dt} = \frac{2F_4}{N\rho\pi r^2}\frac{(T_J - T_{J+1})}{\Delta x} + \frac{2U_{HE}(T_s - T_{J+1})}{\rho r c_{pT}} \qquad for\, t \geq 0$$

From Taylor series, $\frac{dT_T}{dx} = \left(\frac{T_J - T_{J+1}}{\Delta x}\right)$

$$\frac{dT_{J+1}}{dt} = \frac{2F_4}{N\rho\pi r^2}\frac{dT_T}{dx} + \frac{2U_{HE}(T_s - T_{J+1})}{\rho r c_{pT}} \qquad for\, 0 \langle x \langle L, t \geq 0$$

1.4 Pectin concentration over the heat exchanger

Rate of pectin accumulation in generalised region j	=	Rate of pectin flow across the the region j	+	Rate of pectin degradation

$$\rho\pi r^2 \frac{\Delta x}{2}\frac{dC_{pt_1}}{dt} = F_4(C_{ptT} - C_{pt1}) - \pi r^2 \rho \frac{\Delta x}{2}\frac{V_{\max} C_{pt_1}}{K_m + C_{pt_1}} \qquad for\, t \geq 0$$

$$\frac{dC_{pt}}{dt} = \frac{2F_4}{\rho\pi r^2}\left(\frac{C_{ptT} - C_{pt}}{\Delta x}\right) - \frac{V_{\max} C_{pt}}{K_m + C_{pt}} \qquad for\, t \geq 0$$

From Taylor series, $\dfrac{dC_{ptT} - C_{pt}}{\Delta x} = \dfrac{dC_{pt}}{dx}$

$$\frac{dC_{pt}}{dt} = \frac{2F_4}{\rho\pi r^2}\left(\frac{dC_{pt}}{dx}\right) - \frac{V_{\max} C_{pt}}{K_m + C_{pt}} \qquad for\, 0 < x < L, t \geq 0$$

For node j =1

$$\frac{dC_{pt}(1)}{dt} = \frac{2F_4(C_{ptT} - C_{pt}(1))}{\rho\pi r^2 \Delta x} - \frac{V_{\max} C_{pt}(1)}{K_m + C_{pt}(1)} \qquad for\, t \geq 0$$

whereas $V_{\max} = (k_{eo} C_e(1)) \exp\left(\dfrac{-E_e}{R(T(1) + 273.15)}\right)$

For node j =2:J

$$\frac{dC_{pt}(j)}{dt} = \frac{F_4(C_{pt}(j-1) - C_{pt}(j))}{\rho\pi r^2 L} - \frac{V_{\max} C_{pt}(j)}{K_m + C_{pt}(j)} \qquad for\, t \geq 0$$

whereas $V_{\max} = (k_{eo} C_e(j)) \exp\left(\dfrac{-E_e}{R(T(j) + 273.15)}\right)$

For node j =J+1

$$\frac{dC_{pt}(j)}{dt} = \frac{2F_4(C_{pt}(J) - C_{pt}(J+1))}{\rho\pi r^2 \Delta x} - \frac{V_{\max} C_{pt}(J+1)}{K_m + C_{pt}(J+1)} \qquad for\, t \geq 0$$

whereas $V_{\max} = (k_{eo} C_e(J+1)) \exp\left(\dfrac{-E_e}{R(T(J+1) + 273.15)}\right)$

1.5 Enzyme concentration over the heat exchanger

Rate of enzyme accumulation in generalised region *j*	=	Rate of enzyme flow across the the region *j*	+	Rate of enzyme inactivation

$$\rho\pi r^2 \frac{\Delta x}{2}\frac{dk_{eo}C_e}{dt} = F_4(k_{eo}C_{eT} - k_{eo}C_e) - \pi r^2 \rho \frac{\Delta x}{2} k_{do}(k_{eo}C_e)\exp\left(\frac{-E_d}{R(T+273.15)}\right) \qquad for\ t \geq 0$$

$$\frac{dk_{eo}C_e}{dt} = \frac{2F_4}{\rho\pi r^2}\left(\frac{k_{eo}C_{eT} - k_{eo}C_e}{\Delta x}\right) - k_{do}(k_{eo}C_e)\exp\left(\frac{-E_d}{R(T+273.15)}\right) \qquad for\ t \geq 0$$

From Taylor series, $\dfrac{dk_{eo}C_{eT} - k_{eo}C_e}{\Delta x} = \dfrac{dk_{eo}C_{eT}}{dx}$

$$\frac{dk_{eo}C_e}{dt} = \frac{2F_4}{\rho\pi r^2}\left(\frac{k_{eo}C_{eT} - k_{eo}C_e}{\Delta x}\right) - k_{do}(k_{eo}C_e)\exp\left(\frac{-E_d}{R(T+273.15)}\right) \qquad for\ t \geq 0$$

For node $j = 1$

$$\frac{dk_{eo}C_e(1)}{dt} = \frac{2F_4(k_{eo}C_{eT} - k_{eo}C_e(1))}{\rho\pi r^2 \Delta x} - k_{do}(k_{eo}C_e(1))\exp\left(\frac{-E_d}{R(T(1)+273.15)}\right) \qquad for\ t \geq 0$$

For node $j = 2{:}J$

$$\frac{dk_{eo}C_e(j)}{dt} = \frac{F_4(k_{eo}C_e(j-1) - k_{eo}C_e(j))}{\rho\pi r^2 L} - k_{do}(k_{eo}C_e(j))\exp\left(\frac{-E_d}{R(T(j)+273.15)}\right) \qquad for\ t \geq 0$$

For node $j = J{+}1$

$$\frac{d(J+1)}{dt} = \frac{2F_4(k_{eo}C_e(J) - k_{eo}C_e(J+1))}{\rho\pi r^2 \Delta x} - k_{do}(k_{eo}C_e(J+1))\exp\left(\frac{-E_d}{R(T(J+1)+273.15)}\right) \qquad for\ t \geq 0$$

Appendix A3

Matlab programme

Matlab programme was divided into two sections. The function file and script file were shown in section A3.1 and A3.2, respectively.

A3.1 Function file

```
function odes=enzyme(t,DVs)

global J;
global T1;
global F3;
global F2;
global Uhe;
global F1set;
global r;
global CpT;
global Ts;
global Utank;
global DT;
global Atank;
global Ta;
global L;
global N;
global Ahe;
global T2;
global Km;
global kdo;
global Ed;
global R;
global keoCeo;
global Ee;
global C1;
global Mmax;

dx=L/J;

%Break tank variables
MT=DVs(1);
TT=DVs(2)./MT;
CT=DVs(3)./MT;
keoCeT=DVs(4)./MT;
T=DVs(5:J+5);
C=DVs(J+6:2*J+6);
keoCe=DVs(2*J+7:3*J+7);

%Differential equations
odes=zeros(3*J+7,1);
F1=F1set;

%logic statement
if t>=2000
   F1=0;
end
```

```
if t>=2500
   F1=F1set;
end

F4=(F2-F3);

%Breaktank mass
odes(1)=(F1+F4)-F2;

%Breaktank temperature

odes(2)=F1*T1+F4*T(J+1)-F2*TT-(Utank*Atank*(TT-Ta)/CpT);

%Breaktank pectin concentration

Vmax=keoCeT*exp(-Ee/(R*(TT+273.15)));
odes(3)=F1*C1-F2*CT+F4*C(J+1)-MT*Vmax*CT/(Km+CT);

%Breaktank enzyme concentration

odes(4)=F1*keoCeo-F2*keoCeT+F4*keoCe(J+1)-MT*kdo*keoCeT*exp(-
Ed/(R*(TT+273.15)));

F4=(F2-F3);

%1st node in HE
%Temperature
odes(5)=2*F4/N*(TT-T(1))/(DT*dx*pi*r^2)+2*Uhe*(Ts-T(1))/(DT*r*CpT);

%Concentration
Vmax=keoCe(1)*exp(-Ee/(R*(T(1)+273.15)));
odes(J+6)=2*F4*(CT-C(1))/(DT*pi*r^2*dx)-Vmax*C(1)/(Km+C(1));

%Enzyme concentration
odes(2*J+7)=2*F4*(keoCeT-keoCe(1))/(DT*pi*r^2*dx)-kdo*keoCe(1)*exp(-
Ed/(R*(T(1)+273.15)));

%Internal nodes in HE
for j=2:J

%Temperature
odes(j+4)=F4/N*(T(j-1)-T(j))/(DT*dx*pi*r^2)+2*Uhe*(Ts-
T(j))/(DT*r*CpT);

%Pectin concentration
Vmax=keoCe(j)*exp(-Ee/(R*(T(j)+273.15)));
odes(j+J+5)=F4*(C(j-1)-C(j))/(DT*pi*r^2*L)-Vmax*C(j)/(Km+C(j));

%Enzyme concentration
odes(j+2*J+6)=F4*(keoCe(j-1)-keoCe(j))/(DT*pi*r^2*L)-
kdo*keoCe(j)*exp(-Ed/(R*(T(j)+273.15)));

end;

%Last node in HE
%Temperature
odes(J+5)=2*F4/N*(T(J)-T(J+1))/(DT*dx*pi*r^2)+2*Uhe*(Ts-
T(J+1))/(DT*r*CpT);

%Pectin concentration
Vmax=keoCe(J+1)*exp(-Ee/(R*(T(J+1)+273.15)));
```

```
odes(2*J+6)=2*F4*(C(J)-C(J+1))/(DT*pi*r^2*dx)-Vmax*C(J+1)/(Km+C(J+1));

%Enzyme concentration
odes(3*J+7)=2*F4*(keoCe(J)-keoCe(J+1))/(DT*pi*r^2*dx)-
kdo*keoCe(J+1)*exp(-Ed/(R*(T(J+1)+273.15)));
```

A3.2 Script file

```
%Global variables

global J;
global f;
global T1;
global F3;
global F2;
global Uhe;
global F1set;
global r;
global CpT;
global Ts;
global Utank;
global DT;
global Atank;
global Ta;
global L;
global N;
global Ahe;
global T2;
global Km;
global C1set;
global keoCeset;
global kdo;
global Ed;
global R;
global keoCeo;
global Ee;
global C1;
global Mmax;

%System input
Simtime=5000;
tinterval=100;

%Constants
J=50;
T1=80;
F1set=2.3;
F1=F1set;
F3=F1set;
F2=18.4;
Mmax=3487;
Uhe=232;
rt=0.775;
ht=4*rt;
CpT=3700;
Ts=140;
Utank=4.6;
DT=1060;
Atank=10.72;
Ta=20;
r=0.023;
```

```
L=10;
N=15;
Tinit=80;
Minit=3487;
Cinit=4;
C1=Cinit;
Km=0.18;
kdo=1.67*10^18;
Ed=136474;
R=8.314;
f=1;
keoCeo=8.33*10^8;
Ee=75600;

%Initial conditions
Dvi=zeros(3*J+7,1);
DVi(1)=Minit;
DVi(2)=Tinit*Minit;
DVi(3)=Cinit*Minit;
DVi(4)=keoCeo*Minit;
DVi(5:J+5)=Tinit;
DVi(J+6:2*J+6)=Cinit;
DVi(2*J+7:3*J+7)=keoCeo;

%ODE solver options
options=odeset('RelTol',1e-6);
tspan=[0:tinterval:Simtime];

%Solve equations
[t,DV]=ode15s('enzyme',tspan,DVi);

%Create array of results
MT=DV(:,1);
TT=DV(:,2)./MT;
CT=DV(:,3)./MT;
keoCeT=DV(:,4)./MT;
T=DV(:,5:J+5);
C=DV(:,J+6:2*J+6);
keoCe=DV(:,2*J+7:3*J+7);

Xpt=(C1-CT)/C1;
Xet=(keoCeo-keoCeT)/keoCeo;
Xp=(C1-C)/C1;
Xe=(keoCeo-keoCe)/keoCeo;

figure
plot(t,T,'b--');
hold on
plot(t,TT,'r:');
figure
plot(t,MT);
figure
plot(t,C,'b--');
hold on
plot(t,CT,'r:');
figure
plot(t,keoCe,'b--');
hold on
plot(t,keoCeT,'r:');
figure
plot(t,Xp,'b-');
```

```
hold on
plot(t,Xpt,'b--');
plot(t,Xe,'r:');
plot(t,Xet,'r--');
```

Appendix A4

Data for Figure 4.5

Absorbance readings at 575 nm of PG activity at different D-galacturonic acid concentration (0 to 1.000 mg/ml)

Conc.of D-galacturonic acid (mg/ml.)	1	2	3
0	0.005	0.005	0.006
0.202	0.104	0.104	0.106
0.401	0.461	0.446	0.449
0.602	0.782	0.783	0.785
0.802	1.059	1.06	1.06
1.002	1.398	1.392	1.395

Appendix A5

Data for Figure 4.6

The absorbance readings were converted to the concentration of D-galacturonic acid using Regression from Figure 4.5.

$$X=(y+0.1974)/1.5922$$

where y = Absorbance reading at 575 nm.
x = Concentration of D-galacturonic acid (mg/ml)

1.PG activity assay using 2.54 g dark red tomato pulp at 30°C

Absorbance reading at 575 nm				Conc. of D-galacturonic acid (mg/ml)			
Time (min)	1	2	3	1	2	3	mean
0	0.005	0.012	0.018	1.271	1.315	1.353	1.313
5	0.069	0.042	0.072	1.673	1.504	1.692	1.623
10	0.062	0.065	0.041	1.629	1.648	1.497	1.592
15	0.077	0.077	0.089	1.723	1.723	1.799	1.749
20	0.09	0.106	0.105	1.805	1.906	1.899	1.870
25	0.099	0.121	0.111	1.862	2.000	1.937	1.933
30	0.132	0.113	0.119	2.069	1.950	1.987	2.002
40	0.096	0.14	0.158	1.843	2.119	2.232	2.065
50	0.167	0.166	0.19	2.289	2.282	2.433	2.335
60	0.171	0.189	0.195	2.314	2.427	2.465	2.402
90	0.198	0.209	0.21	2.483	2.552	2.559	2.532
120	0.2	0.219	0.241	2.496	2.615	2.753	2.622

2.PG activity assay using 5.04 g dark red tomato pulp at 30°C

Absorbance reading at 575 nm				Conc. of D-galacturonic acid (mg/ml)			
Time (min)	1	2	3	1	2	3	mean
5	0.152	0.161	0.165	2.194	2.251	2.276	2.241
10	0.201	0.201	0.212	2.502	2.502	2.571	2.525
15	0.221	0.246	0.252	2.628	2.785	2.823	2.745
20	0.243	0.259	0.28	2.766	2.866	2.998	2.877
25	0.275	0.262	0.296	2.967	2.885	3.099	2.984
30	0.288	0.317	0.312	3.049	3.231	3.199	3.160
40	0.326	0.359	0.379	3.287	3.495	3.620	3.467
50	0.311	0.368	0.382	3.193	3.551	3.639	3.461
60	0.34	0.366	0.404	3.375	3.539	3.777	3.564
90	0.346	0.366	0.365	3.413	3.539	3.532	3.495
120	0.403	0.411	0.395	3.771	3.821	3.721	3.771

Appendix A6

Data for Figure 4.7

The absorbance readings were converted to the concentration of D-galacturonic acid using Regression from Figure 4.5.

$$x=(y+0.1974)/1.5922$$

where y = Absorbance reading at 575 nm.
x = Concentration of D-galacturonic acid (mg/ml)

1.PG activity assay using 2.50 g green tomato pulp at 30°C

Absorbance reading at 575 nm				Conc. of D-galacturonic acid (mg/ml)			
Time (min)	1	2	3	1	2	3	mean
0	0.012	0.017	0.025	1.315	1.347	1.397	1.353
5	0.042	0.039	0.029	1.504	1.485	1.422	1.470
10	0.028	0.032	0.029	1.416	1.441	1.422	1.426
15	0.026	0.028	0.029	1.403	1.416	1.422	1.414
20	0.023	0.034	0.031	1.384	1.453	1.434	1.424
25	0.023	0.028	0.034	1.384	1.416	1.453	1.418
30	0.042	0.024	0.028	1.504	1.391	1.416	1.437
40	0.027	0.03	0.026	1.409	1.428	1.403	1.414

2. PG activity assay using 2.50 g breaker tomato pulp at 30°C

Absorbance reading at 575 nm				Conc. of D-galacturonic acid (mg/ml)			
Time (min)	1	2	3	1	2	3	mean
0	0.017	0.014	0.015	1.347	1.328	1.334	1.336
5	0.019	0.019	0.035	1.359	1.359	1.460	1.393
10	0.03	0.036	0.043	1.428	1.466	1.510	1.468
15	0.028	0.033	0.031	1.416	1.447	1.434	1.432
20	0.03	0.038	0.039	1.428	1.478	1.485	1.464
25	0.021	0.038	0.034	1.372	1.478	1.453	1.434
30	0.031	0.035	0.042	1.434	1.460	1.504	1.466
40	0.03	0.035	0.044	1.428	1.460	1.516	1.468

3. PG activity assay using 2.54 g turning tomato pulp at 30°C

Absorbance reading at 575 nm				Conc. of D-galacturonic acid (mg/ml)			
Time (min)	1	2	3	1	2	3	mean
0	0.017	0.017	0.015	1.347	1.347	1.334	1.342
5	0.038	0.042	0.044	1.478	1.504	1.516	1.499
10	0.040	0.054	0.048	1.491	1.579	1.538	1.536
15	0.039	0.042	0.046	1.485	1.500	1.526	1.504
20	0.048	0.051	0.047	1.541	1.560	1.535	1.545
25	0.040	0.048	0.044	1.491	1.541	1.516	1.516
30	0.046	0.055	0.057	1.526	1.585	1.595	1.568
40	0.046	0.050	0.047	1.529	1.554	1.535	1.539

4. PG activity assay using 2.55 g orange tomato pulp at 30°C

Absorbance reading at 575 nm				Conc. of D-galacturonic acid (mg/ml)			
Time (min)	1	2	3	1	2	3	mean
0	0.014	0.013	0.015	1.325	1.318	1.334	1.326
5	0.069	0.078	0.078	1.670	1.727	1.730	1.709
10	0.082	0.081	0.089	1.752	1.745	1.799	1.765
15	0.084	0.095	0.092	1.764	1.836	1.818	1.806
20	0.085	0.091	0.090	1.771	1.811	1.802	1.795
25	0.088	0.100	0.096	1.789	1.865	1.840	1.831
30	0.092	0.097	0.100	1.814	1.849	1.868	1.844
40	0.099	0.112	0.116	1.858	1.943	1.965	1.922

5. PG activity assay using 2.53 g dark red tomato pulp at 30°C

Absorbance reading at 575 nm				Conc. of D-galacturonic acid (mg/ml)			
Time (min)	1	2	3	1	2	3	mean
0	0.016	0.014	0.016	1.337	1.325	1.337	1.333
5	0.056	0.075	0.066	1.592	1.708	1.651	1.650
10	0.067	0.074	0.064	1.661	1.705	1.639	1.668
15	0.081	0.076	0.080	1.745	1.714	1.742	1.734
20	0.082	0.090	0.096	1.755	1.802	1.843	1.800
25	0.087	0.102	0.101	1.783	1.880	1.871	1.845
30	0.110	0.117	0.100	1.931	1.971	1.865	1.922
40	0.097	0.124	0.115	1.849	2.019	1.959	1.942

Appendix A7

Data for Figure 4.14

The absorbance readings were converted to the concentration of D-galacturonic acid using Regression from Figure 4.5

$$x=(y+0.1974)/1.5922$$

where y = Absorbance reading at 575 nm.
x = Concentration of D-galacturonic acid (mg/ml)

1.PG activity assay using 2.52 g dark red tomato pulp at 25°C

Absorbance reading at 575 nm				Conc. of D-galacturonic acid (mg/ml)			
Time (min)	1	2	3	1	2	3	mean
0	0.018	0.023	0.015	1.353	1.384	1.334	1.357
5	0.096	0.106	0.119	1.843	1.906	1.987	1.912
10	0.113	0.120	0.129	1.950	1.993	2.050	1.998
15	0.140	0.153	0.141	2.119	2.201	2.125	2.148
20	0.157	0.168	0.169	2.226	2.295	2.301	2.274
25	0.178	0.181	0.186	2.358	2.377	2.408	2.381
30	0.186	0.199	0.203	2.408	2.490	2.515	2.471
40	0.220	0.241	0.235	2.622	2.753	2.716	2.697

2.PG activity assay using 2.54 g dark red tomato pulp at 30°C

Absorbance reading at 575 nm				Conc. of D-galacturonic acid (mg/ml)			
Time (min)	1	2	3	1	2	3	mean
0	0.011	0.014	0.015	1.309	1.325	1.334	1.322
5	0.061	0.066	0.067	1.620	1.651	1.661	1.644
10	0.063	0.073	0.056	1.632	1.698	1.592	1.641
15	0.082	0.080	0.091	1.752	1.739	1.808	1.766
20	0.091	0.102	0.102	1.808	1.877	1.880	1.855
25	0.097	0.120	0.112	1.849	1.990	1.943	1.928
30	0.126	0.123	0.108	2.031	2.009	1.915	1.985
40	0.103	0.143	0.147	1.884	2.135	2.163	2.060

3.PG activity assay using 2.52 g dark red tomato pulp at 35°C

Absorbance reading at 575 nm				Conc. of D-galacturonic acid (mg/ml)			
Time (min)	1	2	3	1	2	3	mean
0	0.018	0.023	0.022	1.353	1.384	1.378	1.372
5	0.120	0.129	0.148	1.993	2.050	2.169	2.071
10	0.162	0.176	0.186	2.257	2.345	2.408	2.337
15	0.188	0.229	0.244	2.421	2.678	2.772	2.624
20	0.243	0.253	0.251	2.766	2.829	2.816	2.804
25	0.257	0.275	0.295	2.854	2.967	3.093	2.971
30	0.279	0.297	0.290	2.992	3.105	3.061	3.053
40	0.323	0.362	0.367	3.268	3.513	3.545	3.442

4.PG activity assay using 2.59 g dark red tomato pulp at 40°C

Absorbance reading at 575 nm				Conc. of D-galacturonic acid (mg/ml)			
Time (min)	1	2	3	1	2	3	mean
0	0.017	0.015	0.018	1.343	1.331	1.354	1.343
5	0.098	0.113	0.122	1.855	1.946	2.006	1.936
10	0.146	0.152	0.172	2.157	2.194	2.320	2.224
15	0.167	0.198	0.204	2.289	2.480	2.521	2.430
20	0.201	0.228	0.236	2.502	2.672	2.719	2.631
25	0.182	0.204	0.263	1.452	1.587	2.892	2.851
30	0.234	0.256	0.280	2.709	2.844	2.995	2.850
40	0.257	0.293	0.313	2.854	3.077	3.202	3.044

5.PG activity assay using 2.48 g dark red tomato pulp at 50°C

Absorbance reading at 575 nm				Conc. of D-galacturonic acid (mg/ml)			
Time (min)	1	2	3	1	2	3	mean
0	0.012	0.014	0.014	1.315	1.330	1.328	1.324
5	0.179	0.186	0.136	2.364	2.408	2.094	2.289
10	0.265	0.256	0.206	2.904	2.848	2.534	2.762
15	0.300	0.287	0.242	3.124	3.042	2.760	2.975
20	0.251	0.311	0.329	2.816	3.193	3.306	3.105
25	0.344	0.313	0.267	3.400	3.206	2.917	3.174
30	0.265	0.322	0.329	2.904	3.262	3.306	3.157
40	0.280	0.338	0.356	2.998	3.363	3.476	3.279

Appendix A8

Data for Figure 4.23

The absorbance readings were converted to the concentration of D-galacturonic acid using Regression from Figure 4.5.

$$x=(y+0.1974)/1.5922$$

where y = Absorbance reading at 575 nm.
x = Concentration of D-galacturonic acid (mg/ml)

1.PG activity assay using 2.53 g dark red tomato pulp at 30°C using 10% PGA solution

Absorbance reading at 575 nm				Conc. of D-galacturonic acid (mg/ml)			
Time (min)	1	2	3	1	2	3	mean
0	0.396	0.418	0.370	3.724	3.862	3.560	3.715
1	0.403	0.454	0.370	3.771	4.091	3.560	3.808
5	0.503	0.477	0.446	4.399	4.233	4.038	4.223
10	0.506	0.517	0.466	4.418	4.484	4.163	4.355
15	0.544	0.532	0.514	4.656	4.581	4.468	4.569
20	0.566	0.561	0.530	4.795	4.760	4.569	4.708
25	0.608	0.576	0.558	5.058	4.854	4.744	4.886
30	0.541	0.590	0.586	4.638	4.942	4.917	4.832
40	0.615	0.664	0.574	5.102	5.410	4.845	5.119

2.PG activity assay using 2.59 g dark red tomato pulp at 40°C using 10% PGA solution

Absorbance reading at 575 nm				Conc. of D-galacturonic acid (mg/ml)			
Time (min)	1	2	3	1	2	3	mean
0	0.343	0.397	0.387	3.394	3.733	3.670	3.599
1	0.376	0.325	0.370	3.601	3.281	3.564	3.482
5	0.377	0.458	0.502	3.608	4.116	4.393	4.039
10	0.589	0.581	0.547	4.939	4.889	4.675	4.834
15	0.600	0.624	0.645	5.008	5.159	5.291	5.153
20	0.685	0.662	0.696	5.542	5.398	5.611	5.517
25	0.768	0.785	0.834	6.063	6.170	6.478	6.237
30	0.838	0.838	0.832	6.503	6.503	6.465	6.490
40	0.958	0.811	0.931	7.257	6.333	7.087	6.892
50	0.782	0.880	0.938	6.151	6.767	7.131	6.683
60	1.075	1.028	0.938	7.991	7.696	7.131	7.606
70	1.005	1.067	1.091	7.552	7.941	8.092	7.862
80	1.162	1.102	1.197	8.538	8.161	8.758	8.486
90	1.055	1.153	1.193	7.866	8.481	8.733	8.360
100	1.227	1.139	1.282	8.946	8.393	9.292	8.877
110	1.169	1.424	1.366	8.582	10.183	9.819	9.528
120	1.306	1.380	1.220	9.442	9.907	8.902	9.417
130	1.452	1.467	1.382	10.359	10.453	9.920	10.244
140	1.580	1.549	1.472	11.163	10.968	10.485	10.872
150	1.512	1.507	1.582	10.736	10.705	11.176	10.872
160	1.515	1.580	1.520	10.755	11.163	10.786	10.901
170	1.601	1.572	1.675	11.295	11.113	11.760	11.389
180	1.694	1.767	1.713	11.879	12.338	11.998	12.072

3.PG activity assay using 2.54 g dark red tomato pulp at 50°C using 10% PGA solution

Absorbance reading at 575 nm				Conc. of D-galacturonic acid (mg/ml)			
Time (min)	1	2	3	1	2	3	mean
0	0.520	0.537	0.469	4.506	4.612	4.185	4.435
1	0.526	0.550	0.560	4.543	4.694	4.757	4.665
5	0.691	0.728	0.697	5.580	5.812	5.617	5.670
10	0.858	0.851	0.898	6.629	6.585	6.880	6.698
15	1.058	1.072	0.947	7.885	7.973	7.188	7.682
20	1.199	1.112	1.090	8.770	8.224	8.086	8.360
25	1.291	1.282	1.254	9.348	9.292	9.116	9.252
30	1.427	1.302	1.421	10.202	9.417	10.165	9.928
40	1.523	1.591	1.587	10.805	11.232	11.207	11.082

4.PG activity assay using 2.58 g dark red tomato pulp at 55°C using 10% PGA solution

Absorbance reading at 575 nm				Conc. of D-galacturonic acid (mg/ml)			
Time (min)	1	2	3	1	2	3	mean
0	0.352	0.399	0.404	3.451	3.746	3.777	3.658
1	0.349	0.443	0.456	3.432	4.022	4.104	3.853
5	0.528	0.591	0.495	4.556	4.952	4.349	4.619
10	0.596	0.638	0.681	4.983	5.247	5.517	5.249
15	0.874	0.895	0.901	6.729	6.861	6.899	6.830
20	1.001	1.018	0.943	7.527	7.633	7.162	7.441
25	1.104	1.160	1.159	8.174	8.525	8.519	8.406
30	1.166	1.234	1.226	8.563	8.990	8.940	8.831
40	1.128	1.335	1.256	8.324	9.624	9.128	9.026
50	1.469	1.598	1.705	10.466	11.276	11.948	11.230
60	1.745	1.661	1.614	12.199	11.672	11.377	11.749
70	1.701	1.679	1.714	11.923	11.785	12.005	11.904
80	1.814	1.714	1.715	12.633	12.005	12.011	12.216
90	1.752	1.723	1.791	12.243	12.061	12.488	12.264

5.PG activity assay using 2.58 g dark red tomato pulp at 60°C using 10% PGA solution

Absorbance reading at 575 nm				Conc. of D-galacturonic acid (mg/ml)			
Time (min)	1	2	3	1	2	3	mean
0	0.508	0.488	0.506	4.427	4.305	4.418	4.383
1	0.552	0.548	0.550	4.707	4.678	4.694	4.693
5	0.797	0.816	0.741	6.242	6.362	5.894	6.166
10	1.060	1.055	1.037	7.897	7.863	7.750	7.837
15	1.503	1.128	1.273	10.676	8.324	9.232	9.411
20	1.427	1.458	1.408	10.199	10.394	10.083	10.225
25	1.497	1.577	1.508	10.642	11.144	10.711	10.832
30	1.691	1.679	1.687	11.857	11.785	11.835	11.826
40	1.780	1.668	1.714	12.567	13.204	13.770	13.180
50	1.701	1.786	1.811	11.923	12.457	12.614	12.331
60	1.898	1.915	1.911	13.160	13.267	13.242	13.223
70	1.982	1.950	1.974	13.688	13.487	13.638	13.604
80	2.204	1.948	2.490	15.082	13.474	16.879	15.145
90	2.063	1.861	2.045	14.197	12.928	14.084	13.736

6.PG activity assay using 2.56 g dark red tomato pulp at 65°C using 10% PGA solution

Absorbance reading at 575 nm				Conc. of D-galacturonic acid (mg/ml)			
Time (min)	1	2	3	1	2	3	mean
0	0.379	0.404	0.326	3.620	3.777	3.287	3.562
1	0.444	0.461	0.427	4.028	4.135	3.922	4.028
5	0.618	0.620	0.610	5.121	5.134	5.071	5.109
10	0.770	0.734	0.761	6.076	5.850	6.019	5.982
15	0.833	0.769	0.851	6.472	6.070	6.585	6.375
20	0.924	0.951	0.950	7.043	7.213	7.206	7.154
25	1.000	1.012	1.057	7.520	7.596	7.878	7.665
30	1.094	1.105	1.100	8.111	8.180	8.148	8.146
40	1.110	1.064	1.122	8.211	7.922	8.287	8.140
50	1.276	1.266	1.160	9.254	9.191	8.525	8.990
60	1.211	1.292	1.253	8.846	9.354	9.109	9.103
70	1.424	1.340	1.410	10.183	9.656	10.095	9.978
80	1.429	1.453	1.477	10.215	10.366	10.516	10.366
90	1.421	1.268	1.504	10.165	9.204	10.686	10.018

7.PG activity assay using 2.55 g dark red tomato pulp at 70°C using 10% PGA solution

Absorbance reading at 575 nm				Conc. of D-galacturonic acid (mg/ml)			
Time (min)	1	2	3	1	2	3	mean
0	0.502	0.432	0.537	4.393	3.953	4.612	4.319
1	0.557	0.482	0.548	4.738	4.267	4.682	4.562
5	0.638	0.732	0.736	5.247	5.837	5.862	5.649
10	0.893	0.831	0.863	6.848	6.459	6.660	6.656
15	0.802	0.887	0.855	6.277	6.811	6.610	6.566
20	0.888	0.985	0.850	6.817	7.426	6.578	6.941
25	0.945	0.964	0.970	7.175	7.294	7.332	7.267
30	1.053	1.063	1.036	7.853	7.916	7.747	7.839
40	1.099	1.014	1.071	8.142	7.608	7.966	7.906
50	1.068	1.101	1.028	7.947	8.155	7.696	7.933
60	1.154	1.013	1.133	8.488	7.602	8.356	8.148
70	1.088	1.198	1.190	8.073	8.764	8.714	8.517
80	1.328	1.308	1.286	9.580	9.455	9.317	9.451
90	1.127	1.230	1.086	8.318	8.965	8.061	8.448

8.PG activity assay using 2.58 g dark red tomato pulp at 80°C using 10% PGA solution

Absorbance reading at 575 nm				Conc. of D-galacturonic acid (mg/ml)			
Time (min)	1	2	3	1	2	3	mean
0	0.526	0.524	0.448	4.543	4.531	4.054	4.376
1	0.529	0.572	0.531	4.562	4.832	4.575	4.656
5	0.524	0.549	0.565	4.531	4.688	4.788	4.669
10	0.558	0.497	0.516	4.744	4.361	4.481	4.529
15	0.582	0.506	0.584	4.895	4.418	4.908	4.740
20	0.469	0.645	0.490	4.185	5.291	4.317	4.598
25	0.598	0.623	0.604	4.996	5.153	5.033	5.061
30	0.642	0.527	0.517	5.272	4.550	4.487	4.770
40	0.586	0.612	0.570	4.920	5.084	4.820	4.941
50	0.636	0.623	0.618	5.234	5.153	5.121	5.169
60	0.644	0.510	0.478	5.285	4.443	4.242	4.656
70	0.642	0.675	0.671	5.272	5.479	5.454	5.402
80	0.655	0.668	0.645	5.354	5.435	5.291	5.360
90	0.709	0.648	0.680	5.693	5.310	5.511	5.504